

# Microfluidic Paper Based Electrochemical Sensing Devices

By

**Clementine Juliat Louw**

A thesis submitted in partial fulfilment of the  
requirements for the degree of Magister Scientiae in  
Chemistry.



Faculty of Natural Science

University of the Western Cape

Cape Town, South Africa

Supervisor: Prof PGL Baker

# Keywords

Polyamic Acid

Cobalt nanoparticles

Carbon ink

Antibiotics

Paper Substrates

Microfluidics

Paper based sensors

Cyclic Voltammetry

Square Wave Voltammetry

Screen Printing

Norfloxacin



# Abstract

Microfluidic paper based electrochemical sensing devices ( $\mu$ PEDs) provides a new way for point of care testing (POCT).  $\mu$ PEDs offer an inexpensive, portable, easy to use technology to monitor the environment and diagnose diseases, especially in developing countries in cases where there is not enough infrastructure and a limited trained medical and health professionals. The aim of this work is to develop a paper based electrode which can be further integrated into a microfluidic paper device to develop miniature point of care devices. Paper was used as a substrate for printing of the electrode because it is found everywhere, inexpensive and it is compatible with a number of chemical, biochemical and medical applications. Polyamic acid (PAA) was incorporated into commercial carbon ink and was used to print the working electrode.

The first part of the study was conducted using the commercial screen printed carbon electrodes (SPCE) to study and understand the electrochemical behaviour of PAA. Cobalt nanoparticles and cobalt nanoparticles-polyamic acid composites were electrochemically deposited onto SPCE. The modified electrodes were characterised using cyclic voltammetry. As synthesised polyamic acid were characterised using Scanning Electron Microscopy (SEM) to evaluate the morphology and chemical composition of polyamic acid. Transmission Electron Microscopy (TEM) was used to study the particle size and chemical composition of cobalt nanoparticles. Fourier Transform Infrared Spectroscopy (FTIR) was used to study the chemical nature of polyamic acid and cyclic voltammetry (CV) was used to study the electrochemical behaviour of polyamic acid and cobalt nanoparticle electrodes. The diffusion coefficients and formal potential of the electrodes were calculated. The modified and bare electrodes were also used to electrochemically detect Norfloxacin in an aqueous solution by CV and square wave voltammetry (SWV) and the analytical performance of the electrochemical systems are reported here. The obtained limit of detection for the bare SPCE was  $3.7 \times 10^{-3}$  M and  $14.7 \times 10^{-3}$  M for the PAA-SPCE.

In the second part of the study novel mixed polymer electrodes were printed as paper based electrodes and optimised with respect to the composition of the polymer PAA mixed with commercial carbon nanomaterials. Different amounts of PAA were mixed with commercial carbon ink and stirred to make a homogenous ink mixture, the ink was then used to screen print the working electrodes onto photo paper using a screen printer. The novel screen printed electrodes were characterized by SEM to study the surface morphology of the working electrode and CV to evaluate the electrochemical performances of the electrodes. The optimised composite electrodes were applied to the electrochemical detection of Norfloxacin in an aqueous solution and a detection of limit of  $7.93 \times 10^{-4}$  M.



# Declaration

I declare that “**Microfluidic paper electrochemical sensing devices**” is my own work, that it has not been submitted before for any degree or assessment in any other university, and that all the sources I have used or quoted have been indicated and acknowledged by means of complete references.

**Clementine Juliat Louw**

Signature .....

Supervisor: **Prof. Priscilla G.L. Baker**



# Acknowledgements

*“I am with you and will watch over you wherever you go, and will bring you back to this land. I will not leave you until I have done what I have promised you.” Genesis 28v15*

I would like to thank God for the strength, guidance and wisdom that He gave me throughout my work.

To the University of the Western Cape, Natural Sciences faculty thank you for allowing me to pursue my Master’s degree.

To my supervisor Professor PGL Baker, thank you for the guidance, encouragement, motivation, advice, time and immense knowledge during the course of this research project.

To my colleagues in SensorLab research group thank for the assistance throughout my work.

To Dr Kevin Land, Mesuli Mbanjwa, Letta Ntuli and Phophi Madzivhandlila and CSIR (MMM) thank you for all the assistance with the screen printed electrodes.

To my mother Ralie Laliswa Louw, my father Joseph Tsietsi Joseph Louw, my sister Ophelia Nicolette Louw, little brothers Tshenolo Dominique Louw and Lebogang Madiba Louw and my grandmother Betty Khetiwe Stander thank you for all the support, encouragements, love and prayers .

To my friends, family and my brothers and sisters in Christ thank you for the support, encouragement and prayers.

To the Council for Scientific and Industrial Research (CSIR)-DST Inter-Bursary Support Programme thank you for funding my studies.

# Dedication

This project is dedicated to everyone who believed in me and encouraged me.

My parents: Ralie Louw and Tsietsi Louw

My siblings: Ophelia Louw, Lebogang Louw and Tshenolo Louw



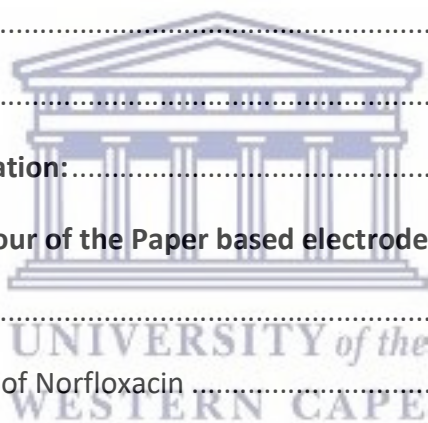
# Table of Contents

Keywords.....	2
Abstract.....	3
Declaration.....	5
Acknowledgements.....	6
Dedication.....	7
Table of Contents.....	8
List of figures and tables.....	11
List of Abbreviations.....	14
Chapter 1.....	16
<i>Introduction</i> .....	16
<b>1.1 Microfluidic devices</b> .....	16
<b>1.2 Microfluidic paper based electrochemical sensing devices</b> .....	16
<b>1.3 Paper Substrate</b> .....	17
<b>1.4 Screen printing technology</b> .....	18
<b>1.5 Carbon paste based electrodes</b> .....	19
<b>1.6 Polyamic Acid</b> .....	21
<b>1.7 Cobalt Nanoparticles</b> .....	22
<b>1.8 Antibiotic residues in aqueous systems</b> .....	22
<b>1.9 Problem statement</b> .....	25
<b>1.10 Aims and Objectives</b> .....	26
<b>1.11 Conceptual diagram</b> .....	27
<b>1.12 Thesis outline</b> .....	28
Chapter 2.....	29



<i>Literature review</i> .....	29
<b>2.1 Electrochemical sensors</b> .....	29
<b>2.1.1 Paper based electrochemical sensors</b> .....	30
<b>2.1.2 Detection of analytes in paper electrochemical sensors</b> .....	31
<b>2.2 Polymer paper based modified electrodes</b> .....	33
<b>2.3 Electrochemical sensor for detection of Norfloxacin</b> .....	35
Chapter 3.....	37
<i>Characterisation techniques</i> .....	37
<b>3.1 Electrochemical Techniques</b> .....	37
<b>3.1.1 Cyclic Voltammetry</b> .....	37
<b>3.1.2 Square wave voltammetry (SWV):</b> .....	39
<b>3.2 Spectroscopic Techniques</b> .....	39
<b>3.2.1 Fourier transform infrared spectroscopy (FTIR):</b> .....	39
<b>3.2.2 Ultraviolet-Visible (UV-Vis)</b> .....	40
<b>3.3 Microscopic Techniques</b> .....	40
<b>3.3.1 Transmission electron microscopy (TEM)</b> .....	40
<b>3.3.2 Scanning electron microscopy (SEM):</b> .....	41
<b>3.3.3 Small angle X-ray scattering (SAXS)</b> .....	42
Chapter 4.....	44
<i>Materials and synthesis</i> .....	44
<b>4.1 Material and synthesis:</b> .....	44
<b>4.1.1 Preparation of Phosphate buffer saline</b> .....	44
<b>4.1.2 Synthesis of Polyamic acid:</b> .....	44
<b>4.1.3 Synthesis of Cobalt Nanoparticles:</b> .....	45
<b>4.1.4 Potassium ferricyanide with potassium chloride as supporting electrolyte</b> .....	45
<b>4.2 Ink Formulation and fabrication of electrodes</b> .....	46

<b>4.2.1 Incorporation of polyamic acid in commercial carbon ink:</b> .....	46
<b>4.2.2 Carbon Nanotubes (CNT) and PAA</b> .....	47
<b>4.3 Characterization</b> .....	50
<b>4.3.1 Spectroscopic characterization</b> .....	50
<b>4.3.2 Microscopic characterization:</b> .....	51
<b>4.3.3 Electrochemical Characterization</b> .....	55
Chapter 5.....	64
<i>Analysis of Norfloxacin</i> .....	64
<b>5.1 UV analysis of Norfloxacin</b> .....	64
<b>5.2 Electrochemical detection of Norfloxacin</b> .....	65
Chapter 6.....	76
<i>Paper based electrodes</i> .....	76
<b>6.1 Microscopic characterization:</b> .....	76
<b>6.2 Electrochemical behaviour of the Paper based electrodes</b> .....	78
6.3 Charge calculation.....	83
6.4 Electrochemical detection of Norfloxacin .....	84
Chapter 7.....	88
<i>Conclusion and Future works</i> .....	88
<b>Conclusion</b> .....	88
<b>Future works:</b> .....	91
References .....	92



# List of figures and tables

Figure 1: Chemical structure of PAA and polyamide (Noah N.M. et al., 2012) .....	21
Figure 2: Conceptual diagram of the thesis .....	27
Figure 3: Chemical structure of Norfloxacin .....	35
Figure 4: PalmSens Potentiostat .....	37
Figure 5: Example of a reversible cyclic voltammogram .....	38
Figure 6: Example of a three electrode system .....	38
Figure 7: Schematic of transmission electron microscopy .....	41
Figure 8: Schematic of scanning electron microscopy .....	42
Figure 9: Schematic of synthesis of cobalt nanoparticles .....	45
Figure 10: Schematic of paper based electrodes fabrication .....	47
Figure 11: Cyclic voltammograms of the electrodes fabricated in this study, A) Commercial carbon ink, B) 6%PAA-Commercial carbon ink, C) MWCNT paste, D) 6%PAA-MWCNT paste, E) 10%PAA-MWCNT paste, F)20% PAA-Commercial carbon ink .....	49
Figure 12: FTIR spectrum of polyamic acid and PAA-Co NP .....	50
Figure 13: HRSEM image of polyamic acid .....	51
Figure 14: EDS of polyamic acid .....	51
Figure 15: HRTEM image of cobalt nanoparticles .....	52
Figure 16: SAED image of the cobalt nanoparticles .....	52
Figure 17: Image of EDX of the cobalt nanoparticles .....	53
Figure 18: Distribution curve of cobalt nanoparticles .....	54
Figure 19: Cyclic voltammogram of PAA-SPCE in pH 7.04 0.1 M PBS at scan rates ranging from 10 mV/s-100 mV/s. Insert shows bare SPCE electrode at scan rate 50 mV/s in pH 7.04 0.1 M PBS .....	56
Figure 20: Cyclic voltammogram of PAA-GCE in pH7.04 0.1 M PBS at different scan rates (10 mV/s-100 mV/s) .....	57
Figure 21: Cyclic voltammogram of commercial cobalt solution and synthesised Co NP in 0.1 M pH 7.04 PBS at scan rate 50 mV/s .....	57

Figure 22: Cyclic voltammogram of Co NP in 0.1M pH 7.04 PBS at different scan rates (10 mV/s-100 mV/s).....	59
Figure 23: Cyclic voltammogram of PAA-Co NP on SPCE in 0.1M pH 7.04 PBS at different scan rates (10 mV/s-100 mV/s).....	60
Figure 24: Randles Sevcik plot of PAA-SPCE in pH 7,04 0.1 M PBS.....	60
Figure 25: Randles Sevçik plot of Co nanoparticles-SPCE in pH 7.04 0.1 M PBS. ....	61
Figure 26: Randles Sevçik plot of Co NP-PAA on SPCE in pH 7.04 0.1 M PBS.....	61
Figure 27: UV-Vis spectrum of 0.1 M Norfloxacin in HCl.....	64
Figure 28: Current response of a bare SPCE at increasing concentrations of Norfloxacin as measured by CV in 0.1M pH7 PBS, scan rate 50 mV/s. ....	65
Figure 29: Current response measured by SWV of bare SPCE at increasing concentrations of Norfloxacin in 0.1 M pH7.04 PBS, scan rate 50 mV/s.....	66
Figure 30: Current response measured by CV of PAA-SPCE at increasing concentrations of Norfloxacin in 0.1 M pH7.04 PBS, scan rate 50 mV/s.....	67
Figure 31: Current response measured by SWV of SPCE-PAA at increasing concentrations of Norfloxacin in 0.1 M pH7.04 PBS, scan rate 50 mV/s.....	68
Figure 32: Current response measured by CV of SPCE-PAA- Co NP at increasing concentrations of Norfloxacin in 0.1 M pH 7.04 PBS, scan rate 50 mV/s.....	69
Figure 33: Square wave voltammogram of PAA-Co NP at different concentrations of Norfloxacin in 0.1 M pH 7.04 PBS at scan rate 50 mV/s.....	70
Figure 34: Calibration curves of bare SPCE at different concentrations of Norfloxacin, at scan rate 50 mV/s, n=3. ....	71
Figure 35: Linear range of the average of the bare electrodes calibration curves at different concentrations of Norfoxacin in 0.1 M pH 7.04 PBS calibration curve,n=3. ....	71
Figure 36: Calibration curves of Modified SPCE with PAA at different concentrations of Norfloxacin.....	72
Figure 37: Linear range of the average of the PAA-SPCE calibration curve at different concentrations of Norfloxacin in 0.1 M pH 7.04, n=3.....	72
Figure 38: Calibration curve of PAA-Co NP at different concentrations of Norfloxacin in 0.1 M pH7.04 PBS, n=3.....	73
Figure 39: HRSEM image of the surface of the commercial carbon ink working electrode prior to modification.....	76

Figure 40: HRSEM image of the surface of the 6%PAA-commercial carbon ink working electrode.....	77
Figure 41: HRSEM image of the surface of 20%PAA-commercial carbon ink working electrode. ....	77
Figure 42: Cyclic voltammogram of the different paper electrodes in 5 mM $K_3[Fe(CN)_6]$ 0.1 M KCl at scan rate 50 mV/s. ....	79
Figure 43: Cyclic voltammogram of 20% PAA-Com carbon ink electrode in 5mM $K_3Fe(CN)_6$ in 0.1 M KCl at scan rates 10-100 mV/s.....	80
Figure 44: Cyclic voltammogram of 20%PAA- Com carbon electrode ink in pH 7.04 0.1 M PBS at scan rates 10 mV/s-100 mV/s.....	80
Figure 45: Randles Sevçik plot of 20%PAA-Commercial carbon ink electrode in 5 mM $K_3Fe(CN)_6$ with 0.1 M KCl. ....	81
Figure 46: Randles Sevçik plot of 20%PAA-Commercial carbon ink electrode in 0.1 M pH 7.04 PBS. ....	82
Figure 47: Electrochemical detection of Norfloxacin at 20%PAA-Commercial carbon ink electrode in pH 7.04 0.1 M PBS. ....	84
Figure 48: Calibration curve of detection of Norfloxacin at 20%PAA-Commercial carbon ink electrode. ....	85
Figure 49: Linear plot of at 20%PAA-com carbon ink electrode at different concentrations of Norfloxacin.....	86

## List of tables:

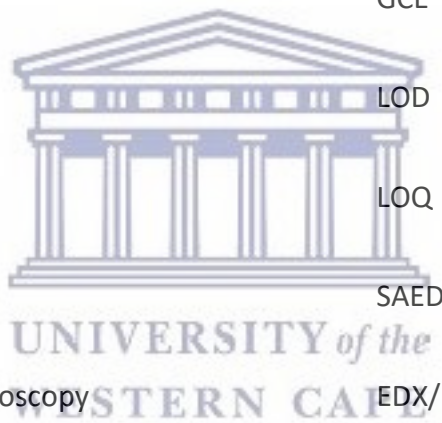
Table 1: Most commonly studied conjugated polymers (Rahman M.D. et al., 2008).....	20
Table 2: Ink formulation of MWCNT-PAA.....	47
Table 3: Electrochemical parameters of PAA, Co NP and PAA-Co NP on SPCE. ....	62
Table 4: Comparison of voltammetric performance of PAA-SPCE with previously reported data for electrochemical detection of Norfloxacin.....	74
Table 5: Response of novel screen printed paper based electrodes.....	83

# List of Abbreviations

Polyamic acid	PAA
Cobalt nanoparticles	Co NP
Polyamic acid- Cobalt Nanoparticles	PAA-Co NP
Microfluidic paper based analytical devices	$\mu$ PADs
Microfluidic paper based electrochemical devices	$\mu$ PEDs
Screen printed carbon electrode	SPCE
Screen print electrode	SPE
Phosphate buffer solution	PBS
Hydrochloric acid	HCl
Potassium Ferricyanide	$K_3Fe(CN)_6$
Potassium Chloride	KCl
Cyclic Voltammetry	CV
Square Wave Voltammetry	SWV
Fourier Transform Infrared	FTIR
Scanning Electron Microscopy	SEM
Transmission Electron Microscopy	TEM
Ultraviolet-Visible Spectroscopy	UV-Vis



Anodic peak current	$I_{p_a}$
Cathodic peak current	$I_{p_c}$
Anodic peak potential	$E_{p_a}$
Cathodic peak potential	$E_{p_c}$
Diffusion coefficient	$D_e$
Formal potential	$E^{\circ}$
Peak separation	$\Delta E_p$
Glassy Carbon Electrode	GCE
Limit of Detection	LOD
Limit of Quantification	LOQ
Selected area diffraction	SAED
Energy dispersive X-ray spectroscopy	EDX/EDS
Small Angle X-ray Scattering	SAXS
Pair distance distribution function	PDDF



# Chapter 1

## *Introduction*

*This chapter gives an introduction to microfluidic devices, microfluidic paper based electrochemical sensing devices and gives a background on conducting polymers and polyamic acid as a conducting polymer. It also gives a review on the methods that are used to detect antibiotic residues.*

### **1.1 Microfluidic devices**

Microfluidic is a field of science and technology that has to do with the way fluids move through micro-channels and the development of microminiaturized devices that contain parts such as chambers and tunnels which allow fluids to flow through or are confined. Microfluidic devices are also referred to as lab on a chip (LOC) is an instrument that uses a tiny amount of fluid on a microchip to do certain laboratory tests (Elveflow.com 2019). These devices integrate all functions of sample pre-treatment, reagent delivery, mixing, separation and detection that are usually are done in a laboratory in a miniaturized chip through the inside micro channels (Xu Y et al., 2016). The advantage of these devices are that they are portable, they do not require a large amount of sample for analysis, short processing time, reduced reagent consumption, real time analysis and automation (Zhang Z et al., 2013).

### **1.2 Microfluidic paper based electrochemical sensing devices**

The most important factors that needs to be taken into consideration when developing diagnostic devices for low resourced countries or under developed countries are low cost, simplicity and speed of results for early screening for diseases and environmental analysis. Microfluidic paper based analytical devices ( $\mu$ PADs) are devices that can be used to quantify and measure concentrations of various analytes at low levels. These devices are fabricated from patterned paper combined with electrodes that are printed on chromatography paper or polyester paper (Nie Z et al., 2010). Microfluidic paper electrochemical sensing devices ( $\mu$ PEDs) are electrochemical sensors that are made up of paper-based microfluidic channels patterned by methods such as photolithography, wax printing, laser printing, flexographic etc. and electrodes that can printed using conductive inks by various different methods like inkjet



printing, screen printing, pencil drawing etc. and are capable of quantifying the concentrations of various analytes (e.g., heavy-metal ions and glucose) in aqueous solutions (Nie Z et al., 2010).  $\mu$ PEDs have been widely used as an alternative point of care (POC) device due to the fact that they offer a combination of simplicity, low power requirements, low limit of detection and ease of quantification. The World Health Organisation (WHO) set a criteria 'ASSURED' to describe the characteristics a diagnostic device should have. The acronym ASSURED stands for affordable, sensitive, specific, user friendly, robust, equipment free and deliverable to those who need them (Mabey D. et al., 2004).  $\mu$ PEDs comply to this criteria as they use materials such as paper which is inexpensive and is found everywhere, they are portable and do not require big machines for manufacturing.

When fabricating these devices there are a number of factors to consider, such as paper design and fabrication method, detection method and the choice of the conductive ink to be used for the electrodes.

### 1.3 Paper Substrate

Paper is a well-known material that is found everywhere that can be used for writing, printing, drawing and packaging. In addition to its traditional uses paper has the potential to be used for other applications due to its physical properties (Liana D et al., 2012). It is a sophisticated material as it can be made thin, lightweight and flexible depending on its pulp processing. The main component of paper is cellulose fibre which makes it very attractive for certain applications because it allows liquid to infiltrate within its hydrophilic fibre matrix without the need of an active pump or external sources (Liana D et al., 2012). The fibrous and porous structure of paper provides; I) capillary action for the movement of the liquids, II) absorbency for storage of reagents in the paper, III) air permeability, IV) network structure, VI) high surface to volume ratio (Akyazi T et al., 2018). Different kinds of paper substrates possess different properties such as grades, sizes, flow rate, thickness and pore size. Therefore, depending on the target analytes, the requirement of the paper substrate will vary. The choice of paper material in an application is important in order to fully make use of the characteristics of the paper substrate of choice, to enhance the sensitivity of analysis and the choice is also important based on the fabrication steps required in the development of the

device (Lee V.B.C et al., 2018). The paper substrate that is commonly used to fabricate paper-based analytical devices is the Whatman grade 1 chromatographic filter paper due to its high alpha-cellulose content, smooth surface, structural uniformity and absence of additives, which guarantee its quality, reproducibility and uniformity (Lee V.B.C et al., 2018).

Electrodes can be patterned on the paper using various techniques. The two commonly used techniques are screen printing and inkjet printing (Xu, Y. et al., 2016). Commercial office paper is usually used as a flexible support for electrodes, other substrates such as glossy paper; paper towels; tissue paper and cardboard paper can be used also as support for electrodes when characteristics like wicking is not important in the application (Nery E.W et al., 2013). Screen printing is used frequently for fabrication of paper based electrochemical sensors. This technique makes use of ink, mesh pore stencil/screen and a squeegee. Screen printing technique offers an inexpensive way to print images by transferring the carbon ink or other printable materials onto paper substrate surface. It is with flexibility in design, ease of chemical modification, and ability to produce with minimal external technology (Xu, Y. et al., 2016).

#### **1.4 Screen printing technology:**

Screen printing technology is a technique that is well-known and it is used to develop economical, portable and disposable electrode systems (Hayat A et al., 2014). The whole electrode which includes the counter electrode, reference electrode and working electrode can be printed on the same substrate. Screen printing technology has a number of advantageous such as design flexibility, the ability for process automation and reproducibility (Couto R.A.S et al., 2016). Fabrication of screen printed electrodes consists of basic steps, such as: (i) selection of the screen or mesh that is used to define the geometry and size of the electrodes, (ii) selection and preparing inks to be used to fabricate the electrodes, (iii) choosing a substrate on which the electrodes will be printed on and that is applicable for your application, (iv) printing of electrodes and (v) drying and curing step (Couto R.A.S et al., 2016). The screen printing technique makes use of a mesh screen to support an ink blocking stencil and a roller or squeegee is used to spread the ink across the mesh screen and to force the ink through screen stencil past the threads of the mesh onto the paper substrate (Li M et al., 2012). A screen printed electrode is made up of a chemically inert substrate on which the

three electrodes can be printed on and the electrochemical reaction takes place on the working electrode while the reference and counter electrode are used to complete the electronic circuit (Hayat A et al., 2014).

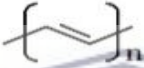




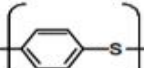
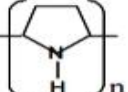
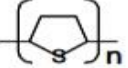
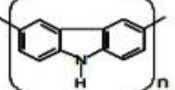
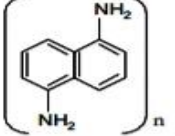
## 1.5 Carbon paste based electrodes

Carbon materials such as graphite, carbon nanotubes, and graphene have been widely used in the development of sensors because of their superior conductivity, high mechanical strength, high stability, high transparency and compatibility with organic semiconductors (Aleeva Y and Pignataro B., 2014). They are attractive for sensing applications due to the fact that carbon materials have high chemical inertness, they provide a wide range of anodic working potentials with low electrical resistivity, readily renewable surface and are relatively inexpensive (Morris A et al., 2007 and Couto R.A.S et al., 2016). Carbon ink that are available commercially and used to fabricate carbon working electrodes are usually made up of graphite particles, polymer binders and other proprietary additives for promotion of dispersion, printing as well as adhesion of the printed material (Wang J et al., 1998). There is a number of factors that can greatly affect the electrochemical performance of printed sensors such as the curing temperature as well as the difference in ink composition so choosing a ink to use to fabricate the electrodes is not an easy task as its exact composition may not be available as well as the fact some of the inks may require a high curing temperature which could affect the ink components negatively and may also affect the substrate that is used to print electrodes on (Wang J et al., 1998). Carbon ink is used as the substrate for further modification of sensing materials on the working electrodes because of the weak catalytic activity of the graphite and resin are rarely used for direct application of the carbon ink for sensing. The surface of screen printed electrodes can be improved by different methods. The commonly used process to modify the surface of screen printed electrodes consists of the alteration of the composition of printing inks by adding different substances such as metals, nanomaterials, enzymes and polymers (Couto R.A.S et al., 2016).

The semiconducting properties of conjugated polymers make them interesting materials for fabrication of electronic devices. Conjugated polymers can be used to improve the properties of sensors, this can be done by modifying or tailoring the polymer for example by modifying

the polymer backbone by attaching side chains on it for an improved solubility or electron affinity (Aleeva Y and Pignataro B., 2014). Conducting polymers (CP) are organic polymers that have an extended  $\pi$  orbital system in which electrons can move from one end of the polymer to the other end and have the ability to conduct electricity (Rahman M.D. et al., 2008). Organic polymers have been used to fabricate accurate, fast and inexpensive biosensors and chemical sensors (Rahman M.D. et al., 2008). The most commonly reported classes of CP are poly(acetylene)s, poly(pyrrole)s, poly(thiophene)s, poly(terthiophene)s, poly(aniline)s, poly(fluorine)s, poly(3-alkylthiophene)s, polytetrafulvalenes, polynaphthalenes, poly(p-phenylene sulfide), poly(para-phenylene vinylene)s etc.

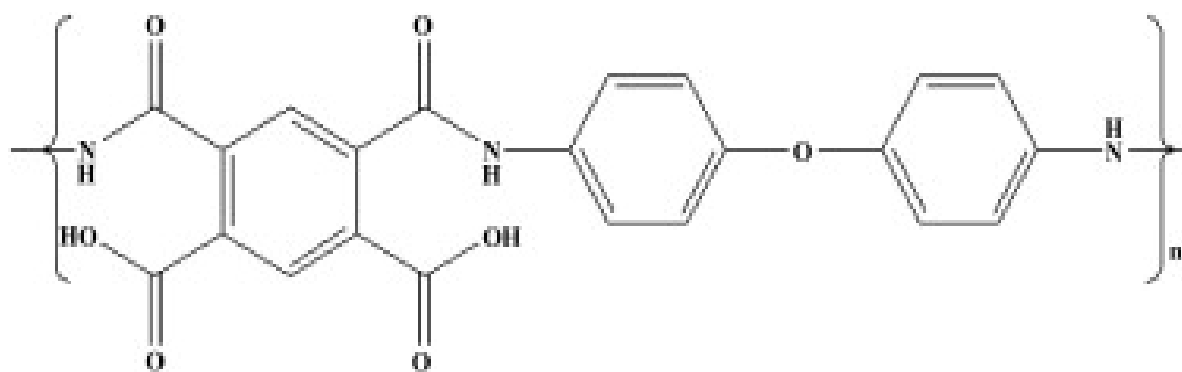
Table 1: Most commonly studied conjugated polymers (Rahman M.D. et al., 2008).

Conducting Polymer	Structure	Conductivity (S/cm)
Polyacetylene		$\sim 1000$
Polyparaphenylene		$100 \sim 500$
Polyparaphenylene vinylene		$\sim 3$
Polyazulene		$\sim 0.1$
Polyaniline		$1 \sim 100$
Polyparaphenylene sulfide		$1 \sim 100$
Polypyrrole		$40 \sim 100$
Polythiophene		$10 \sim 100$
Polycarbazole		$10 \sim 100$
Polydiaminonaphthalene		$10^{-3}$

Using conductive polymers in the fabrication of electrochemical sensors provides a number of advantages such as improvement of sensitivity and selectivity of electrochemical sensors because of their electrical conductivity and they can be easily deposited onto electrodes (Rahman M.D. et al., 2008). When formulating polymer based inks parameters such as molecular weight, concentration and solvent used should be taken into account (Aleeva Y and Pignataro B., 2014)

## 1.6 Polyamic Acid

Polyamic acid (PAA), Figure 1 are part of class of polymers that are formed through a polycondensation reaction between a dianhydride and a diamine (Padavan D.T. et al., 2010). Polyamic acid (PAA) is a semiconductive polymer that is soluble in a number of dipolar aprotic solvents and can be easily processed. PAA can be readily synthesized in the lab and it produces a good yield. It is a precursor of polyamide and it has amide and carboxylic groups in its polymer back bone (Noah N.M. et al., 2012). Aromatic polyimides polymers have a number of outstanding properties like flexibility, low color, high glass transition, temperature, good thermal stability and radiation resistance and they have been applied in a number of things like electronics, fuel cells, membrane separation industries etc (Hua, M.Y. et al., 2011). Due to the presence of the amide and carboxylic groups on the backbone of PAA it has many interesting material applications. PAA has been used in a number of sensor applications (Noah N.M. et al., 2012). In this work we will develop a conductive polyamic acid ink that will be used to fabricate the working electrode in the design of paper based electrochemical sensing device for low environmental analysis.



**Polyamic acid (PAA)**

Figure 1: Chemical structure of PAA and polyamide (Noah N.M. et al., 2012).

## 1.7 Cobalt Nanoparticles

Nanomaterials have unique chemical and physical properties which make them good materials for fabricating and improving sensing devices such as electrochemical and biosensors. Metal nanoparticles are usually used in sensors due to their excellent conductivity and catalytic properties which make them suitable for enhancement of electron transfer and as catalyst to increase electrochemical reactions (Luo X et al., 2006). Merging electrochemical sensors with nanostructured materials have been largely used as a powerful method due to the benefits that are offered by electrochemical sensors as well as the exceptional physiochemical properties of nanomaterials of high surface to volume ratio, high adsorption and reactive capacity and other beneficial properties (Maduraiveeran, G. and Jin, W., 2017). Nanoparticles can be used in electrochemical sensors for immobilization of biomolecules, catalysis of electrochemical reactions and to enhance electron transfer (Luo X et al., 2006). Nanoparticles have become attractive because of their low cost and unique size properties. Modifying electrodes with nanoparticles for electroanalysis offers a number of advantages such as effective catalysis, fast mass transport, large effective sensor area and good control over electrode micro movement (Rassaei, L. et al., 2011). Cobalt nanoparticles (Co NP) have excellent magnetic, electrical and catalytic properties that makes them an interesting material for sensing devices (Ansari et al., 2017).

## 1.8 Antibiotic residues in aqueous systems

There has been a lot of research conducted on the screening of antibiotic residues in aqueous systems. This research has been conducted due to the increase in antibiotic residues in aqueous systems because of the wide use of antibiotics that has raised concern about potential human health effects. One of most common sources of antibiotics in surface and groundwater is the discharge of pharmaceutical waste that comes from the production of antibiotics. Waste water treatment plants (WTP) do not completely remove antibiotics and consequently they can get released into natural waters. Due to the high water solubility that antibiotics have as well as their poor degradation, antibiotics can pass through all the natural filtrations and reach drinking water (Heidari M. et al 2013). Microbes that are harmless that

pass through water treatment systems can also allow dangerous resistant bacteria as well as multiple resistances to antibiotics to reproduce in drinking water supplies (El-Zanfaly, H. T 2015). It is a difficult to examine antibiotics in the environment due to the high complexity of matrices analysed and low concentration ( $\text{ngL}^{-1}$ ) of which the target antibiotics are present in the water (Seifrtová, M. et al., 2009). Due to the different antibiotics from different classes that have been found in the aquatic environment, currently multi-residual analytical methods are preferred for the monitoring of different groups of antibiotics, methods that are sensitive; selective; not time consuming and easily applicable to environmental samples (Seifrtová, M. et al., 2009) .

He K and Banley L., (2015) conducted a study to determine fluoroquinolones in waste water and environmental samples by using selective and ultra-sensitive analytical methods, methods which include solid phase extraction and reversed phase high performance liquid chromatography with fluorescence detection. In their study solid-phase extraction method was employed due to the low concentrations of fluoroquinolones in water and waste water sources which require suitable pre-treatment before analysis. High performance liquid chromatography coupled with fluorescence was used because it has shown to be quite sensitive for determination of fluoroquinolones. The fluoroquinolones were analysed using a high performance liquid chromatography which was equipped with a four channel ultraviolet visible detector and fluorescence detector.

Hernandez et al. (2007) conducted a study based on liquid chromatography-mass spectrometry or liquid chromatography-tandem mass spectrometry for the determination of antibiotic residues in environmental water. The authors mainly concentrated on different approaches for screening, quantification and confirmation of these compounds while paying attention to the difficulties of confirming analytes at low concentrations

Xue Q., et al. (2015) carried out a study to develop an optimized solid-phase extraction and ultra-high performance liquid chromatography coupled with electrospray tandem mass spectrometry method for the analysis of 35 antibiotics. The advantage of this method is that it has short detection times, small sample consumption, excellent reproducibility and high sensitivity. The authors selected sulphonamides, quinolones, tetracyclines and macrolides as their target antibiotics due to their widespread usage and high detection rates. In order to understand the impact of sensitivity and separation efficiency of the 35 antibiotics 3 different

mobile phases was used. The 35 antibiotics were then simultaneously detected in 10 minutes. The author concluded that this method showed high recoveries with a superior detection limit.

A study by (Matongo S, et al., 2015) that was motivated by the little data present about pharmaceutical residues in African water bodies was carried out to study the occurrence of pharmaceutical residues in the water and sediment of Msunduzi River in KwaZulu-Natal province of South Africa and in the Darvill wastewater treatment plant found in Msunduzi catchment. In this study samples were collected along the river and analysed using high performance liquid chromatography and liquid chromatography. In all the samples that were collected and investigated antipyretic ibuprofen had the highest concentration up to 117  $\mu\text{gL}^{-1}$ , 84  $\mu\text{gL}^{-1}$  and 659  $\text{ngg}^{-1}$  in wastewater, surface water and sediment respectively. The detected concentration of antipyretic residues along the Msunduzi River was in agreement with the consumption data of the Republic of South Africa that indicates that Msunduzi contributes to pharmaceutical loading of Umgeni River which joins and therefore may result in deleterious effects to the aquatic life these water bodies.

Methods such as liquid chromatography coupled with mass spectrometry or liquid chromatography coupled with tandem mass spectrometry, ultraviolet, gas chromatography and solid-phase extraction that are used to detect antibiotic residues in water suffer from a number of disadvantages that make constant quality monitoring difficult (Seifrtova M. et al 2009). Chromatographic methods are usually used due to the automation, accurate quantification, simultaneous detection, high specificity based on the structural information of the analytes and are suitable for monitoring analytes with low concentration (Muntteanu, F.D. et al., 2018). However, the disadvantage of these methods that have been used in the work done for detecting antibiotic residues suffer from a number of disadvantages such as being time consuming when a large amount of samples need to be screened, require expensive equipment, require complex preparation steps and often require personal expertise and skills.



## 1.9 Problem statement

The spreading and occurrence of antibiotic resistant-bacteria has become a serious public health problem worldwide and aquatic ecosystems are a recognised reservoir for antibiotic resistant-bacteria and antibiotic resistance genes. Resistant organisms in nature may result from natural production of antibiotics by soil organisms; presence of antibiotics in pharmaceutical industries; runoff from animal feed or crops, or treated waste products from animal or human (El-Zanfaly, H. T. 2015). Antibiotics enter the aquatic environment in different path ways, the antibiotics are excreted as metabolites after administration to humans. Some of the antibiotics are eliminated in an unchanged form as the parent compound via urine and faeces into the sewage (Seifrtová, M. et al., 2009). One of the major contributors of pharmaceuticals in the environment is waste water plants due to the incomplete removal of pharmaceuticals during wastewater treatment process (Seifrtová, M. et al., 2009).

It has been reported that the presence of antibiotics in the environment may have the potential to harm the ecosystem as well as human health and they have been identified as emerging organic contaminants in aquatic environments that have become a worldwide concern. (Xue, Q. et al., 2015). It is important to always keep track of contaminants that are present in source water and the aquatic systems which come from treatment plants, industrial waste and runoff from urban and agricultural lands, by doing that ways can be found to identify the antibiotics that are present in the aquatic systems and to remove them.

Given the increase of antibiotic resistant bacteria in aqueous systems, further development of bacteria resistance has to be stopped, by reducing the contamination of antibiotics in aqueous systems. Therefore it is important to develop devices that are sensitive, environmental friendly, robust, inexpensive, portable and fast as well as devices that are able to detect these contaminants even at very low concentrations. By detecting these contaminants that are present in the environmental waters further contamination can be prevented.

## 1.10 Aims and Objectives

**Overall Aim:** To develop a low cost, environmental friendly, sensitive and highly selective polyamic acid ink based paper based electrochemical sensor for detection of antibiotic residues in water.

**Aim 1:** To synthesis polyamic acid, cobalt nanoparticles and to formulate the screen printable ink

Objective 1: Synthesis of polyamic acid by in situ polymerization and cobalt nanoparticles by a chemical reduction method.

Objective 2: To characterize polyamic acid and cobalt nanoparticles by microscopic, spectroscopic and electrochemical techniques.

Objective 3: To prepare the carbon black and polyamic acid-carbon based screen printable ink by the bulk method.

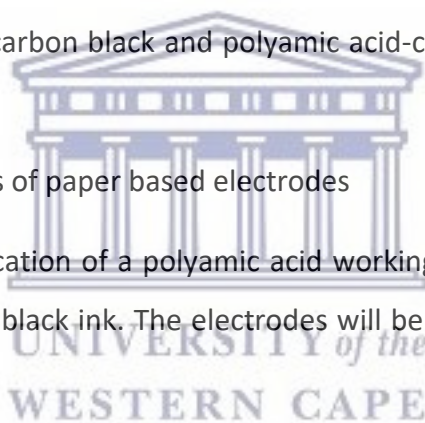
**Aim 2:** Design and fabrications of paper based electrodes

Objective 1: Design and fabrication of a polyamic acid working electrode using commercial ink and polyamic acid-carbon black ink. The electrodes will be fabricated by screen printing technology.

Objective 2: To study the electrochemical behaviour of the printed paper based electrodes.

**Aim 3:** Application of the paper based electrodes to the detection of Norfloxacin

Objective 1: Electrochemical evaluation of carbon ink and PAA ink electrodes in paper printed Microfluidic analytical paper based devices ( $\mu$ PADs). Electrochemical detection of Norfloxacin using paper based electrode.



## 1.11 Conceptual diagram

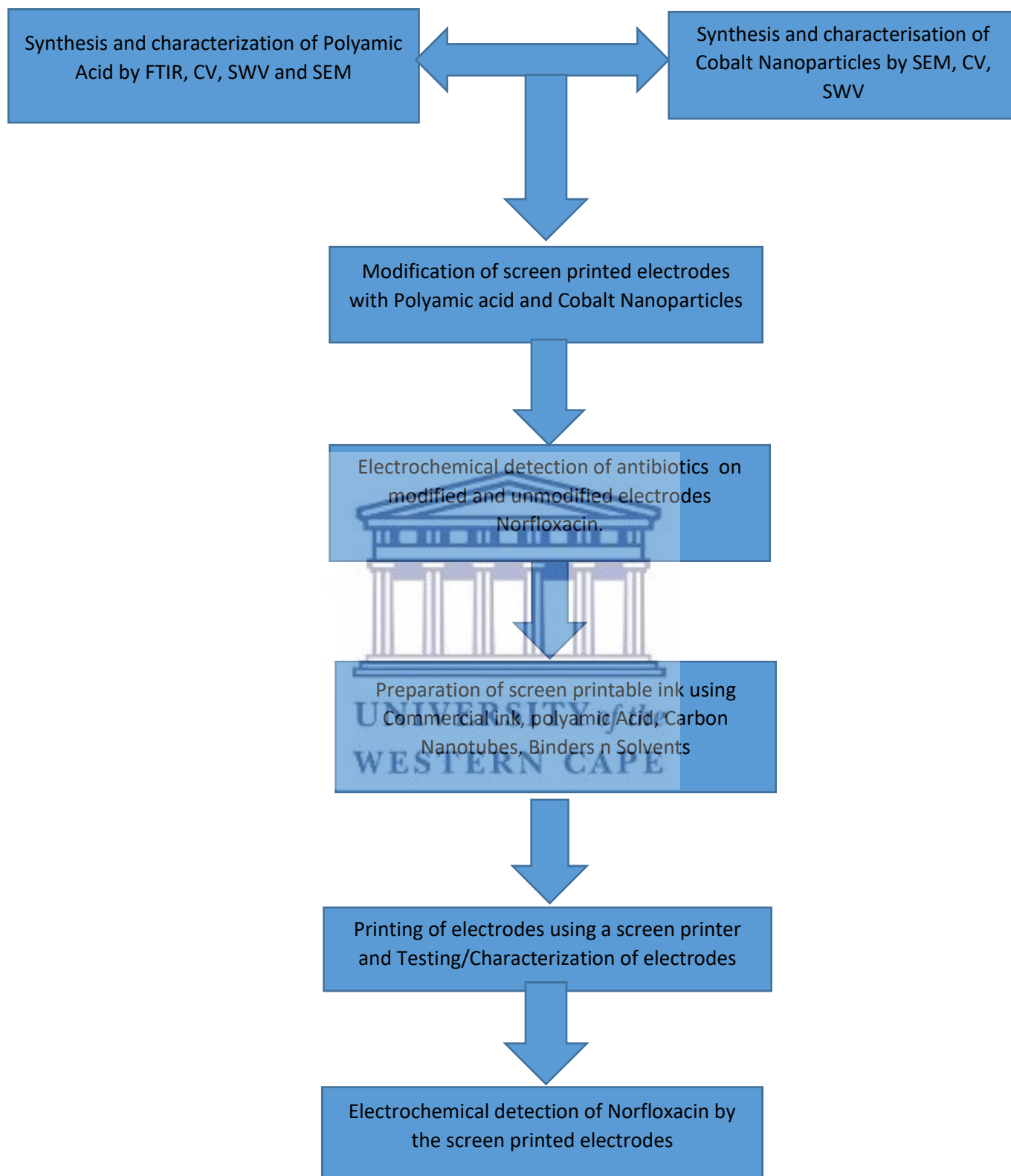


Figure 2: Conceptual diagram of the thesis

## 1.12 Thesis outline

### Chapter 1:

This chapter gives an introduction to microfluidic devices, microfluidic paper based electrochemical sensing devices and gives a background on conducting polymers and polyamic acid as a conducting polymer. It also gives a literature review on the commonly used methods for antibiotic residues detection.

### Chapter 2:

This chapter provides a literature review on electrochemical sensors, paper based electrochemical sensors as well as polymer modified paper based sensors. It also presents work done to detect antibiotics using electrochemical sensors and paper based electrochemical sensors.

### Chapter 3:

This chapter presents information on the principles of the techniques which were used in this work as well as the name of the instruments.

### Chapter 4:

This chapter presents the materials used in the synthesis of polyamic acid and cobalt nanoparticles as well as the ink formulation and the synthesis methods. It also provides microscopic, spectroscopic and electrochemical characterization of cobalt nanoparticles and polyamic acid.

### Chapter 5:

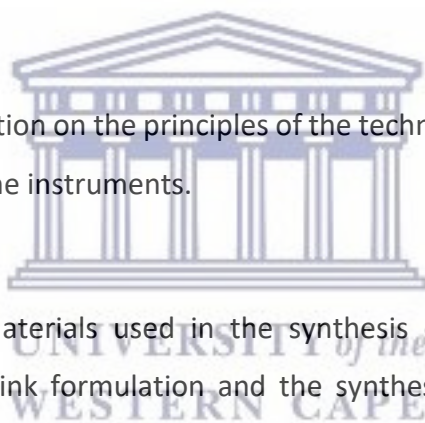
This chapter gives results of the UV-Vis characterization of Norfloxacin and electrochemical detection of Norfloxacin.

### Chapter 6:

This chapter presents characterization of the fabricated paper electrodes. The characterization includes microscopic studies and electrochemical studies.

### Chapter 7:

This chapter gives a summary of the work done and of the results obtained as well as the future works and references.



# Chapter 2

## *Literature review*

*This chapter provides a literature review on electrochemical sensors, paper based electrochemical sensors, polymer based paper electrodes as well as electrochemical detection of Norflaxacin.*

### **2.1 Electrochemical sensors**

An electrochemical sensor is an analytical device that provides information about the composition of a system in real time by coupling a chemically selective layer to an electrochemical transducer and it converts the recognition event to a measurable electrical signal for the purpose of detecting a target compound (analyte) in solution (Antuna J, et al., 2012 and Badihi-Mossberg, M et al., 2007). Electrochemical sensors have been widely used in the fields of industry, medicine and agriculture due to their sensitive, cost effective and rapid form of molecular detection (Jacobs, M et al., 2007). Pilehvah S. et al, 2012 developed an electrochemical sensors for simultaneous detection of phenicol antibiotics at a gold electrode. The electrochemical behaviour of the antibiotics was investigated by cyclic voltammetry and square wave voltammetry in tris buffer solution. A limit of detection of  $1 \times 10^{-6}$  M was found. Zacco E et al, 2007 conducted a study on electrochemical magneto immunosensing of antibiotic residues in milk. They presented an electrochemical immunosensing strategy based on magnetic beads for the detection of sulphonamide antibiotics. The strategy combines advantages taken from immunochemical assays, magnetic beads separation and electrochemical transduction. The authors used spiked milk samples to evaluate the performance of the electrochemical immunosensing strategy based on magnetic beads. They concluded that magnetic beads provide an easy way of completely removing the matrix effect and to improve the non-specific adsorption and also the use of magnetic beads provides improved features regarding sensitivity and selectivity of the assay.

### 2.1.1 Paper based electrochemical sensors

Lab on a chip or microfluidic paper analytical devices are devices that are capable of performing laboratory operations on a microscale with integrated miniaturized equipment. Dungchai W. et al., 2009 introduced the integration of electrochemical detection in microfluidic paper based analytical devices. In their work they screen printed electrodes on a paper substrate using screen printing technology and characterized by cyclic voltammetry to show basic electrochemical performance of the system. Photolithography technique was used to create the barriers according to previous methods recorded. The areas covered with photoresist stayed hydrophobic and the areas without photoresist were hydrophilic. Different inks were used to screen print the electrodes, carbon ink that contained Prussian blue was as the working electrode and counter electrode and silver/silver chloride ink as the reference electrode and conductive pads. To decrease the effect of uncompensated resistance between the working electrode and reference electrode, the working electrode was designed to be as close as possible to the reference electrode. Characterization was carried out by dropping 5 micro litres of 0.1 M potassium phosphate buffer solution on the end of the paper at the detection zone and the solution flowed directly through electrode zone and cyclic voltammetry was performed. This study demonstrated coupling of electrochemical detection and paper microfluidic to provide rapid quantitative measurements of critical health markers in serum.

Screen printed electrodes (SPE) have the advantages of allowing sensitive and selective analysis at low cost, easily disposable, they do not require a lot of sample for analysis, mass production of electrodes that do not require big equipment's; easily modification of the surface of the electrodes in the same way as traditional electrodes to increase sensitivity, and they can be easily integrated into microfluidic analytical devices (Muntteanu, F.D. et al., 2018). Screen printing technology is a great technology tool that can be used to move away the traditional laboratory methods to point of use (Yamanaka K., 2016).

### 2.1.2 Detection of analytes in paper electrochemical sensors

For detection of analytes in paper based microfluidic four detection methods have been reported so far, colorimetric detection, electrochemical detection, chemiluminescence detection and electrochemiluminescence detection (Li, X. et al., 2012). Colorimetric detection concentrate mainly on enzymatic or chemical color change reactions, the results in most cases can be assessed visually which is good for a when a semi quantitative detection is sufficient for diagnosis (Li, X. et al., 2012). The disadvantage of this method is the low sensitivity and variability in environmental illumination (Mettakoonpitak, J. et al., 2016).

Chemiluminescent and electro-chemiluminescent detection methods are mostly used for optical detection methods in microfluidic (Li, X. et al., 2012). These methods have become attractive because of their simplicity, low cost and high sensitivity (Li, X. et al., 2012). The combination of chemiluminescent with electrochemical methods has result in an analysis technique that is known as electrochemiluminescent and the advantage of combining the two techniques is that they provide better sensitivity and increases the dynamic concentration range (Xia Y., et al 2016; Muntteanu, F.D. et al., 2018).

Electrochemical detection in paper based sensors is an attractive detection method because of its inexpensive, portable, high sensitivity, high selectivity, less instrumentation and enables the quantification of analytes in nano-meter range and compared to methods like colorimetric and fluorescent it is the most preferred method due to rapid response, higher sensitivity and for achieving better quantitative results (Xu, Y. et al., 2016 and Lin, Y. et al., 2012). Due to the features that electrochemistry analytical techniques provide its integration with paper based devices is likely to be advantageous. Combining microfluidic paper based analytical devices with electrochemical sensing provides advantages such as: i) electrodes can be miniaturized and easily fabricated on paper using a number of fabrication methods, ii) electrochemistry does not require equipment that are difficult to understand or operate, iii) potentiostats are readily available for on-site measurements, iv) a number of different electrochemical methods are known (Mettakoonpitak, J. et al., 2016).

Smith S et al., 2017 presented a method for monitoring the quality of water by using a paper based electrochemical sensor. The paper based electrochemical sensor were fabricated using inkjet printing and screen printing technology by using carbon inks and silver inks. The three electrode set up was made up of a working electrode, counter and reference electrode. Photo paper was used as the substrate for the electrochemical sensor. The first layer was inkjet-printed using silver ink and the second layer was screen printed using carbon ink. The reference electrode was printed using silver ink and the working and counter electrode were printed using carbon ink. The working electrode was further modified by drop coating 20  $\mu\text{L}$  of bismuth onion like nanoparticle ink onto it. A detection limit of 0.3 ppm was obtained for  $\text{Pb}^{2+}$ .

The conductivity and sensitivity of the electrodes is determined by the kind of material that is used to fabricate the electrode. Depending on the type of analysis and the sample to be analysed, the required materials used to make the reference, counter and working electrodes for paper based electrochemical sensors may differ from each other (Lee, V.B.C. et al., 2018). Electrodes are usually made by using conductive paste like graphene, silver, carbon, platinum, silver/silver chloride and heavy metals (Lee, V.B.C. et al., 2018). Carbon conductive ink/paste is commonly used in the fabrication of the working electrode and counter electrode because it is easy renewal, can be easy modified and reproducibility (Zhang, X. et al., 2011). The conductive ink is usually made up of an active material, binder and solvent and the electrochemical and electroanalytical properties of the electrodes are affected on not only the binder but also the carbon material (Zhang, X. et al., 2011). The electroanalytical performance of the paper based electrochemical device can be improved by altering the conductive ink/paste during or after manufacturing with nanomaterials, conductive polymers or carbonaceous nanomaterials (Cinti, S. et al., 2017).

Lamas-Ardisana P.J et al, 2017, carried out a study that presented a novel method to fabricate an electrochemical paper-based cells by screen printing technology. In this work ultraviolet curable ink were used to create the hydrophobic barriers on chromatography paper and the three electrode system was printed using carbon ink and silver/silver chloride ink over the hydrophilic areas. The printed electrochemical cell was further characterised by cyclic voltammetry in different redox systems and ferricyanide was detected using amperometric. The results showed that the signals for the different redox systems were highly repeatable and



they found that the peak-peak values they obtained were similar to the ones previously reported for conventional screen printed electrodes.

Wang P et al, 2017, developed an inexpensive and disposable paper based electrochemical device for detection of nitrile based on a simple and efficient vacuum filtration system coupled with an in situ electrodeposition technique. The paper based electrodes were functionalized with graphene nanosheets and decorated with gold nanoparticles. The electrochemical platform developed in their work exhibited a high sensitivity and improved electron transfer compared to the commercial gold electrode and glassy carbon electrode.

Nie Z et al., 2010, developed a microfluidic paper based electrochemical sensing device and demonstrated that the device is capable of quantifying the concentrations of various analytes in aqueous solution. They demonstrated the detection of glucose in artificial urine using a chronoamperometric analysis based on glucose oxidase. The group used paper as a substrate for the electrochemical detection and used conductive carbon ink and silver/silver chloride to fabricate the electrodes. Detection of glucose using the device showed high sensitivity and accuracy over the full range of clinically relevant concentrations of glucose in urine. They also showed the use of microfluidic paper based electrochemical sensing devices to detect Pb (II) in aqueous solution which contained a mixture of Pb (II) and Zn (II). The Pb measurement of Pb (II) showed a limit of detection of 1.0 ppb.

## **2.2 Polymer paper based modified electrodes**

The composition of carbon ink can be also altered using different substances such as polymers, nanoparticles, metal, enzymes, complex agents etc. The standard electrodes usually have poor detection sensitivity and selectivity hence modifying the working electrodes with more functional materials can be performed to improve the sensing performance of the electrode (Kit-Anan, W. et al., 2012). Materials such as conjugated polymers can be used to enhance the performance of the electrodes. A number of applications have been reported since the discovery of conducting polymers. Conductive polymers can be used in a number of applications such as electrochemical devices, memory devices, energy storage, chemical sensors and biosensors due to their unique properties (Rahman, M.D. et al., 2018). One of the advantages of sensors fabricated from conductive polymers is that polymers have the potential to exhibit improved response properties and are sensitive to small perturbations

and they improve the sensitivity of the sensors due to their electrical conductivity or charge transport properties (Rahman, M.D. et al., 2018).

Kit-Anan W, et al., 2012, developed a paper based electrochemical sensor utilizing inkjet printed Polyaniline modified screen printed electrode for detection of ascorbic detection. In this work they fabricated the base electrode using screen printing technology and to modify the electrode ink jet printing technology was used. The device consisted of three electrodes, Polyaniline modified carbon working electrode and two bare reference and counter electrodes. The three electrodes were initially screen printed on paper and after the working electrode was modified with Polyaniline using an inkjet printer. The cyclic voltammetry experiments of the Polyaniline modified electrode showed a ten times larger current peak over the bare carbon graphite paste electrode. The results of their work showed a moderately good Ascorbic Acid detection performance with a low concentration range, low limit of detection and good sensitivity compared to other devices in the past works.

Ruecha N et al., 2015, developed an electrochemical sensor using a graphene-polyaniline nanocomposite for simultaneous detection of Zn (II), Cd (II) and Pb (II). The electrode was developed by reverse phase polymerization in the presence of polyvinylpyrrolidone. In this work they used plastic film and filter paper as substrate materials and deposited the nanocomposite by drop casting and electro spraying. The modified electrochemical sensors were fabricated by first printing the hydrophobic barriers by printing solid wax with a commercial printer and melting the wax at 200°C. The three electrodes were then screen printed using a mixture of carbon ink and graphite powder and was dried left to dry for 30 minutes in an oven to remove the remaining solvents. The working electrodes were modified by drop casting and electro spraying the electrode. The electrodes were characterised and the results showed that the G-PANI modified electrodes exhibited high electrochemical conductivity and also showed an increase in the surface area of the electrode.

Electrochemical sensors fabricated using conducting polymers play an important role in the improvement of public health and environment because of the rapid detection, high sensitivity, small size and because of those properties conducting polymer electrochemical sensors can be used for environmental monitoring and clinical diagnostics.

### 2.3 Electrochemical sensor for detection of Norfloxacin

Norfloxacin (1-ethyl-6-fluoro-4-oxo-7-piperazin-1-yl-1H-quinoline-3-carboxylic acid), figure 3 is a chemotherapeutic antibiotic agent which is used to treat common as well as complicated urinary tract infection and respiratory infection (Huang, K.J. et al., 2008). It belongs to a class of antibiotics called fluoroquinolones. Fluoroquinolones are usually used to treat a number of illnesses such as respiratory and urinary tract infections. It has been reported that this antibiotic has been detected in various sources such as surface water, sea water, groundwater, ground water and drinking water. The presence of Norfloxacin in aqueous systems might lead to harmful environmental effects and development of antibiotic resistance to aquatic, direct toxicity to microorganism and can possibly lead to health risk to humans through drinking water (Chen, M. et al., 2012). Methods to detect these antibiotics in aqueous system are needed, methods that are inexpensive, sensitive, not time consuming, simple like electrochemical sensors.

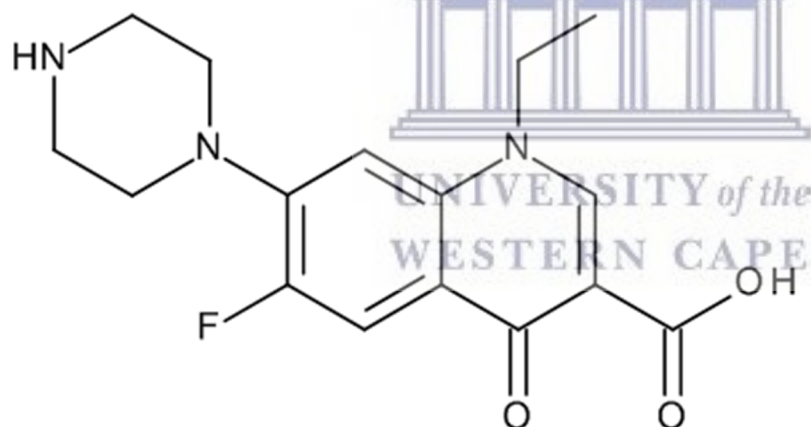


Figure 3: Chemical structure of Norfloxacin.

A study was carried by (Goyal R.N et al., 2012) to determine Norfloxacin in human urine and pharmaceuticals. An electrochemical sensor was developed using edge plane pyrolytic graphite as the sensor material to obtain a low detection limit, high sensitivity and decreased over potentials coupled with increased current values for Norfloxacin using square wave voltammetry. Square wave voltammetry was used because it is a technique that is fast and sensitive. The developed method was selective and Norfloxacin was detected without any interference from common urine metabolites. They obtained detection limit of

$28.3 \times 10^{-8}$  M. According to the authors the results obtained suggested that Norfloxacin can be detected at edge plane pyrolytic graphite using square wave voltammetry.

da Silva H. et al., 2015, developed a molecularly imprinted sensor as an electrochemical sensor for the detection of Norfloxacin. Glassy carbon electrode was modified by depositing multiwalled carbon nanotubes on the surface of the electrode and a molecular imprinted film was prepared by electropolymerization of pyrrole in the presence of Norfloxacin as the template molecule using cyclic voltammetry to achieve selectivity. The multiwalled nanotubes was used to improve sensitivity of analysis by an increase in electrochemical conductivity and the surface area. Selectivity was achieved in their study because the sensor was able to recognise the Norfloxacin. The sensor had a good reproducibility, repeatability and stability. They obtained a limit of detection of  $4.8 \times 10^{-8}$  M and limit of quantification was  $1.0 \times 10^{-7}$  M.

Hamnca S et al., 2017 presented a novel electrode modified with polyamic acid and graphene oxide for electrochemical screening of Norfloxacin and neomycin in aqueous solutions. In this work a screen printed electrode was modified with synthesized polyamic acid and graphene oxide by in situ electrochemical deposition using 5 cycles at a scan rate of 50 mV/s. The modified electrode was further characterized by Raman and AFM. The modified electrode gave a limit of detection of  $0.034 \mu\text{M}$  for Norfloxacin and  $1.07 \mu\text{M}$  for neomycin. The graphene oxide-polyamic acid sensors showed a reproducible and easy to fabricate alternative to measure neomycin and Norfloxacin compared other methods used.

Access to clean and quality water is a major challenge hence it imperative to fabricate devices that are affordable, sensitive, specific, user friendly, robust, equipment free and deliverable. Microfluidic devices integrated with screen printed electrodes offers a number of advantages such as being light weight, portable, flexible/foldable, low cost, high sensitivity, high selectivity and does not require complicated instruments, ability to measure small volumes of samples . Unlike the traditional methods used to detect antibiotic residues in aquatic systems, paper based electrochemical sensors offer an analytical tool that are capable of efficiently monitoring and analysing pharmaceutical pollutants in water.

# Chapter 3

## *Characterisation techniques*

*This chapter presents the techniques and instruments used for characterization and procedures of the polyamic acid synthesis, solvents and analytes preparations.*

### 3.1 Electrochemical Techniques

#### 3.1.1 Cyclic Voltammetry

CV experiments were performed using PalmSens PTrace 4.4 electrochemical work station using a three electrode cell. Cyclic voltammetry is a technique that is used to obtain qualitative information about electrochemical reactions and it can rapidly provide considerable information about the thermodynamics of redox processes and the kinetics of heterogeneous electron transfer reactions and on coupled chemical reactions or adsorption processes (Wang J., 2002). In CV the potential of a stationary working electrode's is scanned linearly using a triangular waveform. The current that results from the applied potential is measured by the potentiostat Figure 4, during a potential sweep. The resulting current-potential plot is known as the cyclic voltammogram Figure 5 (Wang J., 2002). The electrochemical parameters on the cyclic voltammogram can be used for characterization. These parameters consists of two peak currents ( $I_{pa}$  and  $I_{pc}$ ) and two peak potentials ( $E_{pa}$  and  $E_{pc}$ ). The peak currents is used to calculate the diffusion coefficient which is the rate at which the electrons move to and into the interfacial region of the transducer.



Figure 4: PalmSens Potentiostat.

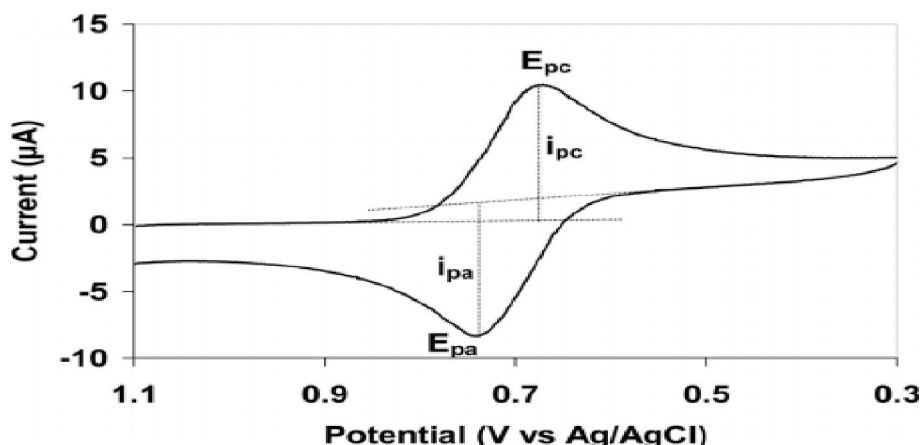


Figure 5: Example of a reversible cyclic voltammogram.

Experimental setup: An electrochemical setup for voltammetric studies is usually made up a potentiostat and three electrodes, Figure 6. A potentiostat is an electronic instrument that is used to control the voltage difference between the working electrode and the reference electrode. The set up includes three electrodes reference electrode, working electrode and counter electrode. At the working electrode the potential is controlled, the current is measured and the chemical reaction takes place at the surface of the working electrode (Bard JA., 2012). Examples of working electrodes are, glassy carbon electrode, gold electrode, platinum electrode etc. The working electrode potential is measured at the reference electrode. The counter electrode carries the current flow through the electrochemical cell and it passes the same current as the working electrode (Bard JA., 2012).

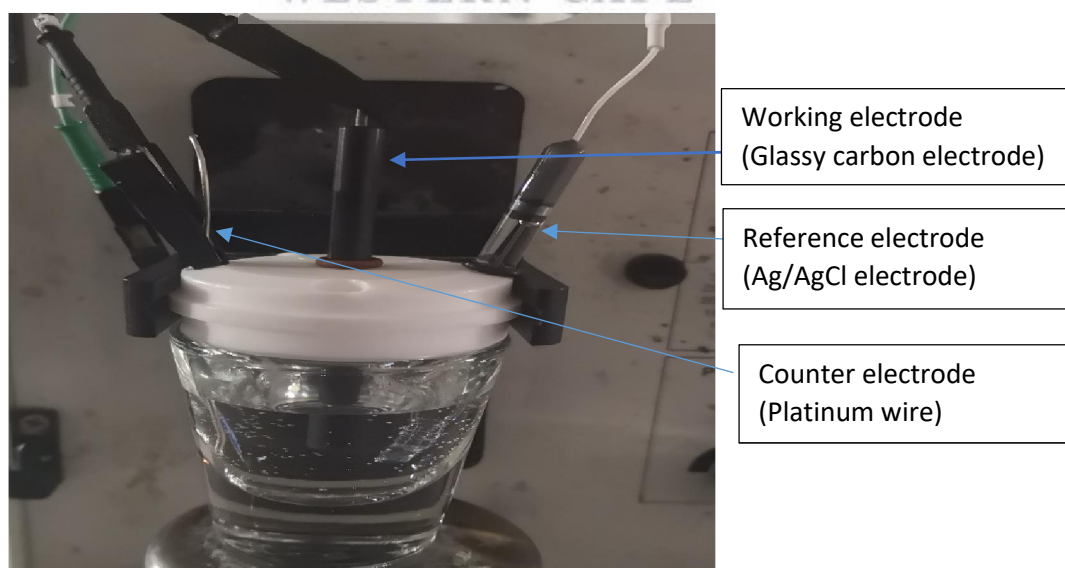


Figure 6: Example of a three electrode system.

In this work cyclic voltammetry was used to understand the redox reactions of PAA (polyamic acid) and Co NP (cobalt nanoparticles) as well as too to provide information about the electrochemical behaviour of PAA and Co NP.

### **3.1.2 Square wave voltammetry (SWV):**

Square wave voltammetry is an electrochemical technique where the cell current is measured as a function of time and as the function of the potential between the working electrode and reference electrode. It is used for quantitative chemical analysis and to study the mechanisms, kinetics and thermodynamics of chemical reactions (Gamry.com, 2019). In a square wave voltammetry experiment the current at a working electrode is measured while the potential among the working electrode and reference electrode is swept linearly in time. SWV experiments were carried out using PalmSens PTrace 4.4 electrochemical work station using a three electrode cell. The advantage of using SWV it is more sensitivity compared to CV, it requires less time per sweep and the square wave frequency can be used to differentiate between processes with fast or slow kinetics (Gamry.com, 2019). SWV can be used also to confirm the peaks observed in CV as it is more sensitive compared to CV.

In this study SWV was used to for the electrochemical detection of Norfloxacin.

## **3.2 Spectroscopic Techniques**

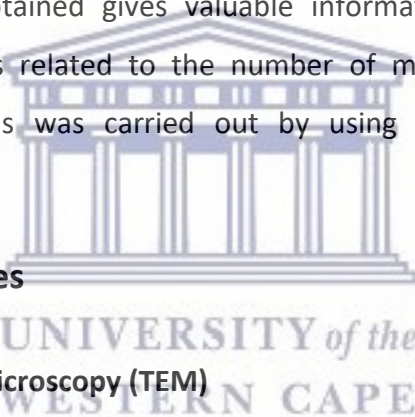
### **3.2.1 Fourier transform infrared spectroscopy (FTIR):**

Fourier transform infrared spectroscopy is an analytical technique that can be used to identify organic and polymeric materials (Materials evaluation and engineering. 2001). It is a useful way to identify functional groups that are present in your material. It uses an infrared light to scan test samples and to observe their properties. When the infrared light passes through the sample, some of the radiation is absorbed by the sample and the other is transmitted and the resulting signal at the detector is a spectrum which represents the molecular finger print of the sample. In FTIR analysis, the spectrometer uses an interferometer to regulate the wavelength from a broadband infrared source. The intensity of the transmitted light or reflected light is measured at the detector as function of its wavelength (Materials evaluation and engineering. 2001). The FTIR spectra is presented as the intensity vs the wave number. FTIR characterization was carried out using a PerkinElmer Spectrum 100, FT.

FTIR was used to study the chemical structure of the chemically synthesized PAA and Co NP and the functional groups. PAA and Co NP were recorded as powder and the pellet was formed using KBr.

### **3.2.2 Ultraviolet-Visible (UV-Vis)**

Ultraviolet-Visible Spectroscopy is a technique used for detection of functional groups, detection of impurities, qualitative and quantitative analysis. It is used to determine the analytes concentration. In this technique the adsorption of light is measured across the ultraviolet and visible light wavelengths through a liquid sample. UV spectroscopy obeys Beers Law which states that the quantity of light absorbed by a substance dissolved in a fully transmitting solvent is directly proportional to the concentration of the substance and path length of the light through the solution. The instrument used in UV-Vis works by passing a beam of light through a sample and measuring the wavelength of the light reaching the detector. The wavelength obtained gives valuable information regarding the chemical structure and the intensity is related to the number of molecules, means quantity or concentration. UV-Vis analysis was carried out by using the NICOLET evolution 100 instrument.



## **3.3 Microscopic Techniques**

### **3.3.1 Transmission electron microscopy (TEM)**

Transmission electron microscopy is a microscopy technique that is used to study the morphology, particle size, defects, elemental composition and crystalline structure of a sample (Tang CY., 2017). This microscopy technique uses a beam of electrons that is transmitted through an ultrathin specimen and interacts with the specimen as it passes through. A high resolution black and white image is then formed due to the interaction of the electrons transmitted through the sample. The image is then magnified and focused onto an imaging device, such as a fluorescent screen, on a layer of photographic film, or to be detected by a sensor such as a CCD camera. TEM has advantages such as that it magnifies samples to a much higher degree than an optical microscope, magnification of 10000 times or more is possible which makes it possible for scientists to analyse extremely small structures.



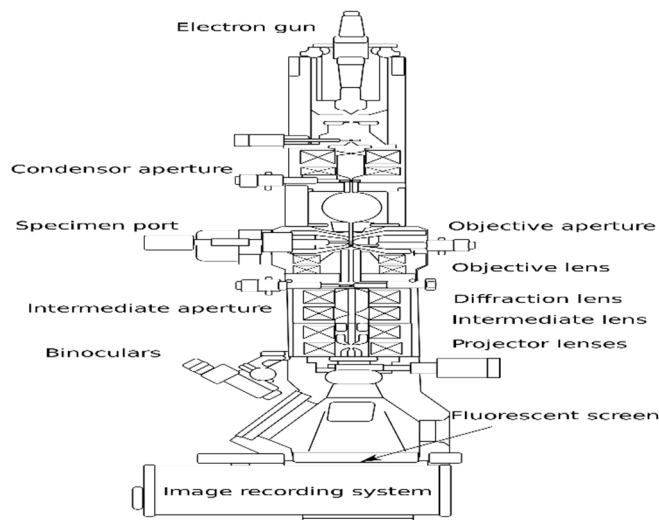
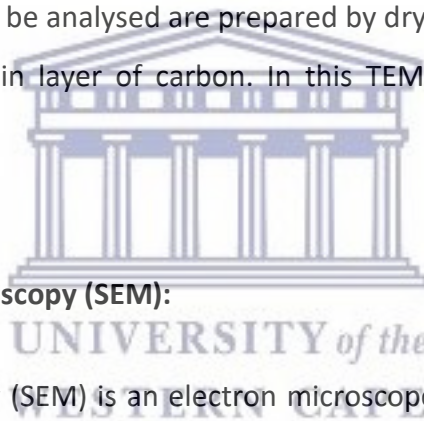


Figure 7: Schematic of transmission electron microscopy.

Imaging of nanoparticles using TEM depends on the contrast of the sample relative to the background. Samples that will be analysed are prepared by drying nanoparticles on a copper grid that is coated with a thin layer of carbon. In this TEM was used to analyse Cobalt nanoparticles.



### 3.3.2 Scanning electron microscopy (SEM):

Scanning electron microscopy (SEM) is an electron microscope technique that produces an image of a sample by scanning across the samples surface with high energy beam of electron in a raster scan pattern (Materials evaluation and engineering. 2001). In this technique electrons interact with atoms in the sample that is being analysed which then produces various signals which give information about the surface topography and the composition of the sample (Liu F., et al 2010). Scanning electron microscopy technique gives information about the topography of the sample being analysed which is the features of the sample or object and the materials properties. SEM can be used to study the morphology of the sample which gives information about the shape and size of the particles of the sample. It can also be used to get information about the elements and compounds that make up the sample and also information regarding the arrangement of the atoms in the sample being analysed.

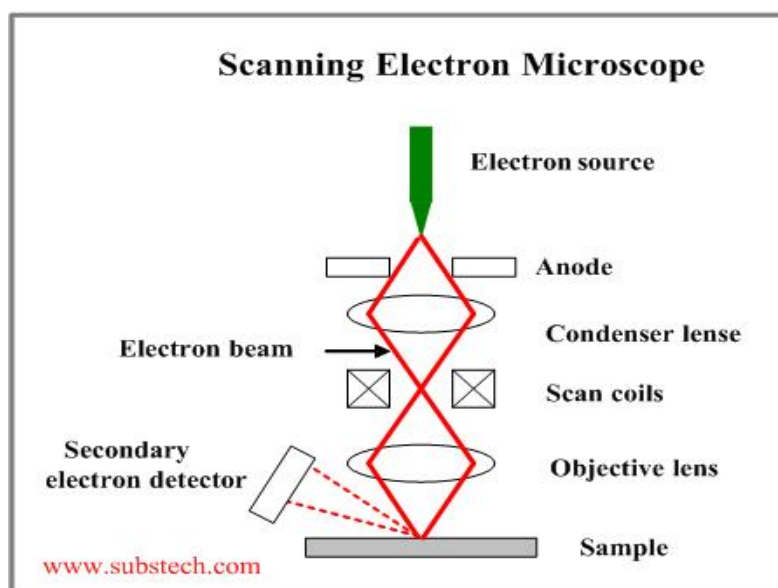


Figure 8: Schematic of scanning electron microscopy.

In this work SEM will be used to study the topography, morphology and composition of the polyamic acid and the surface of the commercial carbon ink incorporated with polyamic acid screen printed electrodes.

### 3.3.3 Small angle X-ray scattering (SAXS)

Small angle X-ray scattering (SAXS) is an analytical technique that is used to determine the size, shape of particles and size distribution (Schnablegger, H. and Singh Y 2012, p. 8). In this analytical method the x-ray irradiates a sample and then the atoms which are present in the sample scatter the incident radiation into all directions that gives a background radiation that is almost constant at small angles (Schnablegger, H. and Singh Y 2012, p. 13). Particles present in the sample produces additional scattering, this happens because the particles are made of the different material or density are the size are in the range of the x-ray wavelength. The average particle structure can be obtained by measuring the angle-dependent distribution of the scattered radiation (Schnablegger, H. and Singh Y 2012, p. 13). This method is an accurate, non-destructive and does not require a lot preparations steps. It can be applied in a number of fields such as biological materials, polymers, colloids, chemicals, nanocomposites, metals etc .The advantage of this technique over the other methods used to analyse size and shape is that it can analyse a variety types of samples such as aerosols, colloidal suspension, powders, solids and thin film (Agbabiaka A. et al., 2013). SAXS also provides better statistically

reliable estimates of nanoparticle size because the particle size distribution of nanoparticles analysed with SAXS is estimated over a large number of nanoparticles as electron microscopy methods analyse particle distribution based on hundreds or thousands particles (Agbabiaka A. et al., 2013). SAXS was performed using SaxSpace Anton Paar (Austria). In this work SAXS was used to estimate the sizes of the cobalt nanoparticles and the shape.



# Chapter 4

## *Materials and synthesis*

*This chapter presents the materials used in the synthesis of polyamic acid and cobalt nanoparticles as well as the ink formulation. It also provides microscopic, spectroscopic and electrochemical characterization of the transducer materials.*

Polyamic acid (PAA) is a semiconductor material that is a precursor of polyamide which is a class of polymers that have good thermal stability, electrical and mechanical properties. In this work PAA was electrodeposited onto screen printed electrodes as thin films to produce thin film electrodes at which the electrochemical behaviour of Norfloxacin was evaluated. Cobalt nanoparticles were incorporated into PAA to enhance the electrochemical performance.

### **4.1 Material and synthesis:**

Sodium phosphate dibasic dihydrate (99.5%), sodium phosphate monobasic dihydrate (99.0%), 4, 4-oxydianiline (97 %) (ODA), 1, 2, 4, 5-benzenetetracarboxylic acid (96 %) (PMDA), acetonitrile (99 %) (ACN), Cobalt (II) Chloride Hexahydrate, Ethylene Glycol anhydrous 99.8%, Hydrazine monohydrate, Hydrochloric Acid 37%, Norfloxacin  $\geq 98\%$ , Potassium hexacyanoferrate(III), Potassium chloride (99.5%). All the reagents were purchased at Sigma Aldrich, South Africa. Carbon ink, Henkel,

#### **4.1.1 Preparation of Phosphate buffer saline**

0.1 M pH 7.04 Phosphate buffer saline (PBS) was prepared by dissolving 3.3818 g of sodium phosphate monobasic dihydrate and 4.83363 g of Sodium phosphate dibasic dihydrate in 500 mL of deionized water. The solution was mixed according to the Henderson- Hasselbach equation to obtain the required pH.

#### **4.1.2 Synthesis of Polyamic acid:**

PAA was prepared by dissolving 0,01 M of 2,0024 g 4,4-oxydianiline (ODA) in 157 ml of acetonitrile, the mixture was stirred until solvation. 50 ml of acetonitrile containing 2,1812 g of pyromellitic dianhydride (PMDA) was added dropwise to the ODA mixture for more than an hour. After the PMDA mixture was added dropwise to the ODA mixture, the solution was

stirred for 24 hours. The resulting yellowish precipitate was filtered through a membrane under suction and dried at room temperature. 2,85 g of PAA was obtained.

#### 4.1.3 Synthesis of Cobalt Nanoparticles:

0,5 g of Cobalt Chloride Hexahydrate was dissolved in 50 ml of ethylene glycol and the solution was heated to 60°C. 2,25 ml of hydrazine was added to the solution and 1 M Sodium hydroxide solution was added with stirring. The resultant solution was kept under magnetic stirrer for 1hr at 60°C. After 1 hr black cobalt nanoparticles were formed. The particles were collected with a magnet and washed with ethanol several times and left to dry at room temperature. Figure 9 displays the synthesis procedure. In picture 9a cobalt chloride hexahydrate was added to the ethylene glycol and the solution turned pink. The colour of the solution then changed to a lighter pink in picture 9b when hydrazine was added. After adding the sodium hydroxide the solution became purple 9c. After 1 hr the solution became clear again, Figure 9d and black cobalt nanoparticles were formed which indicated the reduction of cobalt.

#### 4.1.4 Potassium ferricyanide with potassium chloride as supporting electrolyte

5 mM  $K_3Fe(CN)_6$  with 0.1 M KCl was prepared by dissolving 0.745513 g of potassium chloride in 100ml deionized water. 0.16462 g of potassium ferricyanide was added to the potassium chloride solution and mixed. KCl was used as a supporting electrolyte.

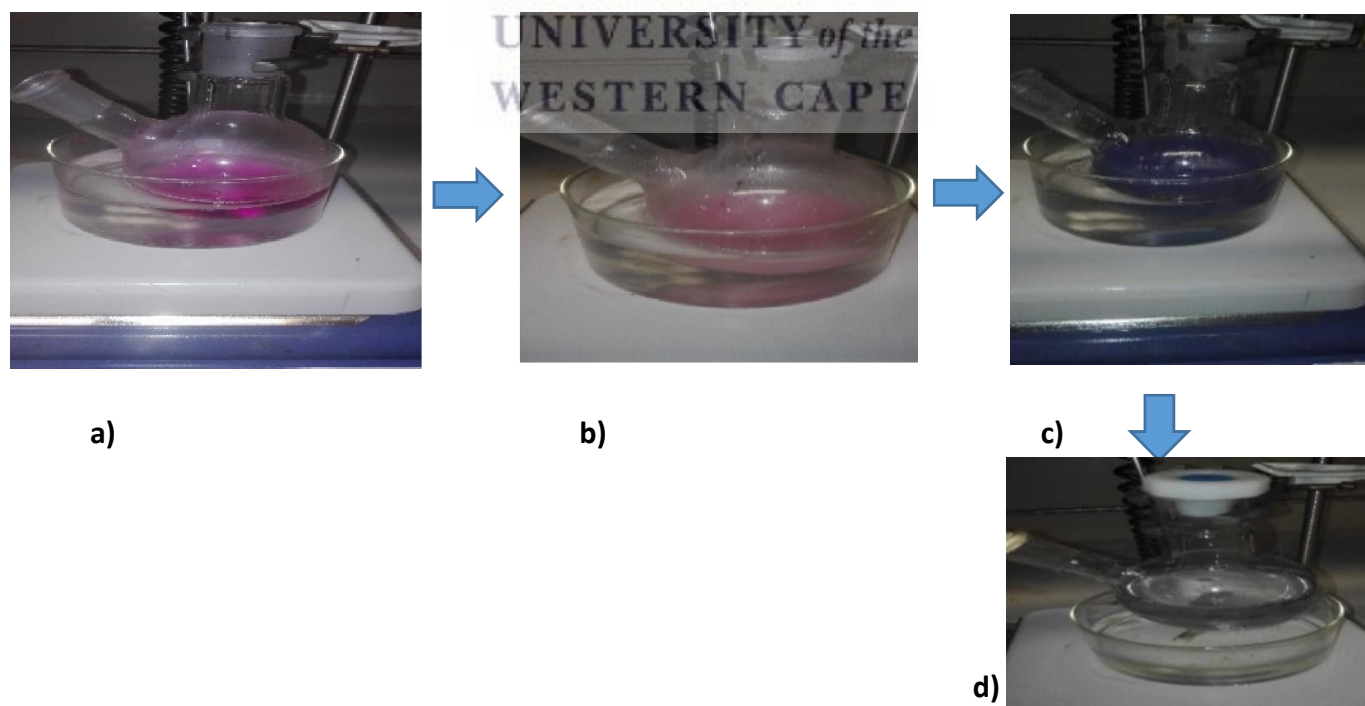


Figure 9: Schematic of synthesis of cobalt nanoparticles.

## 4.2 Ink Formulation and fabrication of electrodes

In order to make a conductive ink that can be used for screen printing of electrodes an active material, binder and solvent are required to make the ink. One of the issues that polymers and monomers face is that they are not soluble in most aqueous based solutions. Polyamic acid is soluble in most polar aprotic solvents like N-Methyl-2-pyrrolidone (NMP), Dimethyl sulfoxide (DMSO), Dimethylacetamide (DMAc) and Tetrahydrofuran (THF) and it is not soluble in solvents such as ethanol, chloroform, cyclohexane, acetic acid and acetone (Li, Q. et al., 2008). A PAA based ink was formulated using different solvents and binders. PAA was mixed with ethylene glycol as the solvent and gum arabic as the binder the problem encountered was that it was not printable as it was difficult to print it onto the paper. PAA was mixed with other solvents like DMSO but the other problem encountered was finding a suitable binder that is suitable with PAA and will not change the chemistry of PAA. Other pastes that were formulated were grainy so the PAA was not finely ground with the mortar and pestle. Therefore because for reasons such as the ones mentioned as well as not being able to dry or cure the working electrode PAA based ink could not be formulated and printed. PAA was then mixed using the bulk method where different amounts of synthesised PAA was mixed with commercial carbon ink to make the PAA-Commercial carbon ink.

### 4.2.1 Incorporation of polyamic acid in commercial carbon ink:

Polyamic acid was incorporated into the working electrode by bulk modification. This was done by mixing controlled amounts of synthesised polyamic acid with commercial carbon ink. The modification was done before the screen printing process of the electrodes. 3.27 g of commercial ink was weighed out and different mass ratios of polyamic acid 0.1962 g (6%) and 0.654 g (20%) was added to the commercial inks. 0.5 ml of Solvent 40 was added to all the inks and the inks were stirred for more than 30 minutes. The resultant ink was then used to screen print the working electrodes. The synthesised PAA was first ground using a mortar and pestle before being added into the commercial carbon ink.

Inks were cured at 75°C in an oven.

#### 4.2.2 Carbon Nanotubes (CNT) and PAA

Table 2: Ink formulation of MWCNT-PAA.

	Polyamic Acid	Carbon Nanotube	Laroflex®	Solvent-40
Multiwalled carbon nanotube paste	0	3 g	1.2 g	8 ml
6%	0.18 g	2.82 g	1.2 g	8 ml
10%	0.3 g	2.7 g	1.2 g	8 ml

The multiwalled carbon nanotube-polyamic acid inks were formulated by weighing and mixing 60% of the active material, Polyamic acid and carbon nanotube and adding 40% of the binding material to the active material, Laroflex®. 8ml of Solvent 40 was added to all the mixtures and the resulting mixture was stirred before screen printing.

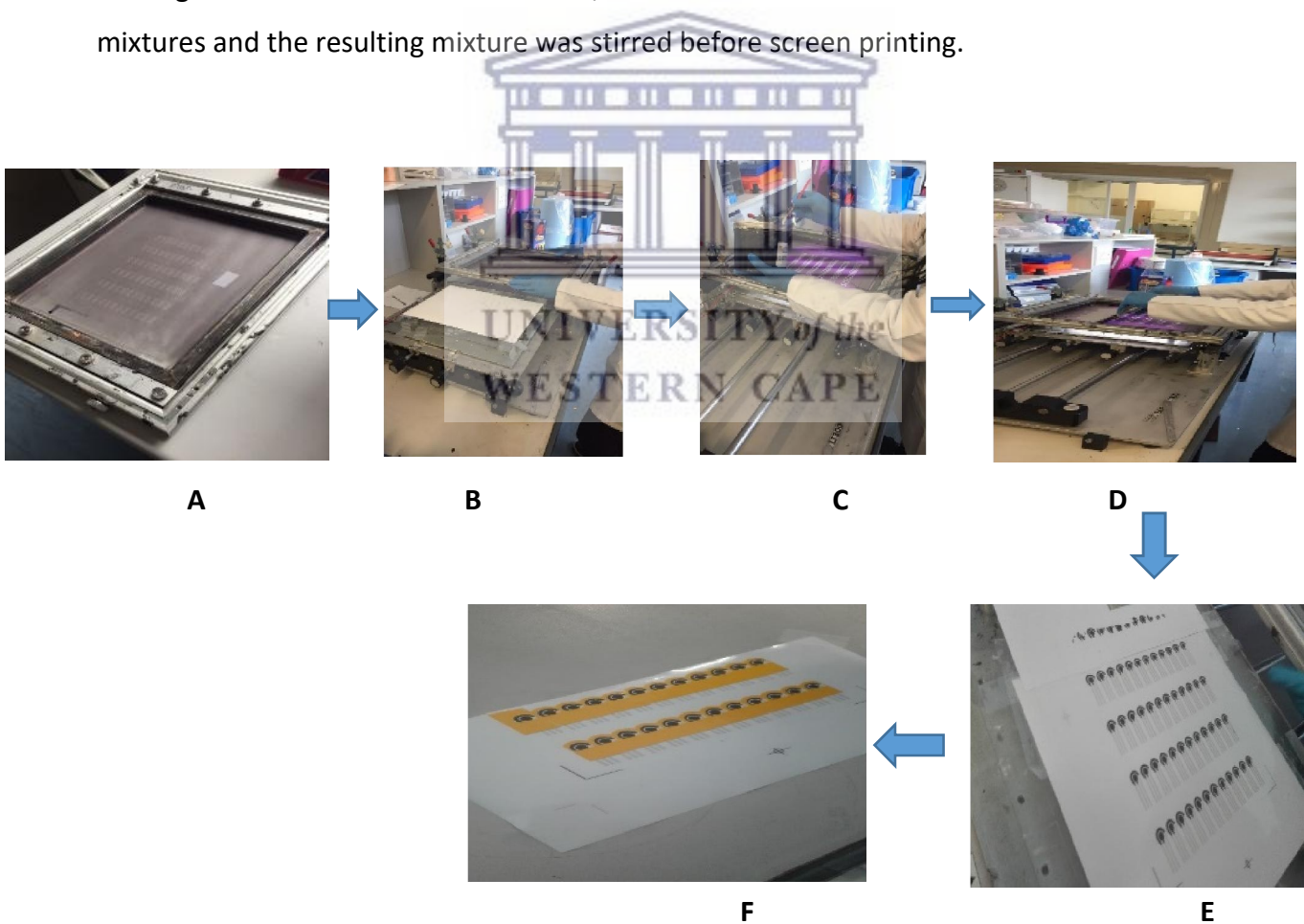


Figure 10: Schematic of paper based electrodes fabrication.

Printing of these paper based electrodes was done at the Council for Scientific and Industrial Research (CSIR) Mechatronics and Micro-Manufacturing unit in Pretoria, South Africa. Photo paper was the substrate for the printing of the electrode. Commercial conductive carbon ink was used as a reference material in the printing process, for comparison with the novel mixed composite working electrodes. These working electrodes were connected in a conventional three electrode electrochemical cell assembly using platinum wire as a counter electrode and Ag/AgCl as a reference electrode. To begin the printing process, a mesh pore screen was first fitted into the frame of the screen printer and a photo paper was placed under the screen (Figure 10a and b). The inks were deposited onto the screen and were spread out with the aid of a squeegee to transfer the ink to the substrate as depicted in picture C and D. The substrate was then removed from the screen printer after printing and placed in the oven for curing. After curing the printed electrodes, they were removed from the oven (Figure 10 E) and left to cool down to room temperature. An adhesive vinyl was used to over the Ag/AgCl tracks and the electrodes were ready to be tested, configured as the working electrode in a classical three electrode electrochemical cell.

The reproducibility of the electrochemical performance of the electrodes was tested by cyclic voltammetry in 0.1 M pH 7.04 PBS using 5 mM  $K_3Fe(CN)_6$ /0.1 M KCl as a redox marker. Figure 11 shows the electrochemical performance of the fabricated electrodes in 0.1 M PBS (pH 7.04). The electrodes showed a high background current which may be due to processing factors such as curing temperature or curing time, the area of the working electrode and the screen printing equipment, since the process was not automated. The composition of the electrode with respect to the polymer and presence of other carbon nanomaterials also play a role.



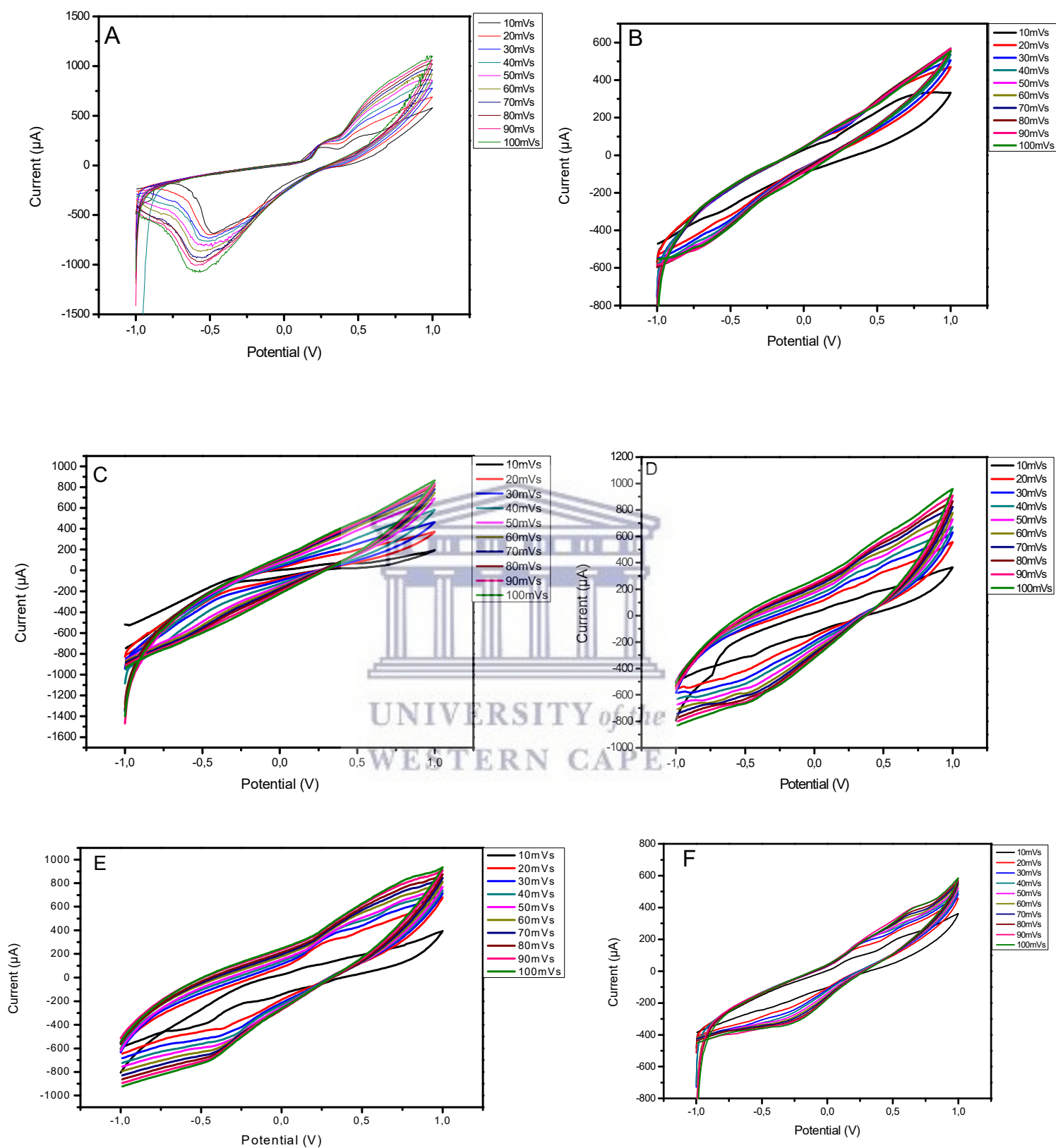


Figure 11: Cyclic voltammograms of the electrodes fabricated in this study, A) Commercial carbon ink, B) 6%PAA-Commercial carbon ink, C) MWCNT paste, D) 6%PAA-MWCNT paste, E) 10%PAA-MWCNT paste, F) 20% PAA-Commercial carbon ink.

## 4.3 Characterization

### 4.3.1 Spectroscopic characterization

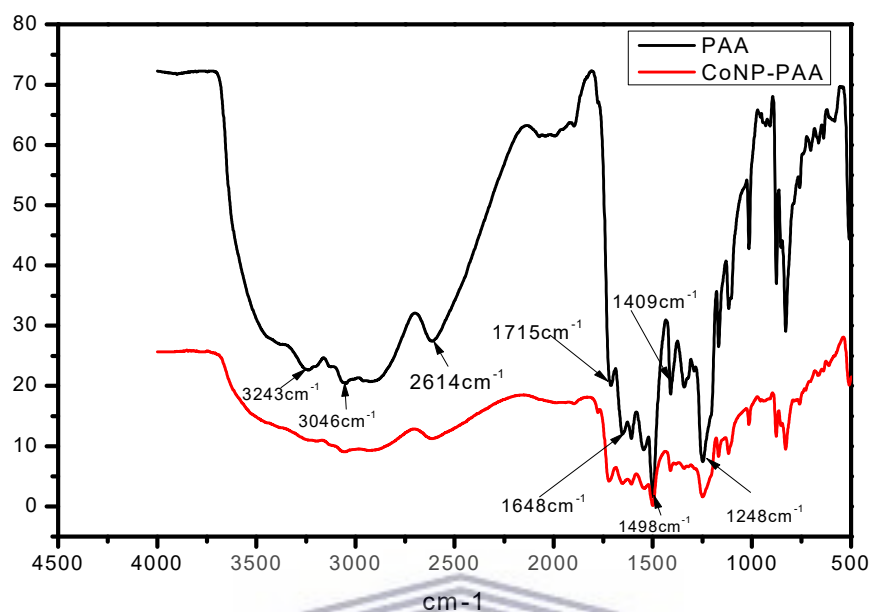


Figure 12: FTIR spectrum of polyamic acid and PAA-Co NP.

All samples were characterized by FTIR as powders by mixing them with KBr (potassium bromide) to form a pellet were recorded over a range of  $4500\text{ cm}^{-1}$  to  $500\text{ cm}^{-1}$ . The absorption bands occurring around  $3243\text{ cm}^{-1}$  (N-H stretch) and  $1648\text{ cm}^{-1}$  (C=O stretch) indicate the presence of the amide group, whereas the absorption band occurring at  $2614\text{ cm}^{-1}$  indicate the vibrational modes of carboxylic acid. The peak appearing at  $3046\text{ cm}^{-1}$  shows the presence of NH. The peak observed at  $1498\text{ cm}^{-1}$  indicates an aromatic group (C=C) and the peak at  $1248\text{ cm}^{-1}$  is associated with a stretching vibration of an ether group (C-O). The peak observed at  $1715\text{ cm}^{-1}$  indicates a C=O stretch and the peak observed at  $1409\text{ cm}^{-1}$  due to  $\nu(\text{CO-NH})$  stretching band. The FTIR spectrum and absorption bands observed of PAA is in agreement with the ones previously reported in literature, therefore the synthesis of PAA was successful. (Li, Q. et al., 2008; Noah, N.M. et al., 2012). The FTIR spectrum of PAA-Co NP is more similar to the PAA spectrum as the peaks that are visible in the PAA spectrum they are also visible in the PAA-Co NP spectrum. There were no new peaks, however the peaks of the composite are less intense compared to the peaks present in the PAA spectrum. The spectrum showed the dominant features of PAA.

### 4.3.2 Microscopic characterization:

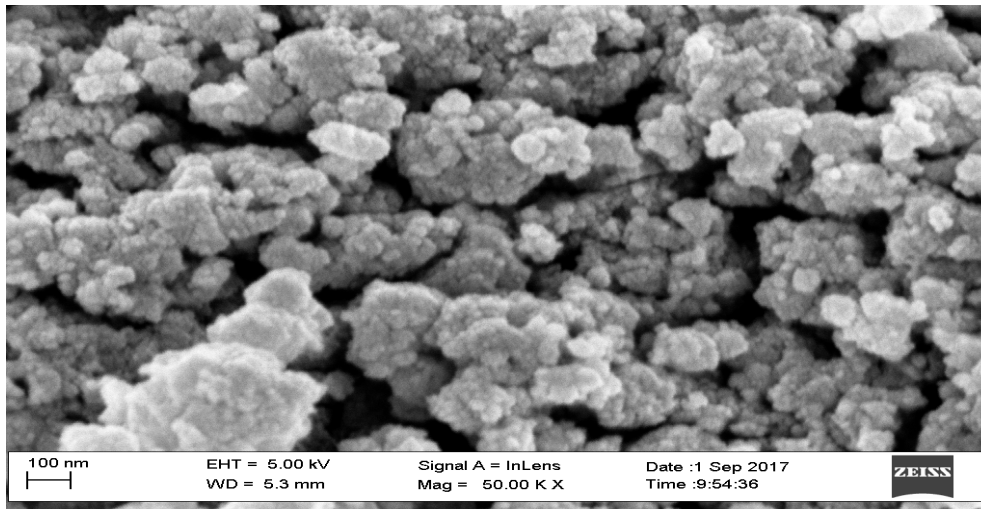


Figure 13: HRSEM image of polyamic acid.

The SEM of PAA shows clusters of PAA with large surface areas. The EDS Figure 14 below shows the chemical composition of PAA, it shows trace amounts of carbon, nitrogen and oxygen which are present in the chemical structure of PAA.

Element	Wt%	Wt% Sigma
C	67,45	1,73
N	7	2,02
O	25,55	1,12
Total:	100	

Figure 14: EDS of polyamic acid.

## Cobalt Nanoparticles

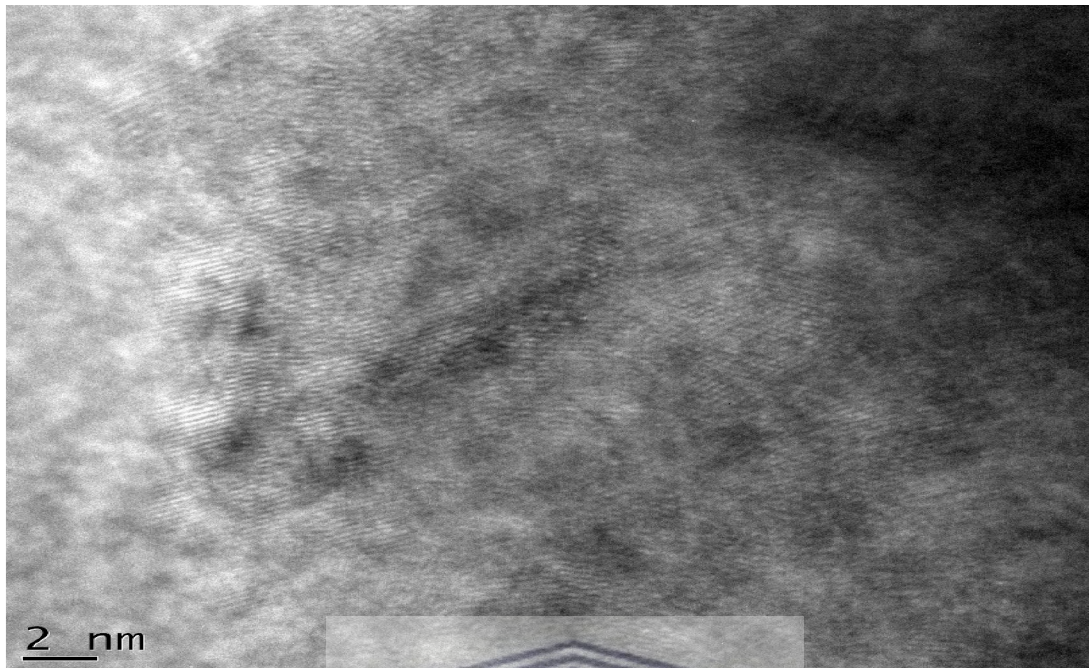


Figure 15: HRTEM image of cobalt nanoparticles.

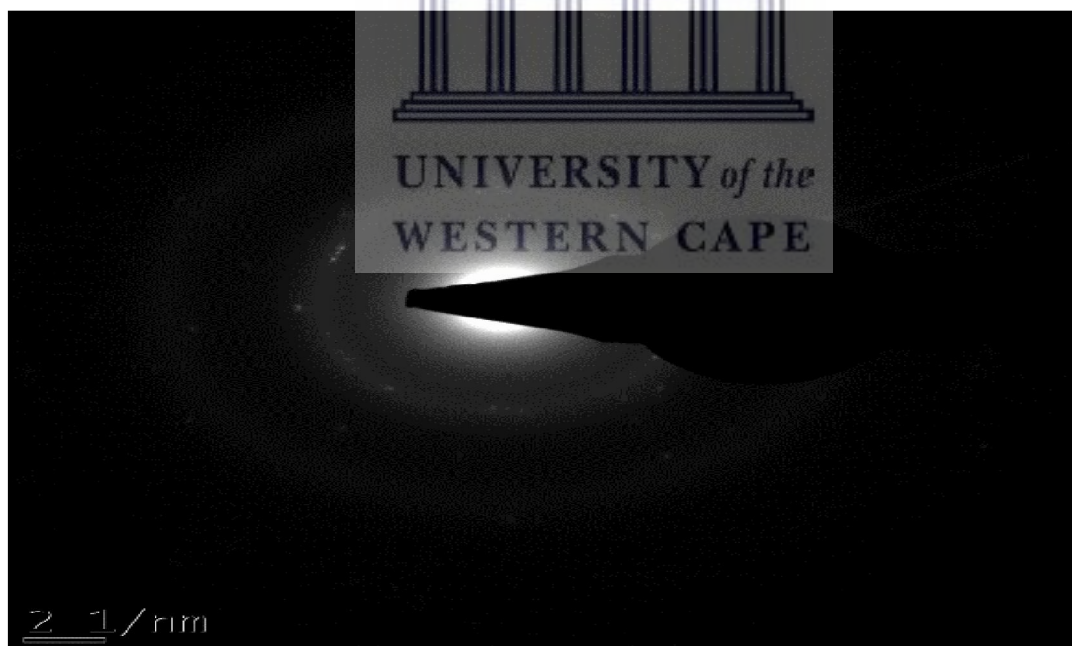


Figure 16: SAED image of the cobalt nanoparticles.

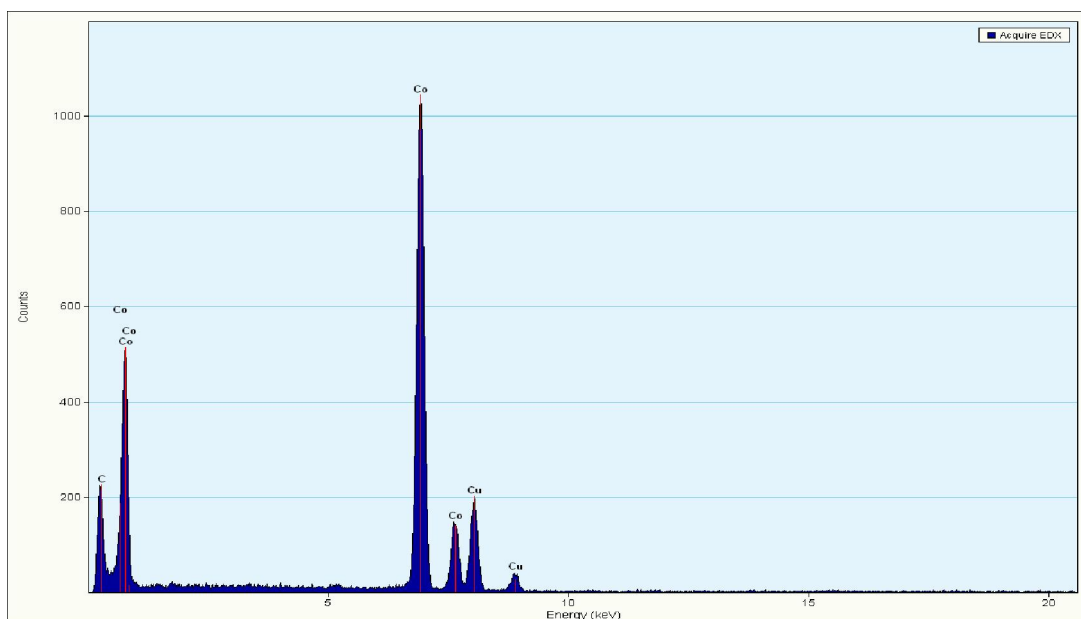


Figure 17: Image of EDX of the cobalt nanoparticles.

The image of the cobalt nanoparticles Figure 15 doesn't give a clear picture of the size and shape of the Co NP this can be due to agglomeration of the nanoparticles. The SAED image Figure 16 which gives information about the crystallinity of the sample being analysed shows that the cobalt nanoparticles are crystalline due to the bright spots observed in the image and the EDX Figure 17 which gives information about the chemical composition of the sample shows that the sample is cobalt. The cobalt nanoparticles were further characterised using SAXS to get the shape and size of the nanoparticles. TEM and SAXS complement each other hence SAXS was used to estimate the size and shape of the nanoparticles due to the fact that they were not clear in the HRTEM image.

## Small angle x-ray scattering (SAXS)

SAXS was performed using SaxSpace Anton Paar (Austria). The sample that was analysed was in the powder form. The powder was spread out between two layers of sticky tape, the two layer sticky layer was then clamped onto frames. The graphs below show the distribution curves of cobalt nanoparticles.

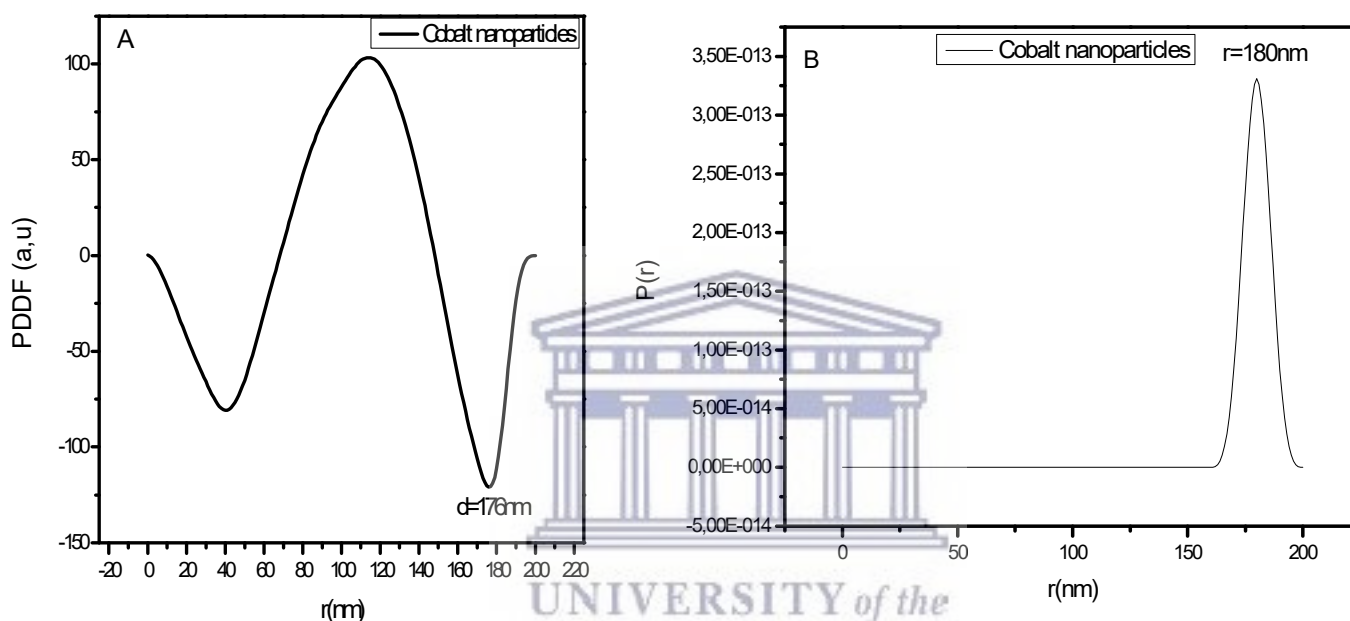


Figure 18: Distribution curve of cobalt nanoparticles.

Small angle x-ray scattering was used to study the shape and size distribution of the Co NPs. The Figure 18 above displays the distribution curves of cobalt nanoparticles, Figure 18a shows the pair distance distribution function (PDDF) graph which gives information about the shape of the particles and the diameter of the particles and Figure 18b is the distribution by number which also gives information about the radius of the particles and number of particles.

The pair distance distribution functions displays a bell shape almost symmetrical which means the particles are spherical. It also shows that there are no aggregates, aggregates are usually identified by a second peak. The PDDF also shows that the nanoparticles have a diameter of 200 nm as the diameter of a particle is observed at the point at which  $p(r)$  goes to zero (Nyman M. et al., 2015). The distribution by number shows the nanoparticles have a radius of 180 nm. (Kamal S.K. et al., 2009) did a study on synthesis of cobalt nanoparticles by

a modified polyol process using cobalt hydrazine complex. In their work they studied the particle size, size distribution and shape of the particles by TEM and SAXS. In their work they first obtained particle sizes with a diameter of 200 nm and the shape of the particles were spherical which is in agreement with the work in this study. When they introduced a stabilizer to the synthesis, polyvinyl pyrrolidone (PVP) the diameter of the particles decreased to 35 nm. In this work a stabilizer was not added in the synthesis of cobalt nanoparticles which may be the reason why the size of the particles were more than 100 nm.

#### **4.3.3 Electrochemical Characterization**

All the CV and SWV experiments were carried out using PalmSens Ptrace work station. All the experimental solutions were purged using Argon. The chemically synthesised PAA was dissolved in 0.1 M pH 7.04 PBS and electrodeposited onto screen printed electrodes (SPCE) using 5 cycles at a potential window of -1000 mV to 1000 mV at a scan rate of 50 mV/s. The modified electrode were further characterized using CV.

Co NP were dissolved in 0.1 M HCl and sonicated for 30-45 minutes. The Co NP solution was then added to 0.1 M pH 7.04 PBS and electrochemically deposited onto SPCEs using 5 cycles between -1000 mV to 1000 mV at a scan rate of 50 mV/s. The modified electrodes were further characterized at different scan rates by CV.

#### **Electrode surface preparation:**

All the CV and SWV experiments were carried out using PalmSens Ptrace work station and PalmSens Trace software. Before using the glassy carbon electrode (GCE) it was cleaned with 0.1  $\mu\text{m}$ , 0.3  $\mu\text{m}$  and 0.05  $\mu\text{m}$  fine alumina powder and sonicated in ethanol for 10 minutes and the electrode was rinsed with distilled water and sonicated again in deionized water for 10 minutes. All the experimental solutions were purged using Argon. The chemically synthesised PAA was dissolved in 0.1 M 7.04 pH PBS and were electrochemically deposited onto the GCE using 5 cycles between -1000 mV to 1000 mV at a scan rate of 50 mV/s. The modified electrode was further characterized at different scan rates.

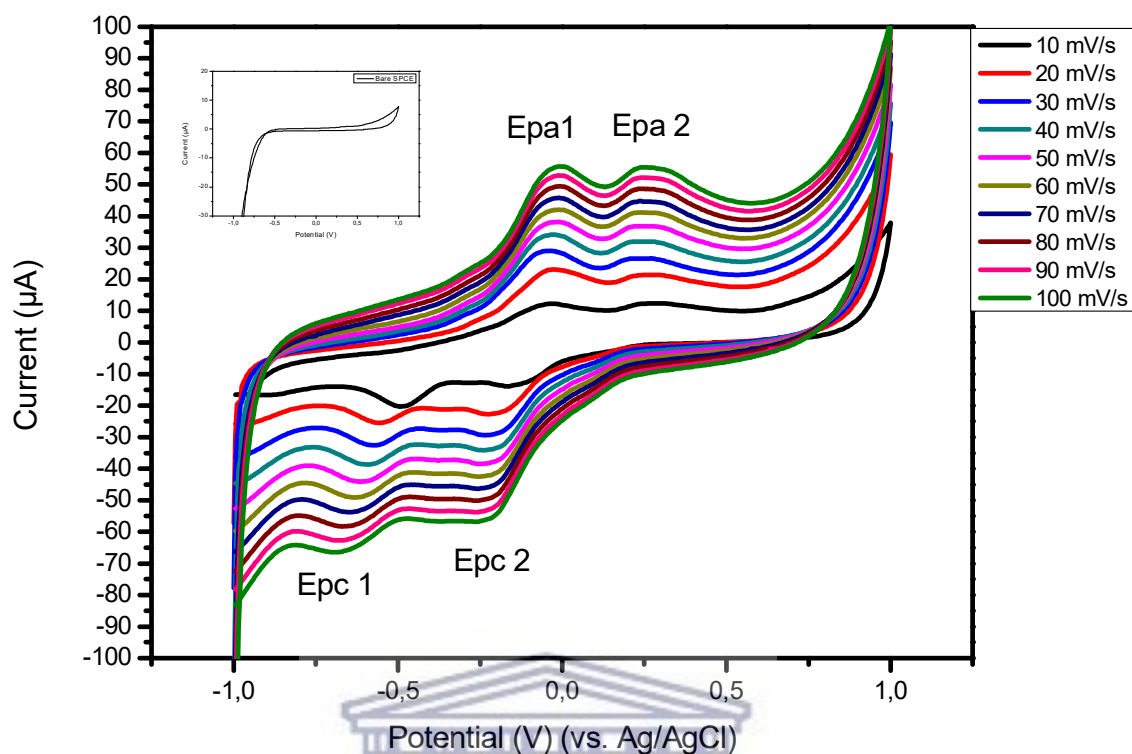


Figure 19: Cyclic voltammogram of PAA-SPCE in pH 7.04 0.1 M PBS at scan rates ranging from 10 mV/s-100 mV/s. Insert shows bare SPCE electrode at scan rate 50 mV/s in pH 7.04 0.1 M PBS.

The oxidation peaks of PAA were identified as Epa1 and Epa2 with complimentary reduction peaks (Figure 19). These peak currents showed an increase with the increasing scan rate indicating good diffusion controlled electron mobility. The electrochemistry of PAA showed two reversible redox couples. It has been reported that the peaks at Epa1 and Epa2 are associated with the oxidation of NH and OH groups that are present in the polyamic acid structure (Hess, E.H. et al, 2014). The effect of the polyamic acid on the surface of glassy carbon and screen print carbon electrodes shows negligible differences (Figure 20). For both transducers modified with PAA respectively, 2 redox couples were observed in keeping with the expected signature of PAA electrochemistry. The graphitic carbon used in SPCE electrodes produced amplified redox currents due to the increased surface area of SPCE compared to glassy carbon electrode surface.



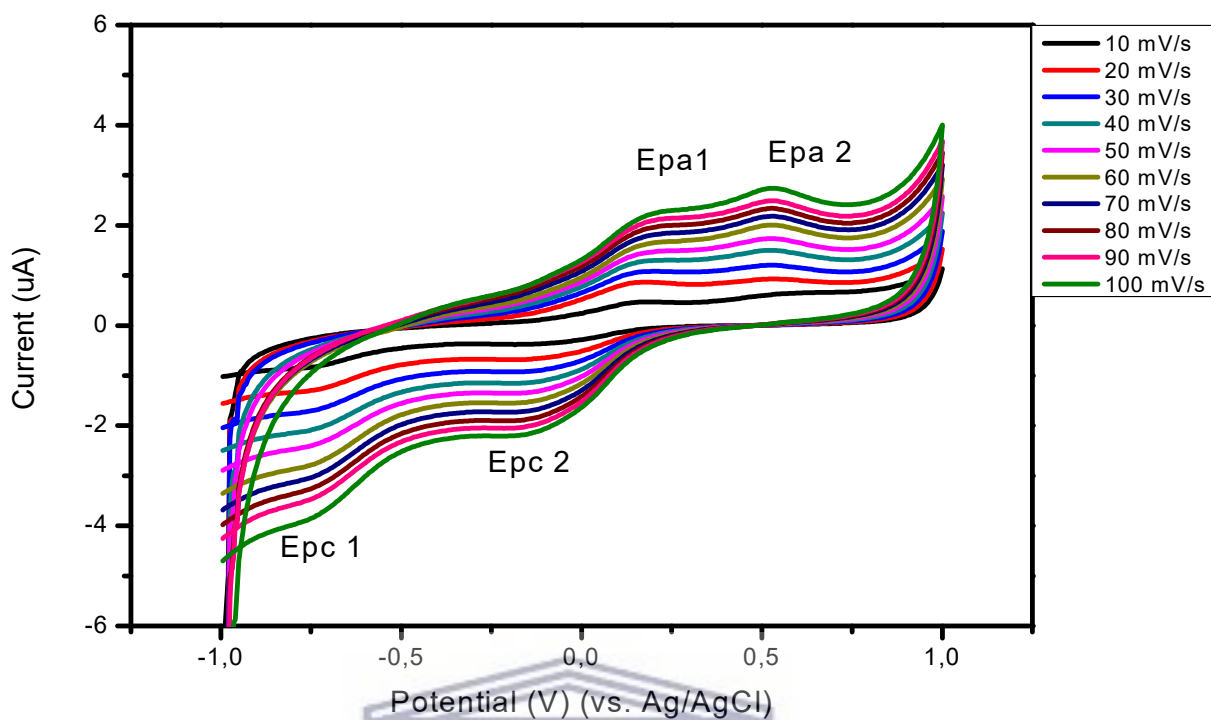


Figure 20: Cyclic voltammogram of PAA-GCE in pH7.04 0.1 M PBS at different scan rates (10 mV/s-100 mV/s).

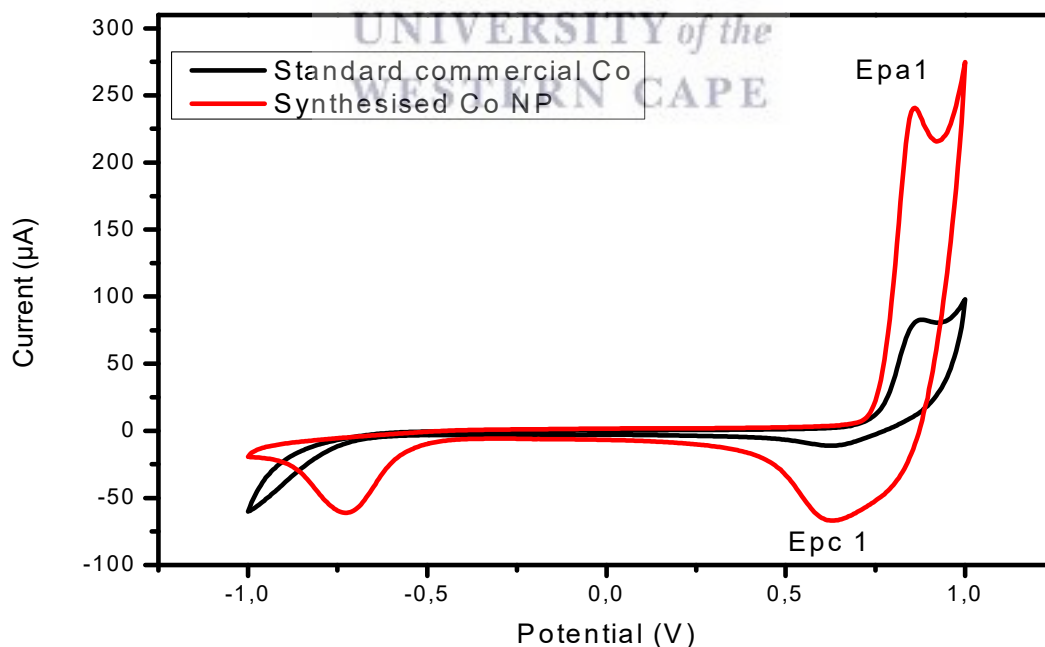
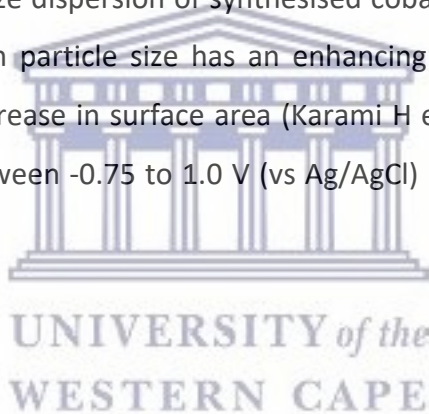


Figure 21: Cyclic voltammogram of commercial cobalt solution and synthesised Co NP in 0.1 M pH 7.04 PBS at scan rate 50 mV/s.

500 ul of standard solution of commercial cobalt solution was added to 3 ml of PBS and electrodeposited onto a SPCE, the electrode was then characterised by CV in 0.1 M pH 7.04 PBS. The cyclic voltammogram of the commercial cobalt solution (black) and the cyclic voltammogram of the synthesised Co NPs (red) at scan rate 50 mV/s were not in agreement with the peak position predicted by Standard Redox Potential of  $-0.27\text{ V}$  for  $\text{Co}^{2+}$  but the peak positions of the commercial cobalt and synthesized cobalt nanoparticles were in agreement to the previously reported in literature by (de Groot M.T et al., 2007). In the commercial cobalt solution an oxidation peak was observed at  $0.87\text{ V}$  (vs. Ag/AgCl) and a reduction peak was observed at  $0.64\text{ V}$  (vs. Ag/AgCl). The cyclic voltammogram of synthesised cobalt nanoparticles displayed an oxidation peak at  $0.86\text{ V}$  (vs. Ag/AgCl) and a reduction peak at  $0.63\text{ V}$  (vs. Ag/AgCl) (Figure 21). The peak currents observed for the synthesised cobalt nanoparticles were larger and sharper compared to the ones observed for commercial cobalt, due to the smaller size and size dispersion of synthesised cobalt nanoparticles as measured by SAXS analysis. Decrease in particle size has an enhancing effect on the oxidation and reduction currents due to increase in surface area (Karami H et al., 2009). The irreversible reduction peak observed between  $-0.75$  to  $1.0\text{ V}$  (vs Ag/AgCl) is believed to be a feature of the carbon electrodes used.



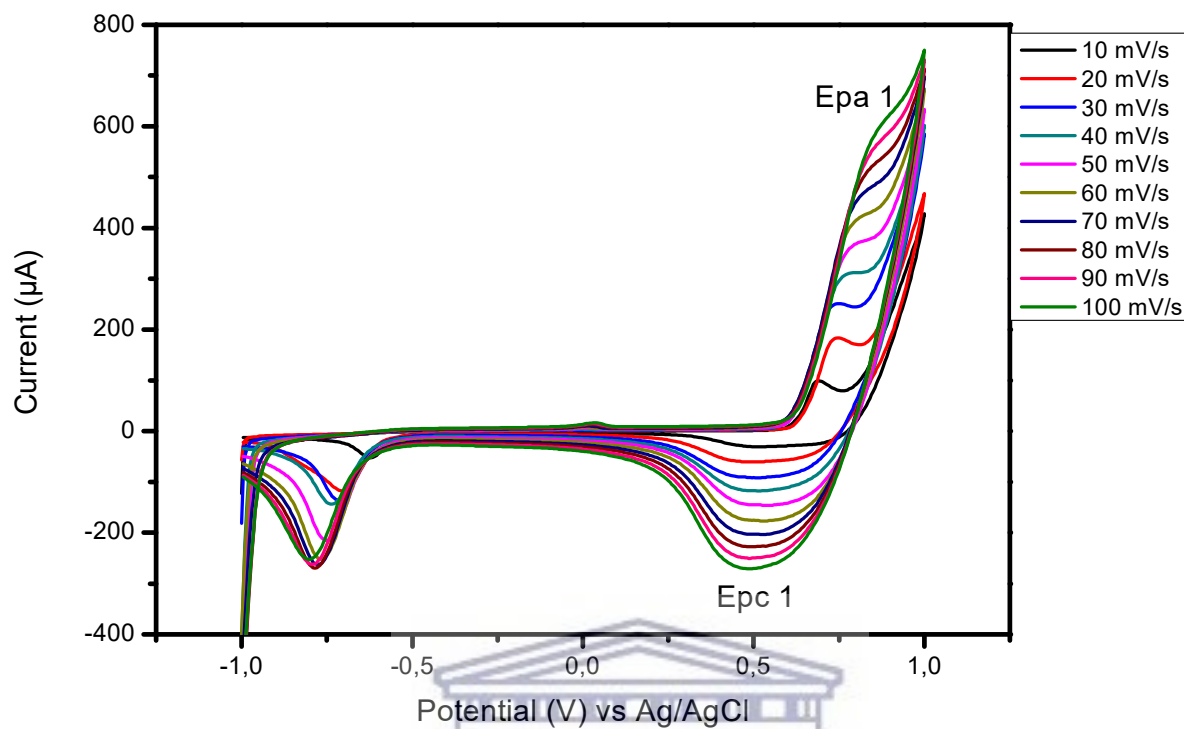


Figure 22: Cyclic voltammogram of Co NP in 0.1M pH 7.04 PBS at different scan rates (10 mV/s-100 mV/s).

The cobalt nanoparticles cyclic voltammogram in Figure 22 shows a reversible system with one redox couple. The peak currents of cobalt nanoparticles increased with the scan rate. The anodic peak Epa1 can be attributed to the  $\text{Co}^{2+}$ .

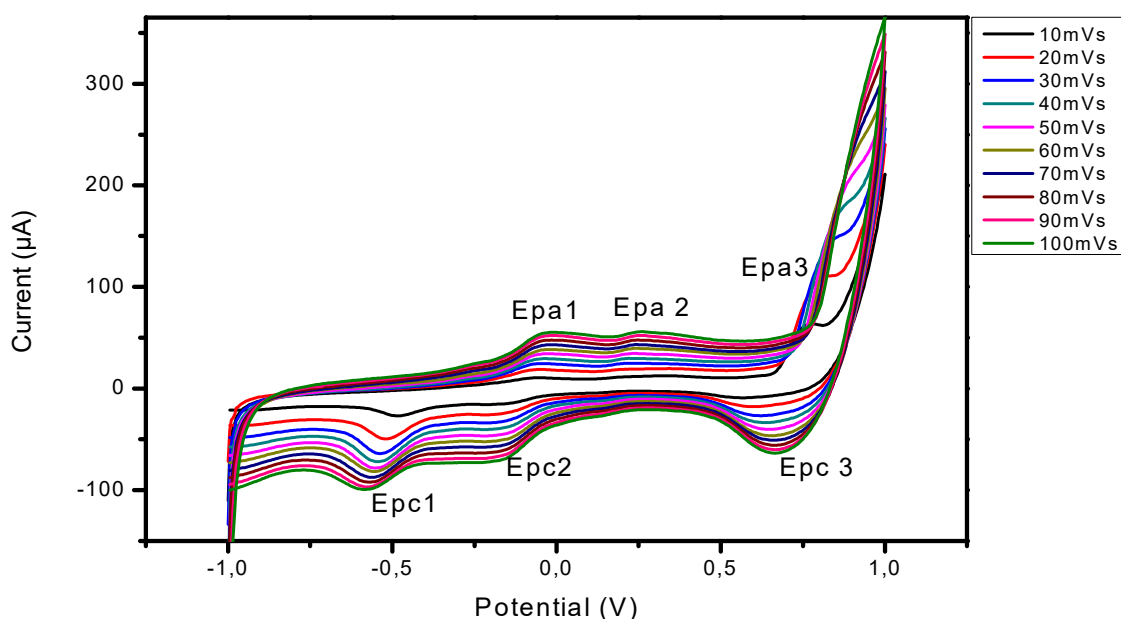


Figure 23: Cyclic voltammogram of PAA-Co NP on SPCE in 0.1M pH 7.04 PBS at different scan rates (10 mV/s-100 mV/s).

Cyclic voltammogram of polyamic acid-cobalt nanoparticles composite showed a reversible system with three redox couples. The cyclic voltammogram shows the integration of the polyamic acid and the cobalt nanoparticles as the PAA and Co NP peaks are both visible on the cyclic voltammogram. The potential peaks at -0.041 V (Epa1), 0.24 V (Epa2), -0.54 V (Epc1), 0.22 V (Epc 2) (vs. Ag/AgCl) are due to the presence polyamic acid and the potential peaks 0.51 V (Epa 3) and 0.64 V (Epc 3) (vs. Ag/AgCl) are due to the presence of the cobalt nanoparticles. The peak currents increased as the scan rate increased.

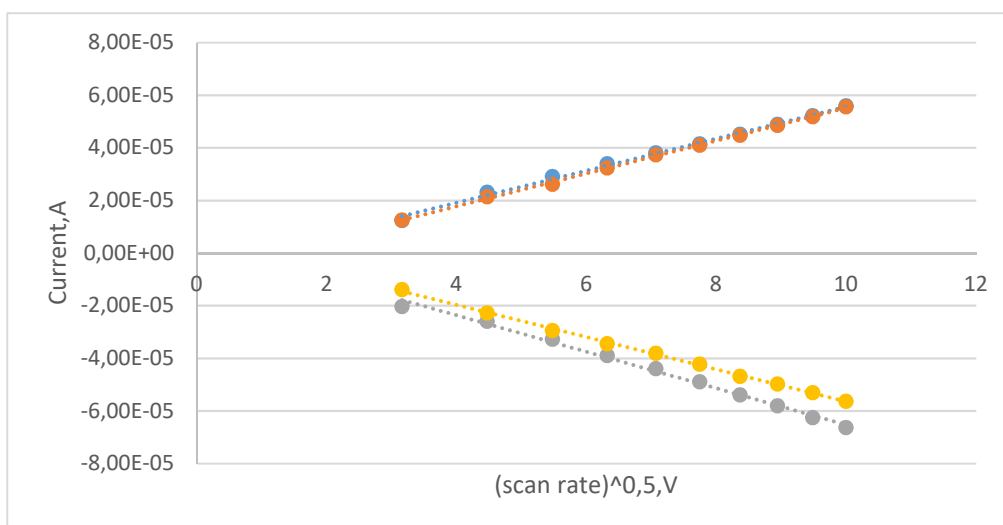


Figure 24: Randles Sevcik plot of PAA-SPCE in pH 7,04 0.1 M PBS.

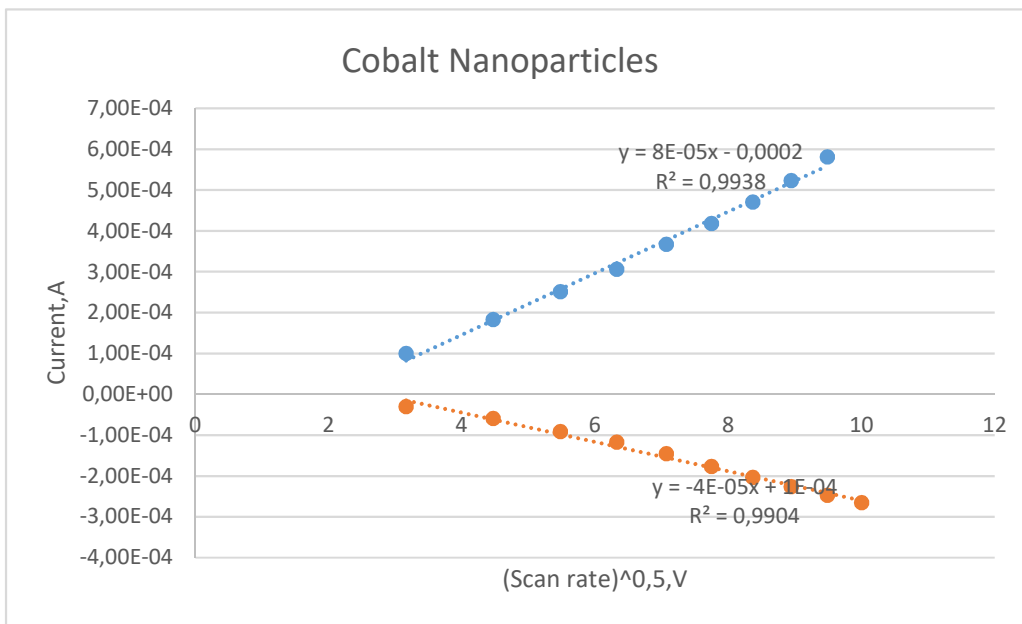


Figure 25: Randles Sevcik plot of Co nanoparticles-SPCE in pH 7.04 0.1 M PBS.

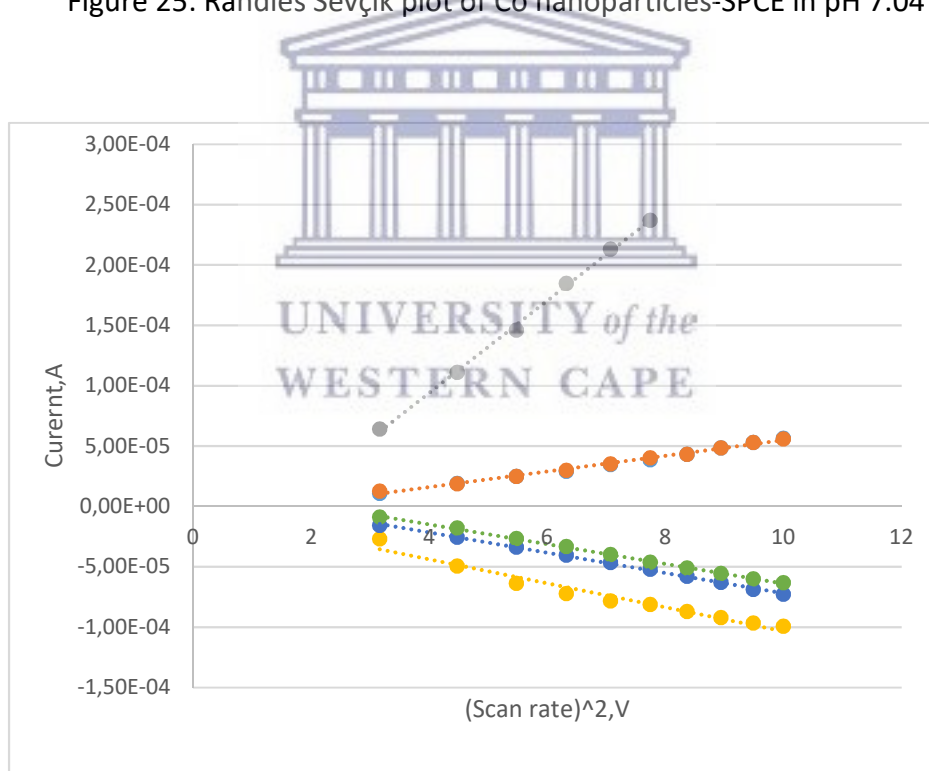


Figure 26: Randles Sevcik plot of Co NP-PAA on SPCE in pH 7.04 0.1 M PBS.

Table 3: Electrochemical parameters of PAA, Co NP and PAA-Co NP on SPCE.

Electrodes	Epa 1, V	Epa 2, V	Epa 3, V	Epc 1, V	Epc 2, V	Epc 3, V	ΔE, V	E° V	Diffusion coefficient, cm <sup>2</sup> /s
PAA-SPCE	-0,02322	0,2605	-	-0,6105	-0,2245	-	ΔE1 = 0,587 and ΔE2=0,485	E°1= -0,32 and E°2= 0,018	Epa1= 0,0013; Epa2= 0,0013; Epc1= 0,0014; Epc2 0,0013
Co-SPCE	0,7894	-	-	0,5340	-	-	ΔE= 0,176	E°=0,62	Epa1= 0,000023; Epc1= 0,00012
PAA/Co-SPCE	-0,0411	0,2462	0,5131	-0,5475	-0,2179	0,6374	ΔE1= 0,506; ΔE2= 0,464; ΔE3= 0,124	E°1= -0,29; E°2= 0,014; E°3=0,57	Epa1= 0,0014; Epa2= 0,0013; Epa3= 0,0034, Epc1= 0,00054, Epc2= 0,0015; Epc3= 0,0015

Table 4 provides a summary of the formal potential, peak separation and diffusion coefficients calculated for each electrode system in PBS, without the addition of any analyte species to PBS solution. A plot of peak current vs the square root of the scan rate produced a linear plot for each of the peaks. The diffusion coefficients of the modified PAA, Co NP and PAA-Co NP electrodes were evaluated, from the slope of the Randles Sevçik plots obtained using the Randles Sevçik equation (Equation 1).

N: Number of electrons

A: electrode area cm<sup>3</sup>

C: concentration mol/cm<sup>3</sup>

D: Diffusion coefficient  $\frac{cm^2}{s}$

V: potential scan rate V/s

$$I_{pc} = 2.687 \times 10^5 \times n^{\frac{3}{2}} \times v^{\frac{1}{2}} \times D^{\frac{1}{2}} \times A \times C \dots \text{Equation 1}$$

The peak potential separation for the redox couples of PAA 0.587 V and 0.485 V were slightly higher than the peak separation obtained for the PAA-Co NP platform of 0.506 V and 0.464 V, which shows that the cobalt nanoparticles may have enhanced the electron transfer rate. The formal potentials obtained for the PAA were -0.32 V and 0.018 V for Epac<sub>1</sub> and Epac<sub>2</sub> respectively and -0.29 V and 0.014 V for Epac<sub>1</sub> and Epac<sub>2</sub> respectively for the PAA-Co NP platform. The diffusion coefficient calculated for Epac<sub>2</sub> of PAA were comparable to Epac<sub>2</sub> of PAA-Co NP as the values obtained for the diffusion coefficient were not very different from each other. The D<sub>e</sub> for Epac<sub>1</sub> for PAA and PAA-Co NP were observed to 10 x lower than the D<sub>e</sub> values typically measured for the conjugated polymer layer only. Hence the incorporation of the Co nanoparticles into the polymer did not show a marked difference in electron mobility of the overall system as measure by the diffusion of electrons into and through the Co- modified conjugated polymer system.

The diffusion coefficients calculated for PAA i.e.  $13.0 \times 10^{-4} \text{ cm}^2/\text{s}$ ,  $14.0 \times 10^{-4} \text{ cm}^2/\text{s}$  were observed to be bigger compared to previously reported D<sub>e</sub> of  $7.10 \times 10^{-6} \text{ cm}^2/\text{s}$  and  $9.11 \times 10^{-6} \text{ cm}^2/\text{s}$  by (Hess E.H. et al., 2014). The difference may be attributed to concentration of the electrolyte used in their study and also different surface area of the electrodes used in the studies since different types of electrodes were used. It is also observed that the diffusion coefficient of Epc 1 decreased from  $0.0014 \text{ cm}^2/\text{s}$  for the PAA-SPCE to  $0.000054 \text{ cm}^2/\text{s}$  for the electrode modified with polyamic acid and cobalt nanoparticles which shows that the PAA-CoNP-SPCE may have had a faster electron transfer.

PAA was successfully characterised by SEM, FTIR and CV. The FTIR and EDS of SEM showed the functional groups and elements of polyamic acid. Co NPs were successfully characterised by TEM, SAXS and CV. The EDX of TEM showed that the cobalt was indeed synthesised. The results obtained from CV with respect to the redox behaviour of the PAA and PAA-Co NP showed that the materials were electroactive and obeyed diffusion controlled interfacial electron transfer kinetics.

# Chapter 5

## Analysis of Norfloxacin

In this chapter we focus on the analytical reporting of the modified and unmodified screen printed electrodes towards the quantitative analysis of Norfloxacin at unmodified and modified electrode. Norfloxacin is representative of the fluoroquinolone class of antibiotics and very few reports of its electrochemical detection have been published to date.

### 5.1 UV analysis of Norfloxacin

0.1 M of Norfloxacin solution was prepared by dissolving 0.1 g of Norfloxacin in 10 ml of HCl with subsequent dilutions for UV/vis analysis, performed using a Nicolet evolution 100 UV/vis instrument, in wavelength scanning mode.

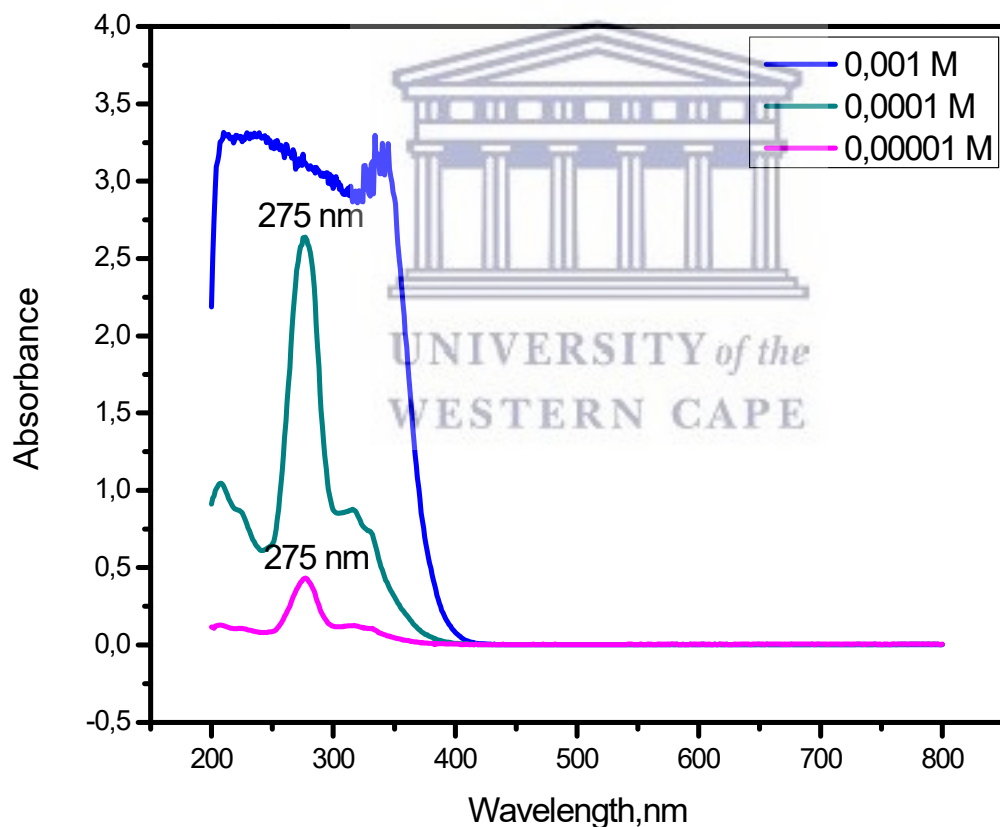


Figure 27: UV-Vis spectrum of 0.1 M Norfloxacin in HCl.

At 0.001 M of Norfloxacin showed a very high absorbance and a lot of noise was observed which can be due to solution being too concentrated. As the solution was further diluted the noise disappeared and the Norfloxacin peak became more visible. The peak wavelength of



the prepared 0.1 M Norfloxacin was observed at 275 nm which is in agreement with the ones reported in literature (Pant M et al., 2012). UV/vis absorbance at 275 nm may be assigned to transitions of n or  $\pi$  electrons to the  $\pi^*$  excited state and is characteristic of this highly conjugate type of molecule, containing N-hetero atoms.

## 5.2 Electrochemical detection of Norfloxacin

Electrochemical detection of Norfloxacin was studied using cyclic voltammetry and square wave voltammetry at bare commercial screen printed electrode and at modified electrodes in 0.1 M pH7,04 PBS, scan rate of 50 mV/s at different concentrations of Norfloxacin.

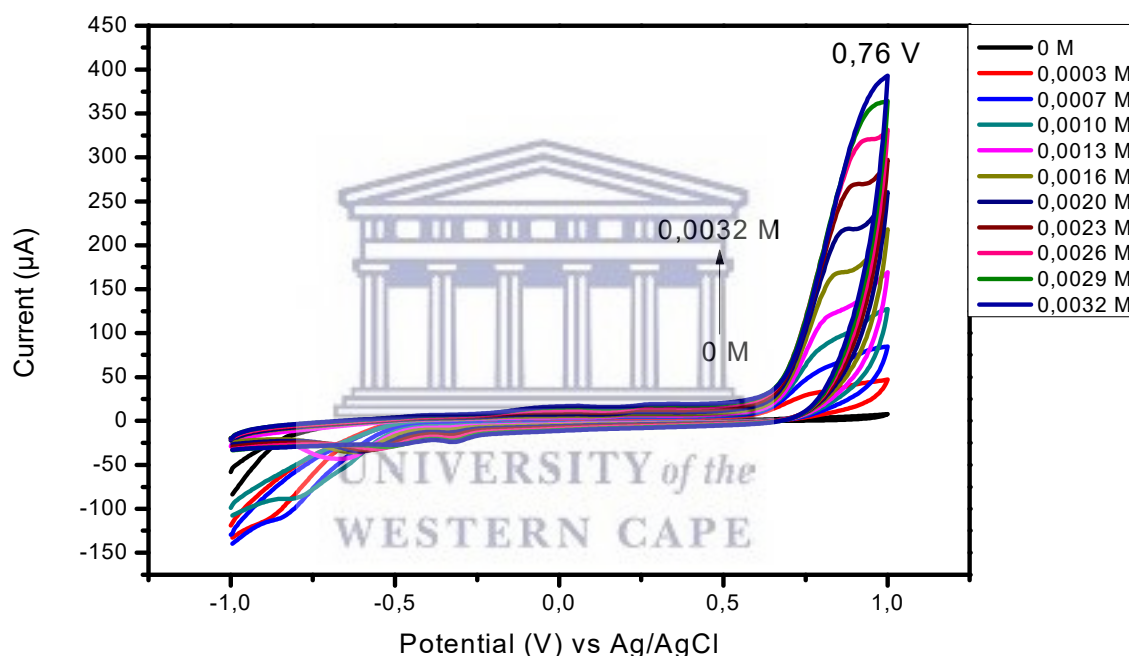


Figure 28: Current response of a bare SPCE at increasing concentrations of Norfloxacin as measured by CV in 0.1M pH7 PBS, scan rate 50 mV/s.

The current response for the oxidation of Norfloxacin was observed as a clearly resolved peak at 0.76 V (vs Ag/AgCl). The peak current responded positively to increasing Norfloxacin concentration in the range of 0.3 to 3.2 mM and from this concentration trend a calibration curve was developed for quantitative assessment of Norfloxacin oxidation. The peak identified at 0.76 V (vs Ag/AgCl) will be used consistently as a marker to monitor current response due to increasing Norfloxacin concentration at all the modified electrodes as well.

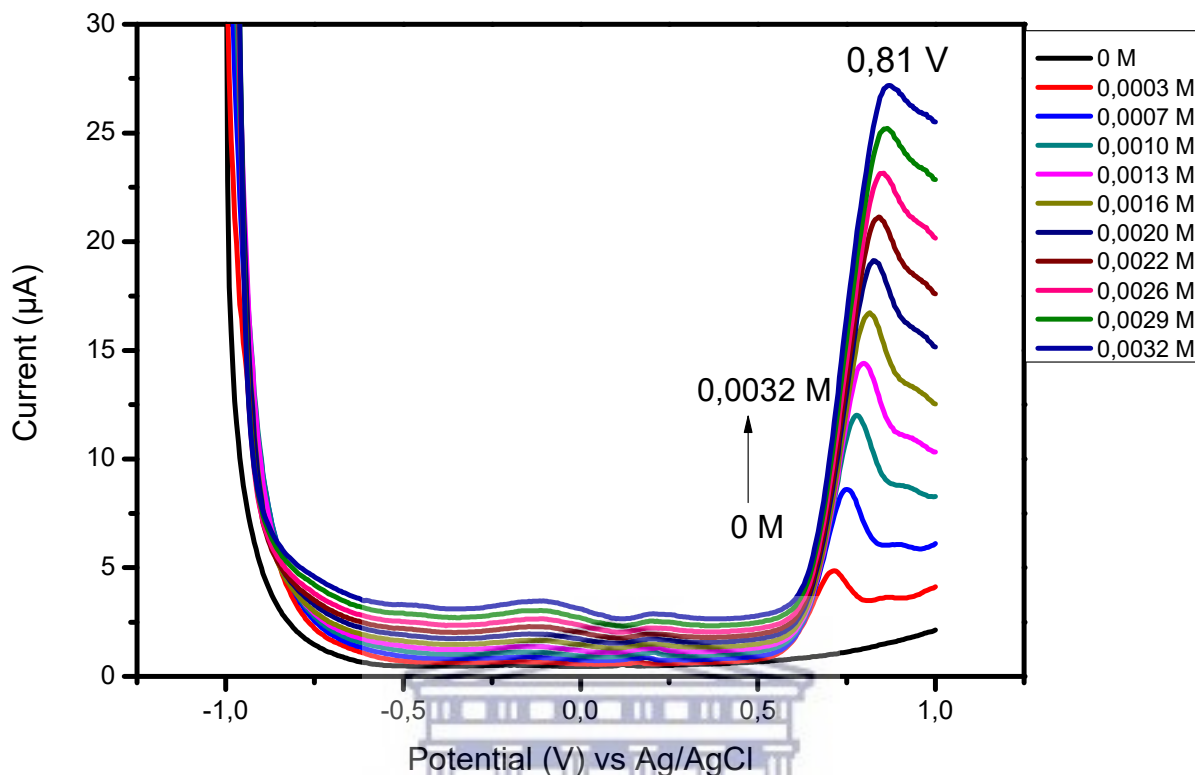


Figure 29: Current response measured by SWV of bare SPCE at increasing concentrations of Norfloxacin in 0.1 M pH7.04 PBS, scan rate 50 mV/s.

Figure 29 shows the current response as a function of Norfloxacin concentration, as measured by square wave voltammetry at a bare screen printed electrode. SWV has the advantage of reporting redox currents with greater sensitivity, due to the fact that the capacitive component of the overall analytical current is removed. Therefore the oxidation peak current associated with Norfloxacin was observed between 0.70 to 0.81 V (vs Ag/AgCl) and the same positive trend was observed over the concentration range investigated.

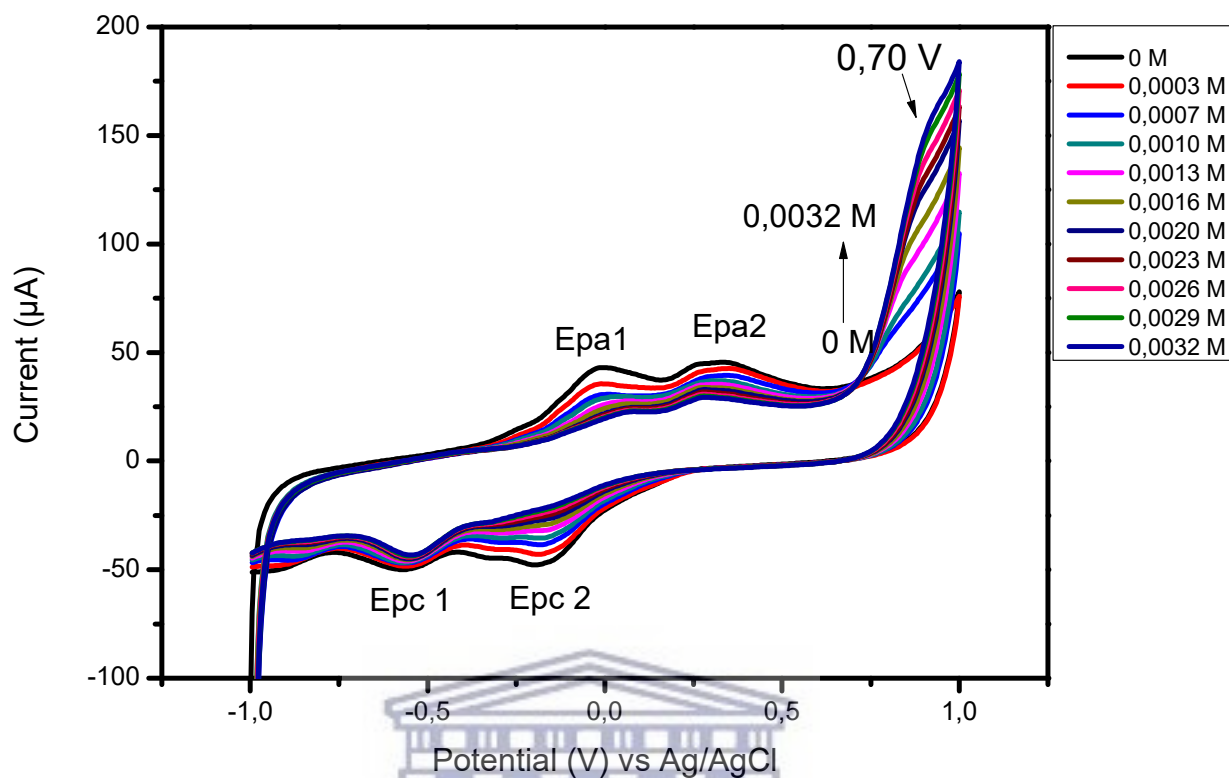


Figure 30: Current response measured by CV of PAA-SPCE at increasing concentrations of Norfloxacin in 0.1 M pH7.04 PBS, scan rate 50 mV/s.

The current response of Norfloxacin at a polyamic acid modified screen printed electrode (Figure 30) as measured by cyclic voltammetry, initially showed no observable response to the presence of Norfloxacin at low concentration (below 0.7 mM). However, continued increase in the analyte concentration produced a poorly resolved peak at 0.7 V (vs Ag/AgCl) after addition of 1.0 mM. During the addition of Norfloxacin to the analytical solution, the reporting peaks of PAA was observed to decrease, particularly in the very low concentration region, indicating that the oxidation mechanism at the PAA modified electrode may involve an initial adsorptive process before the oxidative peak current reverts to the increasing trend associated with oxidation of Norfloxacin.

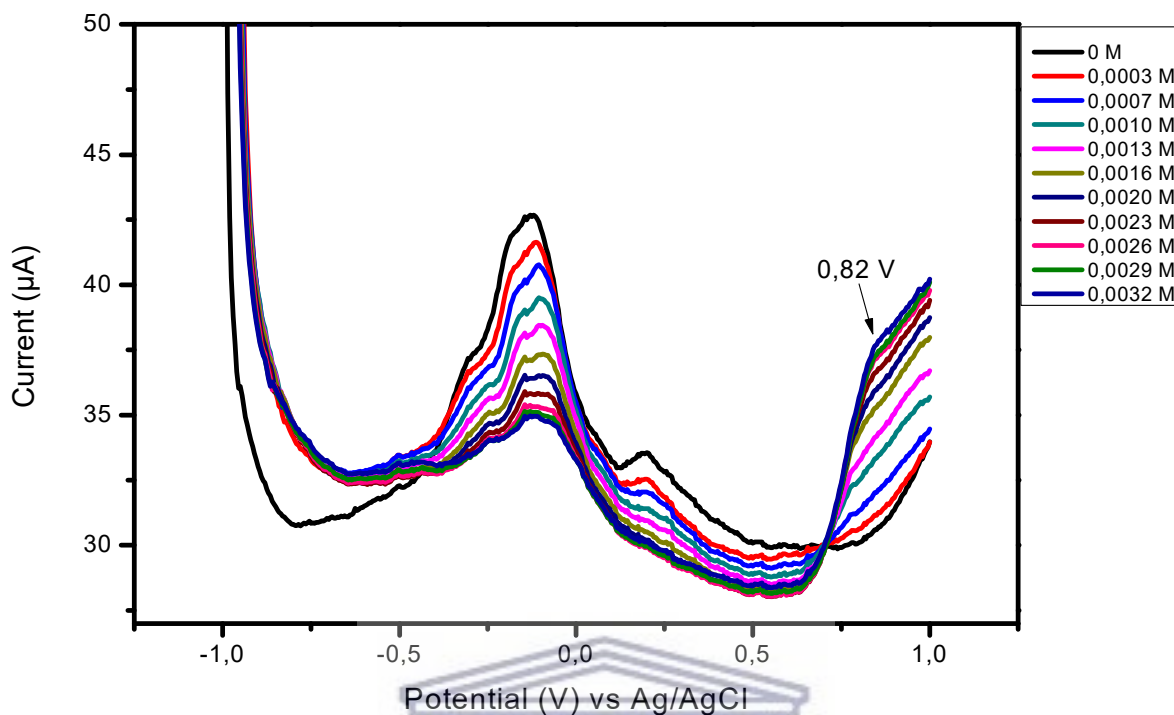


Figure 31: Current response measured by SWV of SPCE-PAA at increasing concentrations of Norfloxacin in 0.1 M pH7.04 PBS, scan rate 50 mV/s.

The oxidative square wave voltammetry of PAA modified screen printed electrode confirmed the increasing current with concentration behaviour observed with cyclic voltammetry with improved resolution of the oxidation peak at 0.82 V (vs Ag/AgCl). The reductive SWV voltammogram did not display a reduction peak which indicated that the oxidation of Norfloxacin is irreversible at PAA modified electrode.

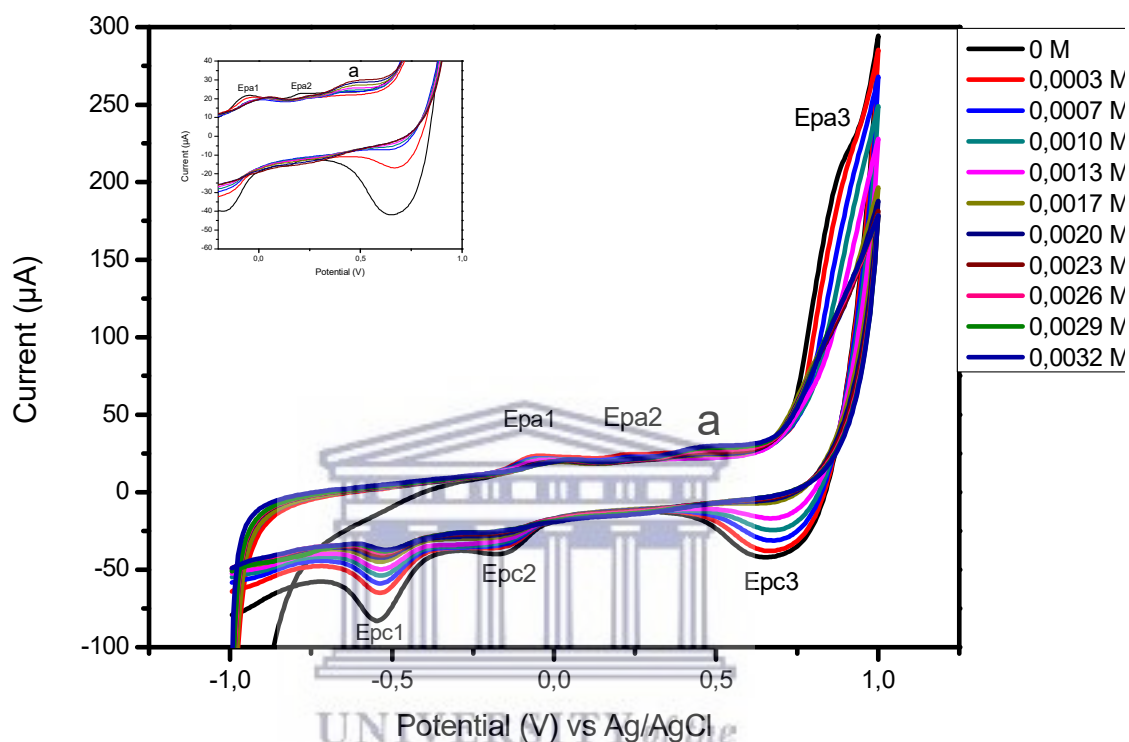


Figure 32: Current response measured by CV of SPCE-PAA- Co NP at increasing concentrations of Norfloxacin in 0.1 M pH 7.04 PBS, scan rate 50 mV/s.

Cyclic voltammetry of the PAA-Co NP modified electrodes showed a similar trend as that of PAA modified electrodes (Figure 32). As the concentration of Norfloxacin increased the peak currents of PAA-Co NP decreased, this could be due to Norfloxacin being adsorbed onto PAA-Co NP in the composite electrodes. At 0.0017 M the peak Epa2 shifted to the peak labelled 'a' as displayed in the zoomed insert (Figure 32) and started to increase with increase in concentration from 0.0017 M. This experiment was done three times but only one electrode showed the peak labelled a.

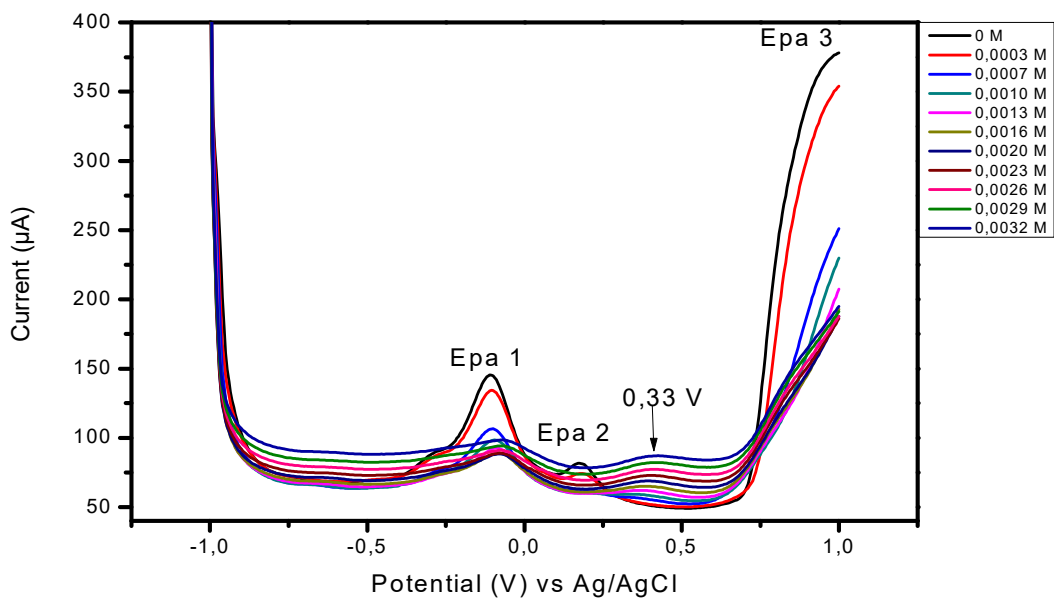


Figure 33: Square wave voltammogram of PAA-Co NP at different concentrations of Norfloxacin in 0.1 M pH 7.04 PBS at scan rate 50 mV/s.

The square wave voltammogram of PAA-Co NP at increasing Norfloxacin concentrations showed that the PAA-Co NP thin films signature peaks first showed a decreasing trend, before responding positively to increased concentration of Norfloxacin (Figure 33). This was consistent with the behaviour of the PAA modified electrodes. At 0.0010 M of Norfloxacin oxidation peak, Epa 2 peak shifted to the right and increased with increase in analyte concentration.

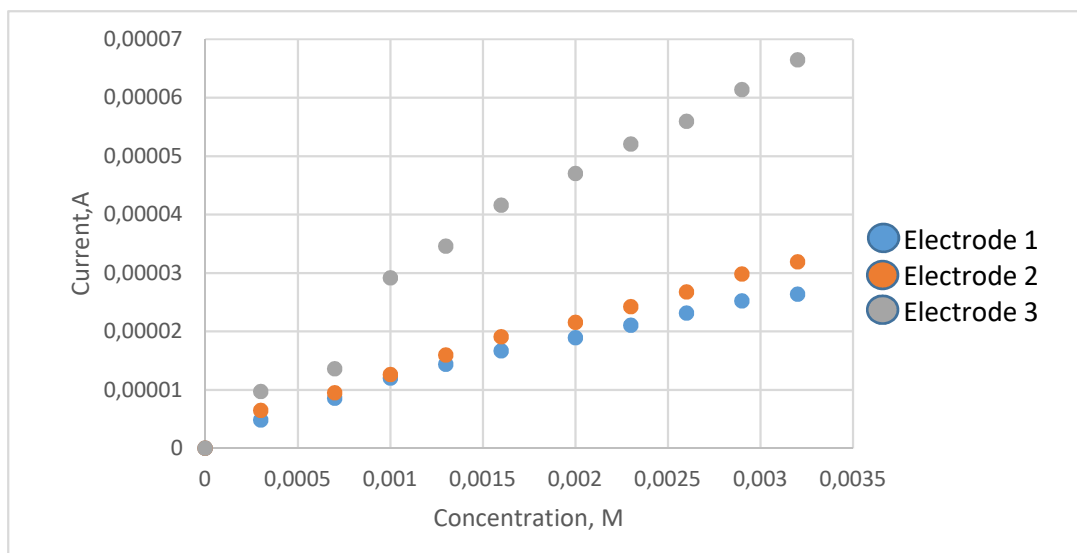


Figure 34: Calibration curves of bare SPCE at different concentrations of Norfloxacin, at scan rate 50 mV/s, n=3.

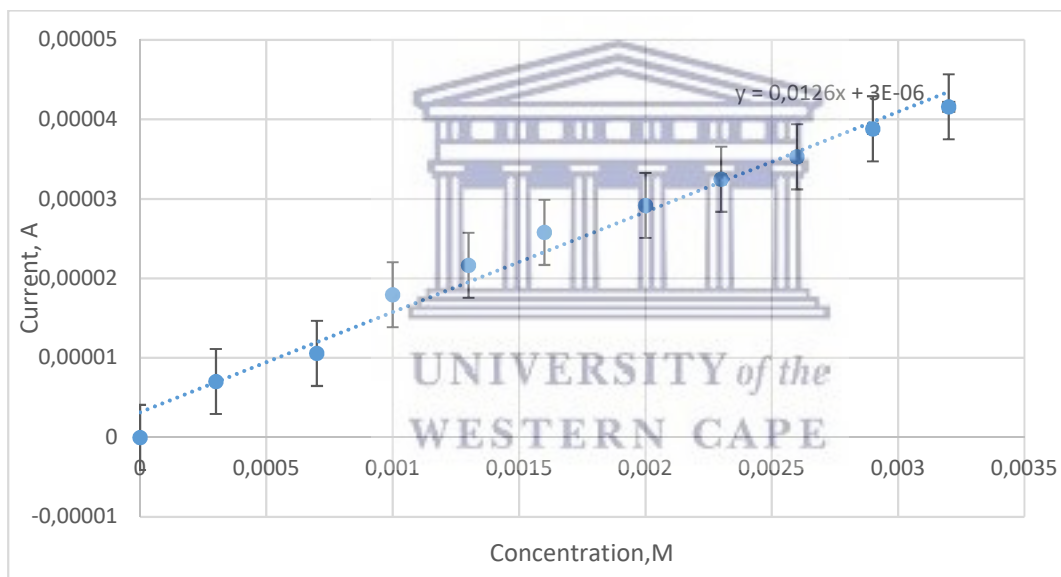


Figure 35: Linear range of the average of the bare electrodes calibration curves at different concentrations of Norfloxacin in 0.1 M pH 7.04 PBS calibration curve, n=3.

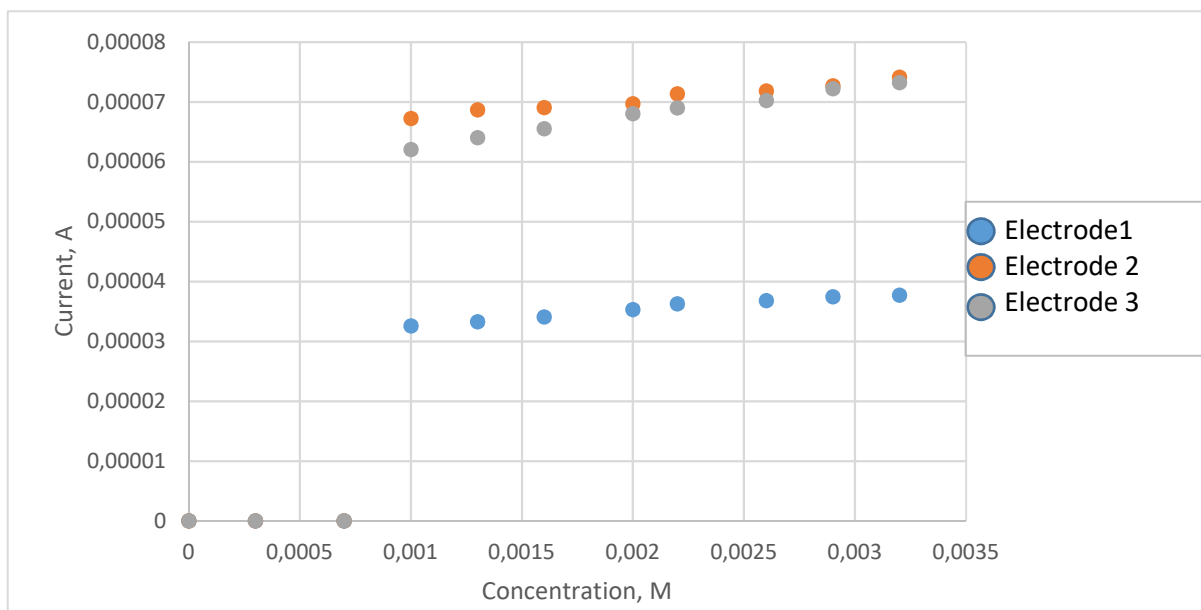


Figure 36: Calibration curves of Modified SPCE with PAA at different concentrations of Norfloxacin.

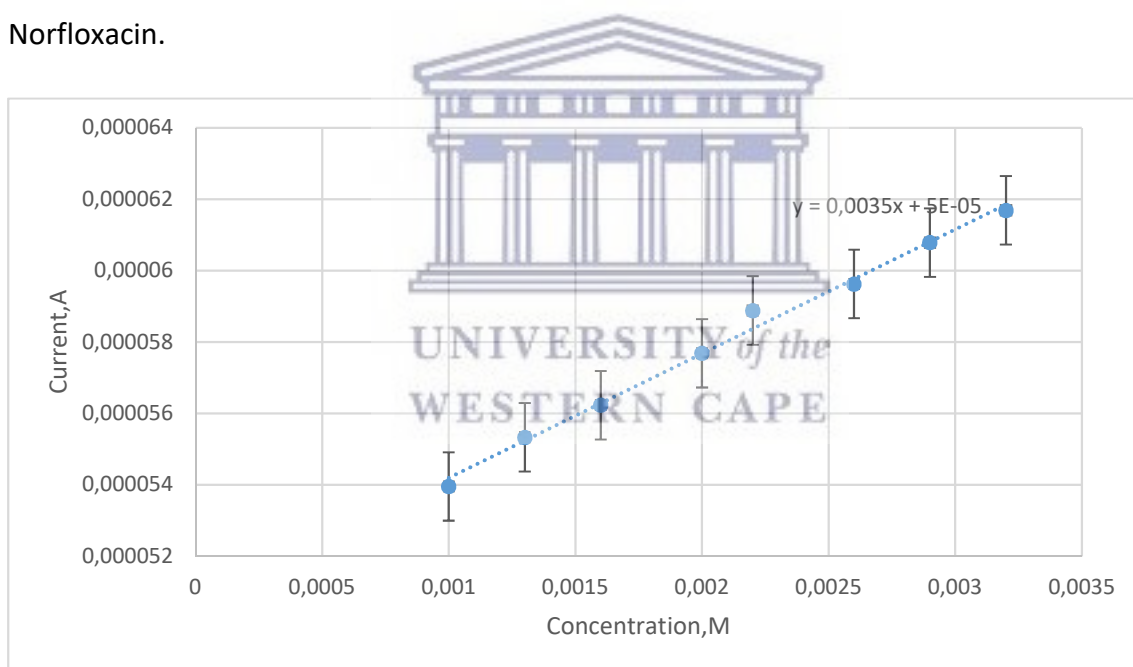


Figure 37: Linear range of the average of the PAA-SPCE calibration curve at different concentrations of Norfloxacin in 0.1 M pH 7.04, n=3.



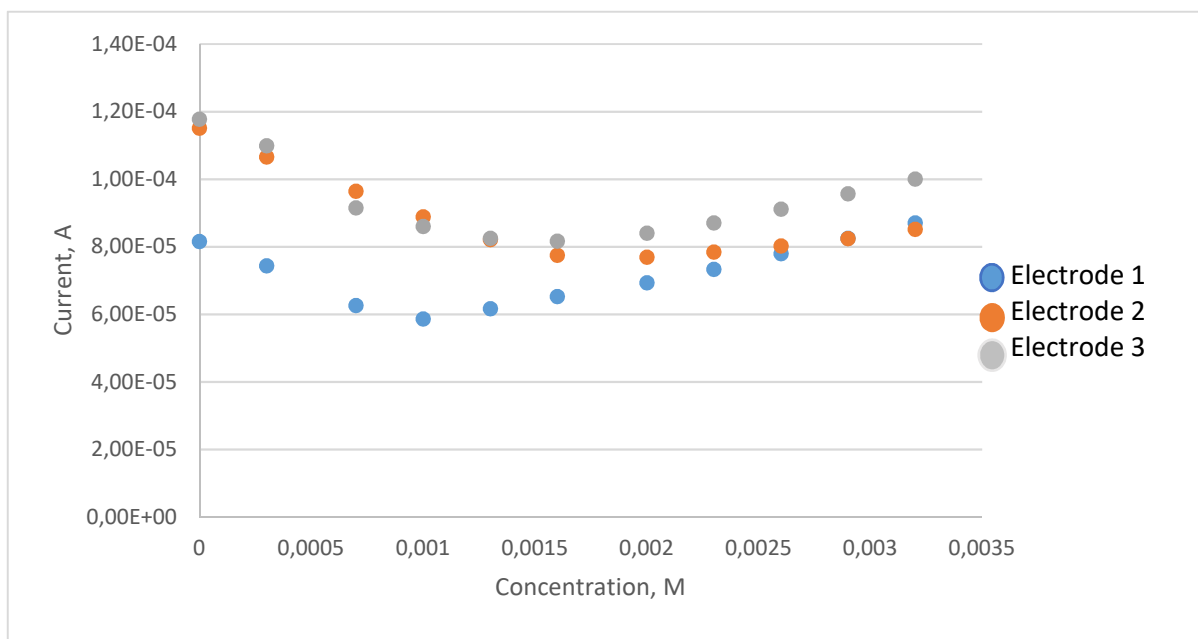


Figure 38: Calibration curve of PAA-Co NP at different concentrations of Norfloxacin in 0.1 M pH7.04 PBS, n=3.

The figures above show the cyclic voltammetric and square wave voltammetric current response of Norfloxacin at bare SPCE, SPCE/PAA and SPCE/PAA-Co NP electrodes. The limit of detection (LOD) which is a measure of the lowest amount of analyte in a sample that the sensor can detect, was calculated using equation 2. All the experiments were repeated three times for each of the three types of electrodes.

$$LOD = 3.3 \times \frac{\sigma}{b} \quad \text{.....Equation 1: Limit of detection}$$

$\sigma$ : Standard deviation of the blank

b: The slope of the calibration curve.

The bare SPCE electrode reported an average for the limit of detection as  $3.7 \times 10^{-3}$  M (STD =  $1.198 \times 10^{-5}$  A, n=3). The calibration curve of the bare electrode at different concentrations of Norfloxacin in Figure 34 showed a linear relationship in the range (0.0 M- 0.0032 M) between the peak current and the Norfloxacin concentration (Figure 35). The linear range for the PAA-SPCE electrodes were observed to be between 0.001 M-0.0032 M and an average of  $14.7 \times 10^{-3}$  M (STD =  $1.426 \times 10^{-5}$  A, n=3) was obtained for the limit of detection for the three modified electrodes at different concentrations of Norfloxacin.

The calibration curve shows that a linear relationship between the peak current and the Norfloxacin concentrations for the electrode modified with PAA was obtained in the range of 0.0010 M-0.0032 M (Figure 37). The obtained limit of detection of the PAA-SPCE sensor at concentrations of Norfloxacin in this study is higher compared to the ones previously reported in literature of  $2,37 \times 10^{-6}$  M by (Goyal, R.N. et al., 2012) and  $3.37 \times 10^{-5}$  M by (Hamnca S. et al 2017), Table 4. It has been previously reported that at a bare electrode the response of Norfloxacin is not good, in this work bare SPCE showed a good response to Norfloxacin as the peak current increased at increasing concentration of Norfloxacin and the peaks were sharp and well defined.

Table 4: Comparison of voltammetric performance of PAA-SPCE with previously reported data for electrochemical detection of Norfloxacin.

Method	LOD	Reference
PAA/Graphene oxide/SPCE	$3.37 \times 10^{-5}$ M	Hamnca S. et al 2017
Basal plane pyrolytic graphite	$2,37 \times 10^{-6}$ M	Goyal, R.N. et al., 2012
PAA-SPCE	$14.7 \times 10^{-3}$ M	present study

The calibration curve for SPCE/PAA-Co NP didn't show an immediate linear response (Figure 38). The Epa 2 (Figure 32) peak started off by decreasing and at 0.0010 M it shifted to the right, to 0.33 V and started to increase as the concentration increased. The chemistry of PAA may have changed due to the presence of Norfloxacin species on the electrode surface which then caused a shift in the peak Epa 2 attributed to PAA hence the peak increased after the shift. The norfloxacin peak was not observed at the PAA-Co NP SPCE. The calibration also displays a decrease at first and then an increase at a certain concentration.

At the unmodified SPCE electrode the peaks of Norfloxacin appear to be sharper and broader compared to the modified electrodes which means at bare electrode the oxidation peak of Norfloxacin had a much faster electron transfer. At the modified electrodes the peaks attributed to PAA were decreasing initially with increase in analyte concentration and the Norfloxacin peak was only observed from 0.0010 M. The decrease in the PAA peaks was due to adsorption of analyte species onto the surface creating a passivating layer that slows down the electron transfer hence the decrease in the peaks of the electrodes. At the electrode

modified with PAA-Co NP the Norfloxacin peak was not observed, in spite of the potential catalytic presence of the Co NP. The peaks attributed to PAA and Co NP decreased with increase in concentration of Norfloxacin which may again be ascribed to fouling at the electrode surface caused by the adsorption of the Norfloxacin or intermediate species from the solution onto the surface of the electrode. PAA also has a strong background electrochemical signature which may further complicate the detection of Norfloxacin.

Norfloxacin was detected at bare SPCE, PAA-SPCE in pH 7.04 0.1 M PBS using cyclic voltammetry and square wave voltammetry. The Norfloxacin peak was observed between 0.70-0.82 V (vs. Ag/AgCl). The obtained  $D_e$ 's for bare SPCE  $3.7 \times 10^{-3}$  M and  $14.7 \times 10^{-3}$  M for PAA-SPCE.



# Chapter 6

## *Paper based electrodes*

*This chapter presents characterization of the fabricated paper electrodes produced by blending the commercial carbon ink with PAA to test the feasibility of polymer blends for the production of screen printing inks. The characterization includes microscopy studies and electrochemical studies. It also includes the electrochemical detection of Norfloxacin at paper based electrode.*

### **6.1 Microscopic characterization:**

Scanning electron microscopy was performed for topographical studies of the paper based screen printed electrodes. The analysis was performed using on a Hitachi Model X-650 Scanning electron analyser.

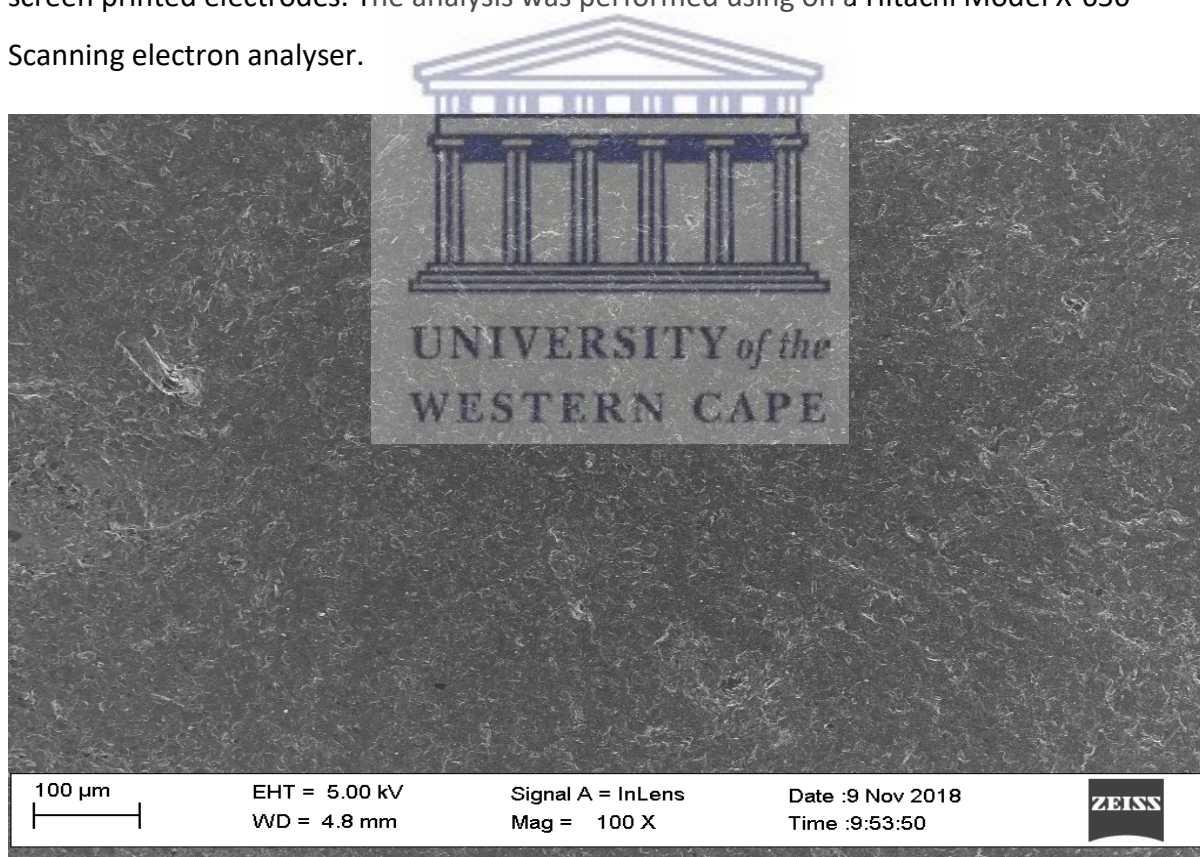


Figure 39: HRSEM image of the surface of the commercial carbon ink working electrode prior to modification.

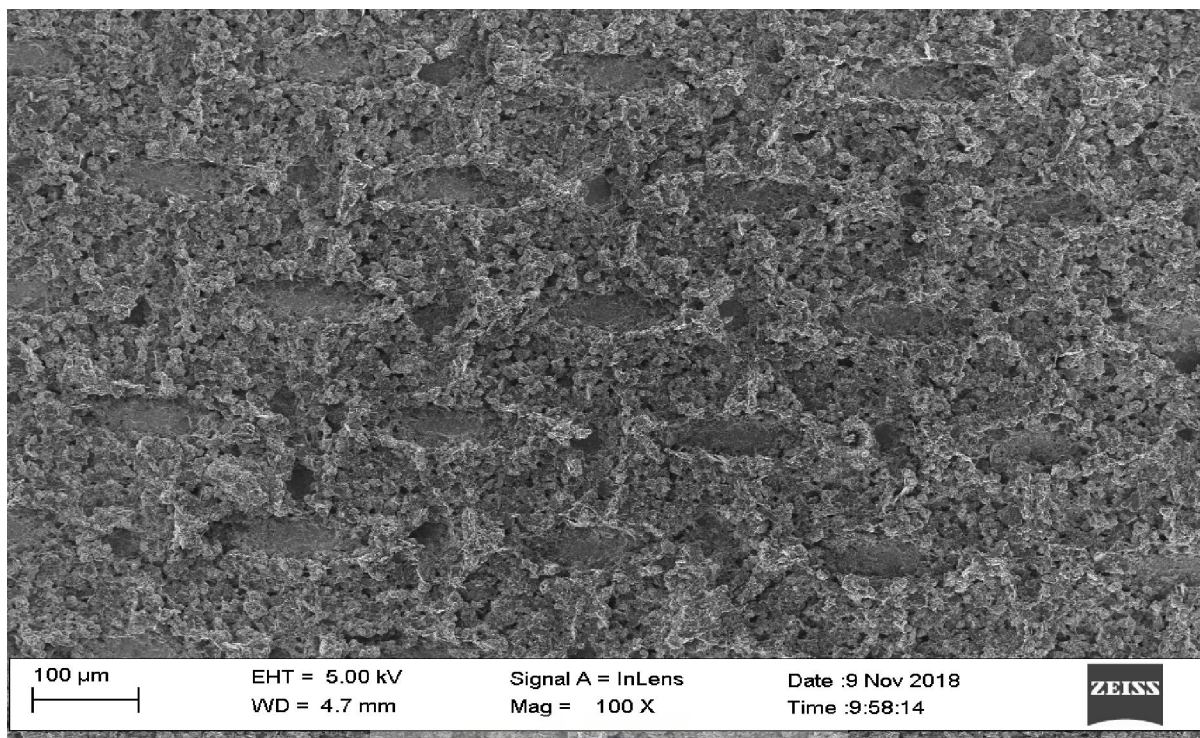


Figure 40: HRSEM image of the surface of the 6%PAA-commercial carbon ink working electrode.

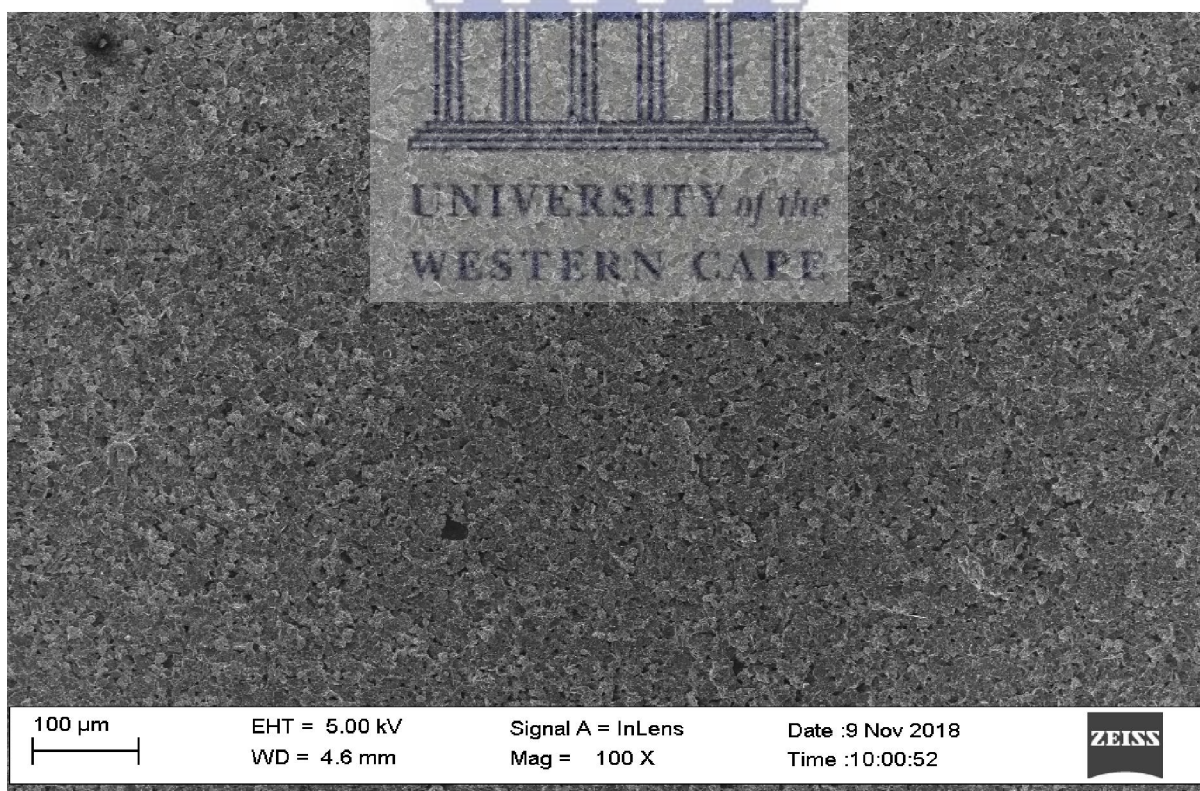


Figure 41: HRSEM image of the surface of 20%PAA-commercial carbon ink working electrode.

Polyamic acid was incorporated into the blended screen printing ink by the bulk method which is usually done before screen printing of the electrodes. In this method different amounts of polyamic acid was mixed with the commercial carbon ink to produce ratios of 6% and 20% PAA, respectively by mass. After thorough mixing the resultant ink was used to print the working electrodes onto photo paper. The paper based electrodes were self-prepared by the screen printing method at the CSIR microfabrication facility (chapter 4) and were characterised using HRSEM to study the surface of the electrodes. The commercial carbon ink electrode displayed a rough surface with a flaky appearance similar to that of a commercial carbon screen printed electrode (Figure 39). The SEM image of 6% of PAA mixed with commercial carbon ink working electrode, displayed dense clusters of polyamic acid (Figure 40). The 20% of PAA mixed with commercial ink shows higher coverage of PAA and the flaky nature of the carbon ink is hardly evident. The surface is fully covered by the polymer and a uniform distribution was observed (Figure 41).

Based on the results obtained from SEM, PAA was uniformly incorporated into the blended ink mixtures and the deposition of the blended inks produced uniformly dispersed blended ink electrodes. Hence the bulk modification method was regarded as successful for introducing polymers into the printing ink mixture in a controlled and systematic manner. As the amount of polyamic acid was increased in the surface of the working electrode took on the micro topography associated with the polymer and the electrode coverage remained optically uniform.

## 6.2 Electrochemical behaviour of the Paper based electrodes

The electrochemical behaviour of the novel screen printed blended ink paper based electrodes were evaluated by cyclic voltammetry. The experiments were carried out in 0.1 M pH 7.04 PBS as well as 5 mM Potassium Ferricyanide in 0.1 M Potassium Chloride as the supporting electrolyte at different scan rates from 10 mV/s to 100 mV/s at a potential window of -1000 mV to 1000 mV. Platinum wire was used as the counter electrode, Ag/AgCl electrode was the reference electrode and the blended ink printed electrodes were configured as the working electrode, in a classical 3 electrode electrochemical cell.

The resolution and position of the  $\text{Fe}^{2+}/\text{Fe}^{3+}$  couple was evaluated, in the electrochemical window between -1000 mV to 1000 mV, at 50 mV/s. The  $\text{Fe}^{2+}/\text{Fe}^{3+}$  peaks were not observed at the commercial carbon ink printed electrode or the 6%PAA-carbon ink modified electrode. However, the peaks of  $\text{Fe}^{2+}/\text{Fe}^{3+}$  were observed at the 20% PAA-carbon ink electrode (Figure 42). The oxidation peak at 317.51 mV and the reduction peak at 71.5 mV showed quasi reversible behaviour based on peak separation of 246 mV.

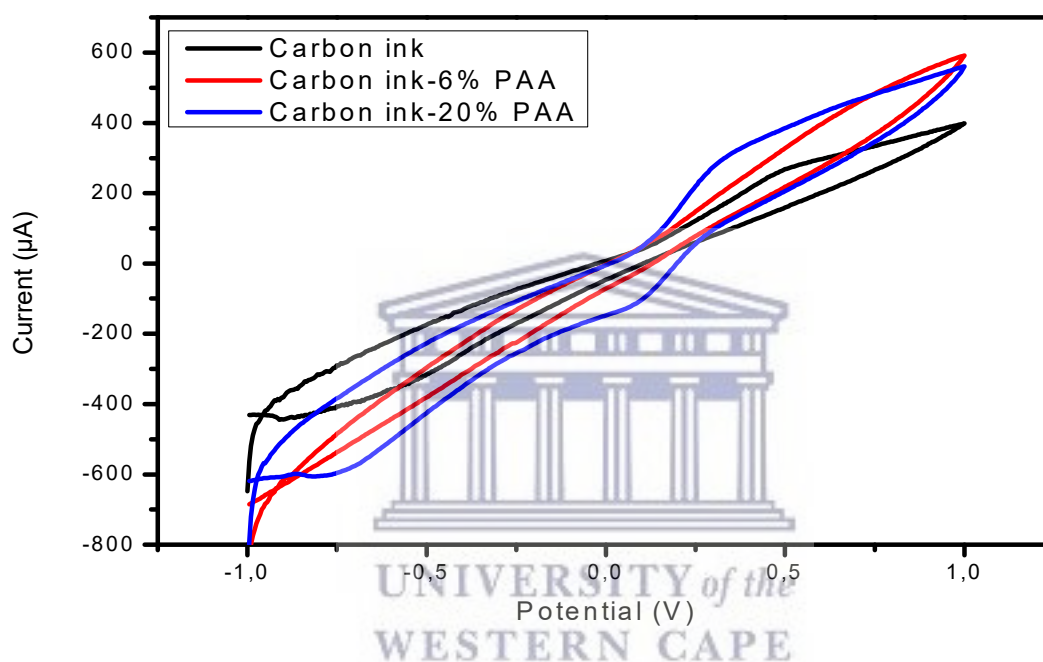


Figure 42: Cyclic voltammogram of the different paper electrodes in 5 mM  $\text{K}_3[\text{Fe}(\text{CN})_6]$  0.1 M KCl at scan rate 50 mV/s.

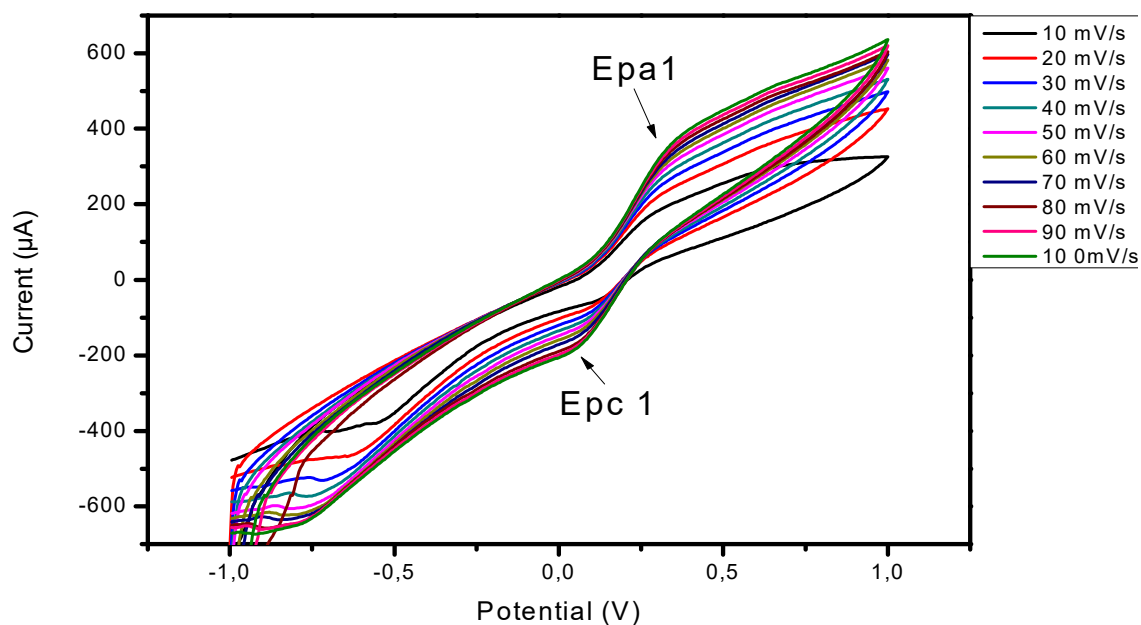


Figure 43: Cyclic voltammogram of 20% PAA-Com carbon ink electrode in 5mM  $K_3Fe(CN)_6$  in 0.1 M KCl at scan rates 10-100 mV/s.

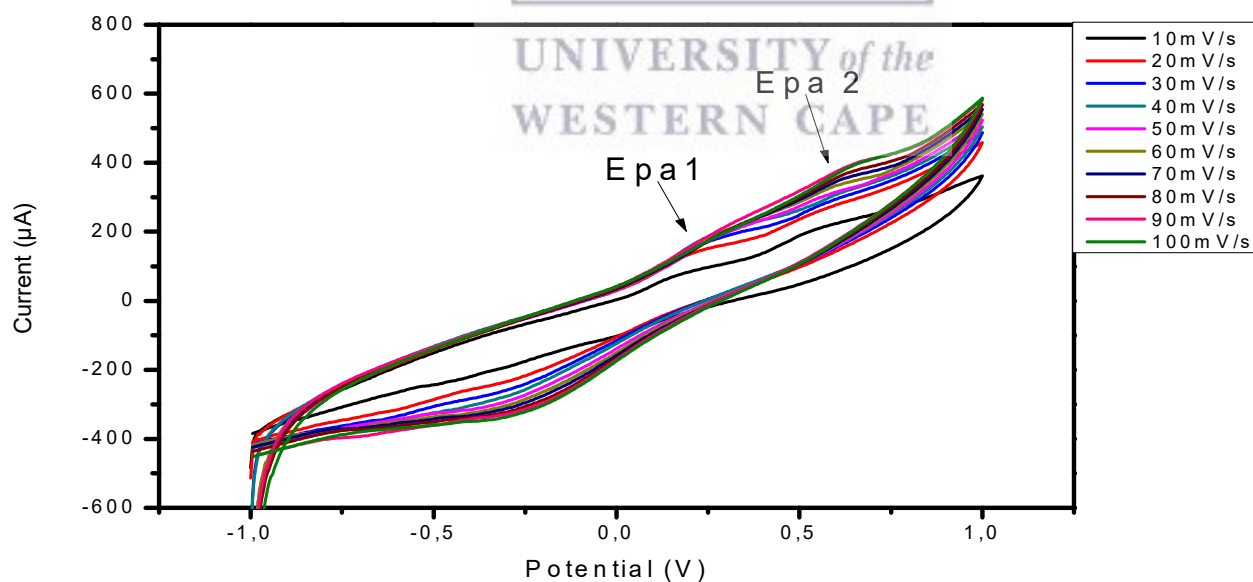


Figure 44: Cyclic voltammogram of 20%PAA- Com carbon electrode ink in pH 7.04 0.1 M PBS at scan rates 10 mV/s-100 mV/s.



The cyclic voltammogram in Figure 44 displayed an irreversible system with only oxidation peaks. The peaks may be due to the presence of PAA in the ink formulation, since the oxidation peaks of PAA do appear between the regions 0.0 V-0.5V. The current peaks increased with increase in scan rate. Figure 43 shows the cyclic voltammogram of the 20%PAA in 5 mM potassium ferricyanide with 0.1 M KCl as the supporting electrolyte. The peak currents increased with increase in scan rate. The cyclic voltammogram displayed a quasi-reversible system with one redox couple. The peak separation  $\Delta E_p$  which gives information about the electron transfer kinetics of the electrochemical process was calculated, and a  $\Delta E_p=0.246$  V was obtained. From the cyclic voltammograms we also see the background current is a bit high, things like the electrode area, concentration of the analyte can have an effect on the magnitude of the current. Electroanalytical performance and sensitivity of the electrode is influenced by the ink composition, the curing temperature, inter electrode distance as well as the kind of ink used. Since commercial carbon ink was used in this study, it is difficult to know what is in the ink as it is proprietary information of the manufacturer so the mixing of the commercial ink with the PAA may also have had an effect on the conductivity of the sensors.

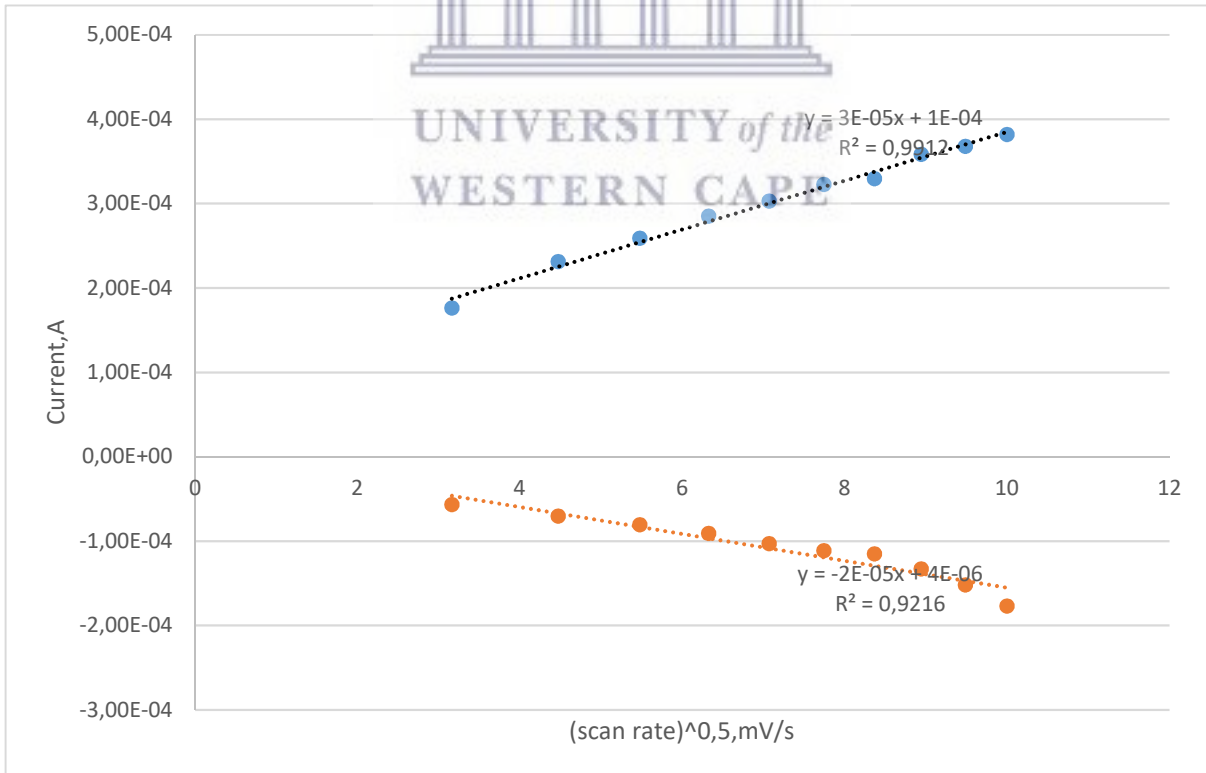


Figure 45: Randles Sevcik plot of 20%PAA-Commercial carbon ink electrode in 5 mM  $K_3Fe(CN)_6$  with 0.1 M KCl.

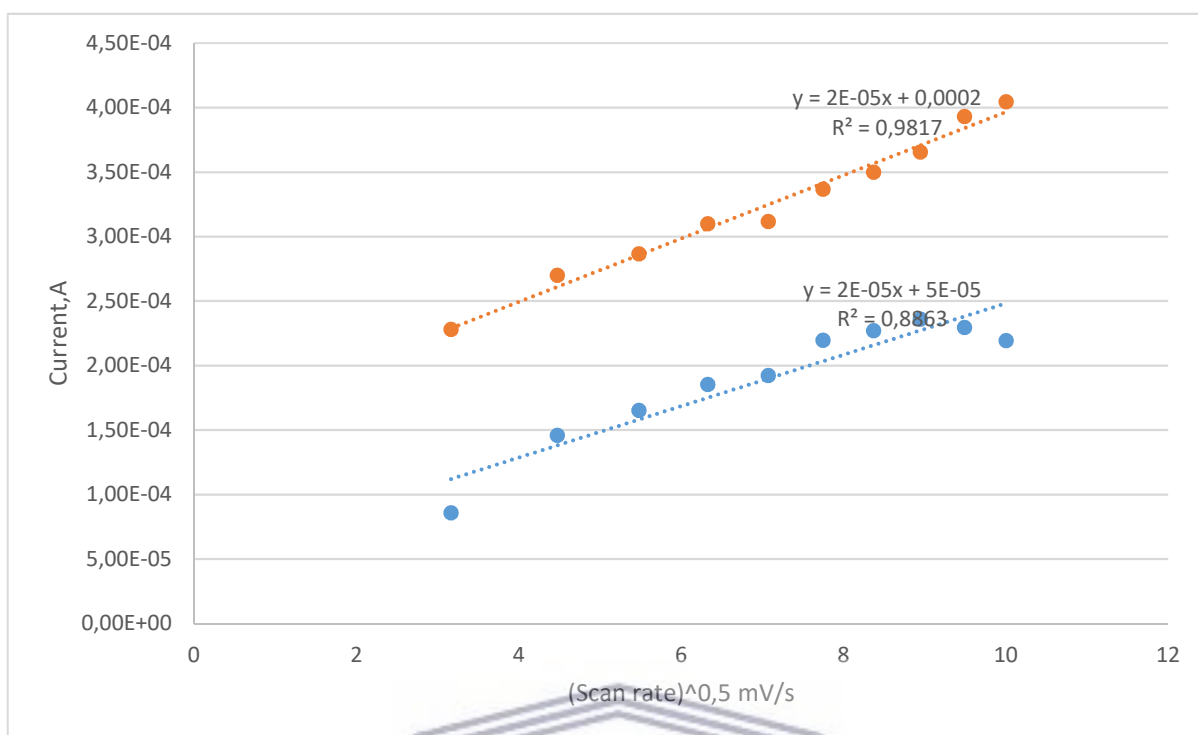


Figure 46: Randles Sevcik plot of 20%PAA-Commercial carbon ink electrode in 0.1 M pH 7.04 PBS.

Randles Sevcik plot was used to study the relationship between the square root scan rate and the current. Both Figure 45 and 46 showed that the current increased linearly with the square root scan rate. The voltammetric response was further assessed in terms of Randles Sevcik equation. Since Figure 46 displayed an irreversible system therefore equation 3 was used to calculate the diffusion coefficient:

$$I_p = 2.99 \times 10^5 \times n \times (\alpha n_a)^{0.5} \times A \times C \times D^{0.5} \times V^{0.5} \dots \text{Equation 3}$$

Where  $\alpha$  is the transfer coefficient,  $n_a$  is the number of electrons involved in a charge transfer step. The calculated  $D_e$  for Figure 46 was 0.012273 cm<sup>2</sup>/s. Figure 45 Randles Sevcik plot of 20%PAA-commercial carbon ink electrode in 5 mM K<sub>3</sub>Fe(CN)<sub>6</sub> with 0.1 M KCl displayed a reversible system therefore equation 1 was used to calculate the diffusion coefficient. The obtained  $D_e$ 's were 0.013326 cm<sup>2</sup>/s for  $E_{pa}$  and 0.010881 cm<sup>2</sup>/s for  $E_{pc}$ .

### 6.3 Charge calculation

Charge is associated with the electron transfer of the reaction. Faraday's law states the number of moles of a substance  $m$ , produced or consumed during an electrode process is proportional to the electric current passed through the electrode so the amount of chemical reaction caused by a flow of current is proportional to the electricity passed. Charge transfer reactions that take place at an electrochemical interface are equal to the product of the number of the reacting species  $N$ , the stoichiometric number of the electrons  $n$  as well as the elementary charge. Following the success of the polymer inclusion in commercial printing ink, the feasibility of blending the PAA polymer with another high surface area carbon material i.e. multiwall carbon nanotubes, were also investigated. In this way 6 sets of electrodes were fabricated in total in this study.

Table 5: Response of novel screen printed paper based electrodes.

Electrode	Epa	Epc	Peak separation	Charge, C	Standard deviation, n=3
6%PAA-MWCNT	X	X	-	$6.19 \times 10^{-5}$	$1.15 \times 10^{-5}$
10%PAA-MWCNT	X	X	-	$5.4 \times 10^{-5}$	$5.11 \times 10^{-6}$
6%PAA-Com carbon ink	X	X	-	$3.591 \times 10^{-5}$	$5.02 \times 10^{-6}$
20%PAA-Com carbon ink	√	√	0,246 V	$4.37 \times 10^{-5}$	$1.66 \times 10^{-6}$
Com carbon ink	X	X	-	$2.41 \times 10^{-5}$	$3.39 \times 10^{-7}$
MWCNT ink	X	X	-	-	-

x- No peaks observed, √- Peaks observed

Electrodes at which Faradaic process occur, are usually referred to as charge transfer electrodes. Therefore, the charge of the electrode was calculated by applying a simplified equation (4) at a fixed point in time (s) corresponding to the maximum oxidation current for  $Fe^{2+}/Fe^{3+}$ , when the peaks were present in the voltammogram.

$$Q = I \times T \dots\dots 4$$

where Q is the charge C, I is the current A and t is the time in seconds.

Table 5 summarises the parameters evaluated for the electrodes fabricated in this study. The electrodes were all characterized by cyclic voltammetry and all experiments were repeated three times for all the electrodes. Only the 20%PAA-commercial carbon ink electrode

responded better compared to the other electrodes as the ferricyanide peaks were only present in the 20%PAA-commercial carbon ink. The charge was also calculated using a simplified formula for calculating charge. The table displays the calculated charge. The charge obtained for the MWCNT/PAA electrodes displayed a greater charge compared to the commercial carbon ink/PAA electrodes. The MWCNT/PAA also showed a very high background current compared to the Com carbon ink/PAA electrodes hence they were not used for further studies. As displayed on the table, as the content of PAA increased in all the electrodes the charge also increased.

## 6.4 Electrochemical detection of Norfloxacin

The 20%PAA-Carbon ink working electrode was further used for electrochemical detection of Norfloxacin since it was the only electrode that responded better in the electrochemical characterization in 5 mM  $K_3Fe(CN)_6$  with 0.1 M KCl.

Electrochemical detection of Norfloxacin was performed using square wave voltammetry at the paper based electrode in 0.1 M pH7.04 PBS at a scan rate of 50 mV/s.

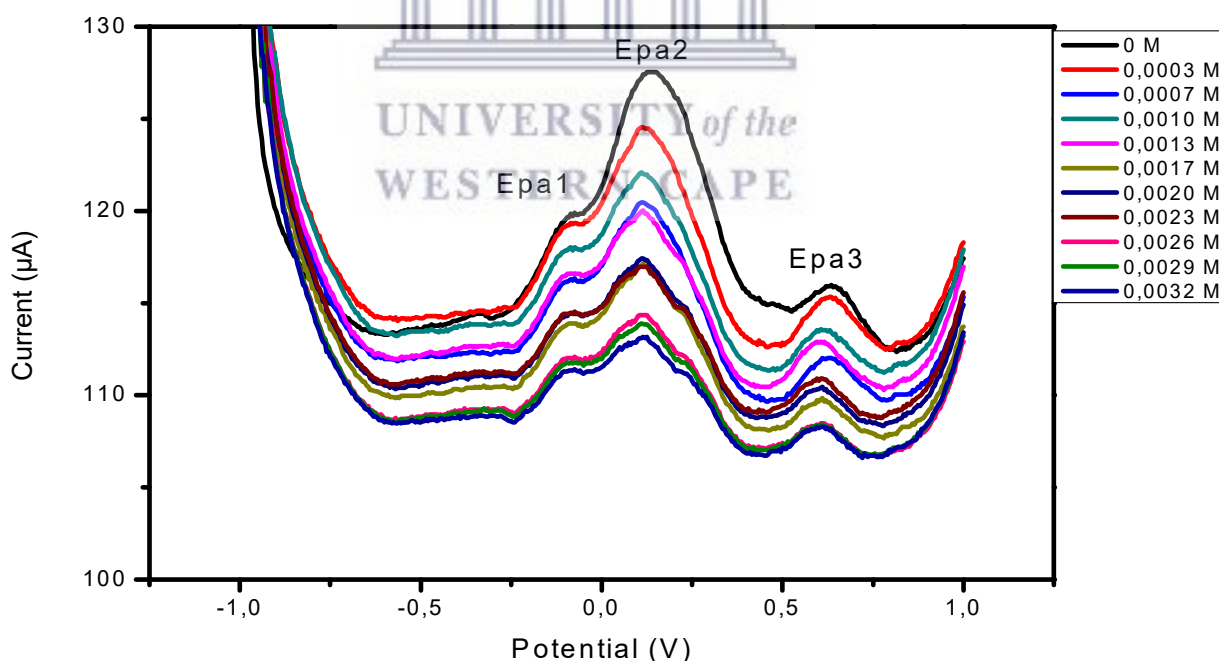


Figure 47: Electrochemical detection of Norfloxacin at 20%PAA-Commercial carbon ink electrode in pH 7.04 0.1 M PBS.

Figure 47 displays the square wave voltammetry response of Norfloxacin at the paper based electrode. At 0 M we see the peaks that are attributed to PAA and as Norfloxacin was added the peaks started to decrease as the concentration of Norfloxacin was increased. The Norfloxacin peak which usually appears between 0.70 V and 0.90 V (vs Ag/AgCl) was not observed in this case. This can be due to Norfloxacin having a blocking effect at the electrode surface and electrolyte interface, which suggest the species from Norfloxacin are getting adsorbed to the electrode surface which then slows down electron transfer, hence the decrease of peak currents as the concentration increases. The calibration curve observed in Figure 48 also shows that the current decreases linearly as the concentration increased.

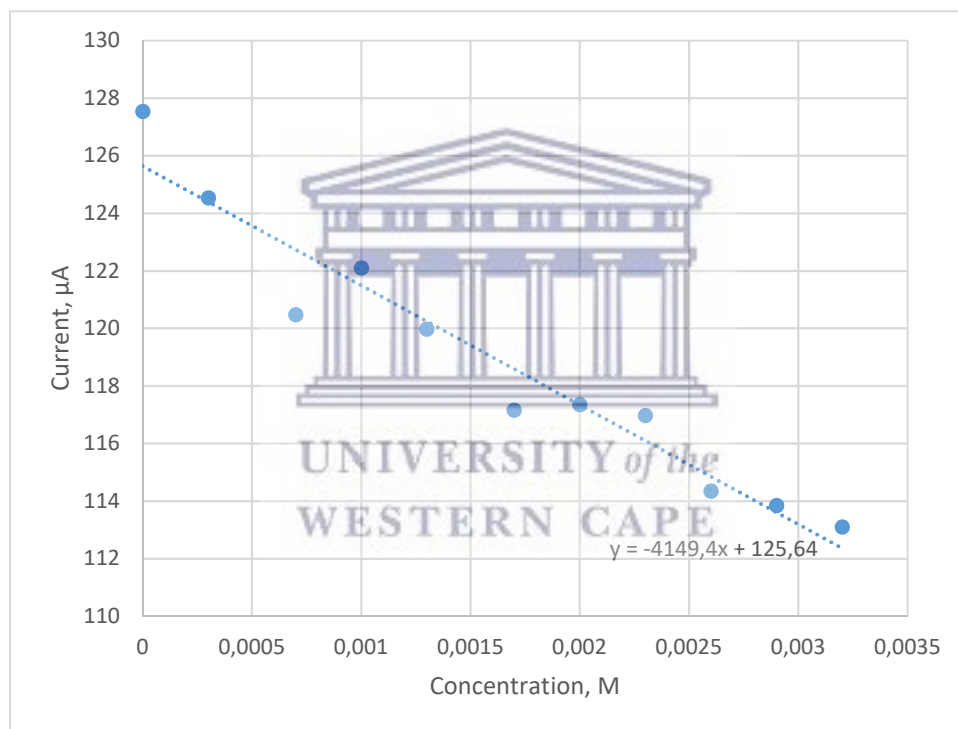


Figure 48: Calibration curve of detection of Norfloxacin at 20%PAA-Commercial carbon ink electrode.

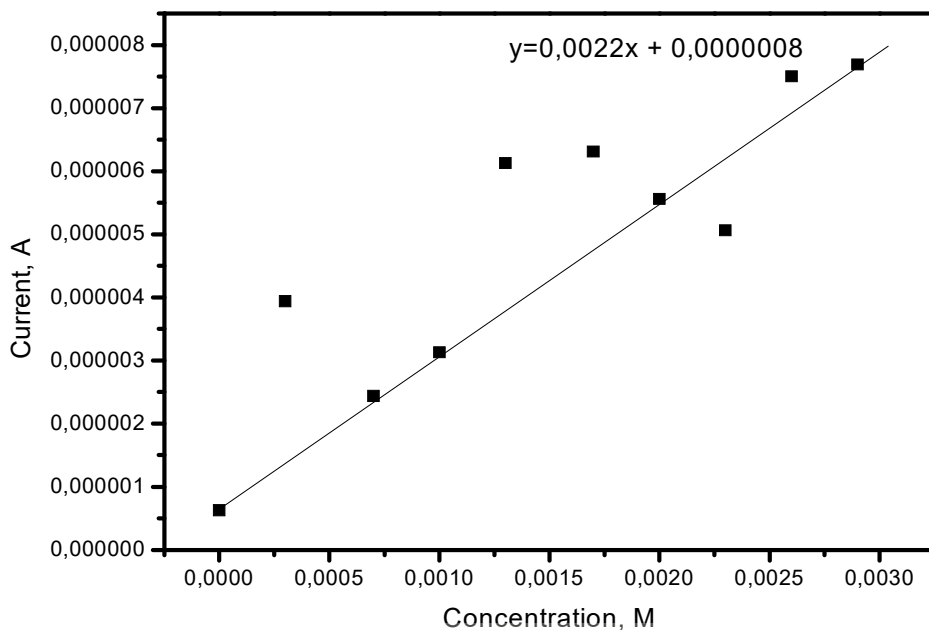


Figure 49: Linear plot of at 20%PAA-com carbon ink electrode at different concentrations of Norfloxacin.

The limit of detection for the electrochemical detection for Norfloxacin by square wave voltammetry at the 20%PAA-Commercial carbon working electrode in pH 7.04 0.1 M PBS was calculated. A limit of detection of  $7.93 \times 10^{-4}$  M was obtained with a sensitivity of 0.0022 A/M. There has not been work reported on screen printable ink made from polyamic acid or polyamic acid screen printable ink incorporated with other materials, but there has been work reported on polymer based modified screen printed paper based electrode. In the study that was reported by Kit-Anan Worrarpong et al, 2012, where they modified the working electrode with polyaniline they obtained a good detection limit when detecting ascorbic acid.

The paper based screen printed electrodes were characterised by HRSEM and CV. The HRSEM images showed as the amount of PAA increased in the PAA-Commercial ink working electrodes the surface of the working electrode became more uniform and less rough. The 20% PAA-Commercial ink working electrode was further characterised by cyclic voltammetry. The obtained diffusion coefficient for the 20%PAA-Commercial carbon ink working electrode in pH 7.04 0.1 M PBS was  $0.012273 \text{ cm}^2/\text{s}$ . The diffusion coefficient for the 20%PAA-Commercial carbon ink working electrode in 5 mM  $\text{K}_3\text{Fe}(\text{CN})_6$  with 0.1 M KCl  $0.013326 \text{ cm}^2/\text{s}$  and  $0.010881$

$\text{cm}^2/\text{s}$  . The obtained limit of detection for Norfloxacin at the 20%PAA-Commercial carbon ink electrode was  $7.93 \times 10^{-4}$  M.



# Chapter 7

## *Conclusion and Future works*

### **Conclusion**

Paper based electrodes provide a sensing platform that is cost effective, simple to fabricate, accurate, rapid detection of analytes. This tool uses paper as a substrate for printing the electrodes. The World Health Organisation set the criteria, ASSURED for diagnostic devices and microfluidic paper based electrochemical sensing devices comply with this criteria as they are affordable, sensitive, specific, user friendly, robust, equipment free and deliverable to those that need them. The methods that are currently being used for detection of antibiotic residues in an aqueous system suffer from a number of disadvantages such as being time consuming, expensive and they also require large expensive equipment. By developing sensors like paper based electrochemical sensors, it will make it easier to keep track and to quantify the concentrations of the pharmaceutical contaminants in the water. According to the WHO report titled *Pharmaceuticals in Drinking Water*, most countries do not have programmes that can be used to monitor pharmaceuticals in drinking water this is due to lack of availability of routine analytical technologies and laboratory infrastructure to detect pharmaceuticals. Paper based electrodes can further be integrated into microfluidic paper devices to develop point of care devices that can used for environmental analysis and monitoring of pharmaceutical contaminants in water especially in countries that do not have access to laboratories.

This study reported on the development of a screen printable ink for paper based electrochemical sensor for detection of antibiotic residues in water. A screen printable ink was successfully fabricated using commercial carbon black ink and synthesised polyamic acid and paper based electrodes were successfully fabricated by screen print technology. Paper based electrodes can be characterised by SEM to study the way the sensing elements are distributed as well as the materials used for the modification of the working electrode surface. Cyclic voltammetry and square wave voltammetry are electrochemical techniques that can be used to study the electrochemical behaviour or performance of the paper electrodes.

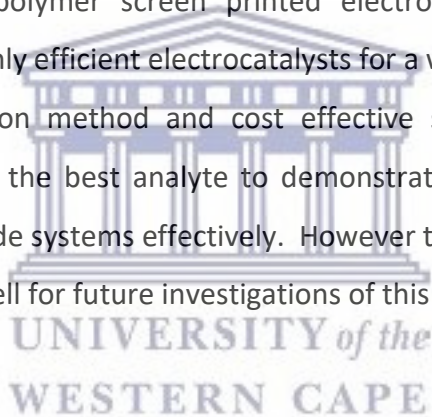


Polyamic acid and cobalt nanoparticles were successfully synthesised and characterized. Cobalt nanoparticles were synthesised using a chemical reducing method and polyamic acid was synthesised by in situ polymerization. PAA and Co NP were characterised by CV, HRSEM, SAXS, and HRTEM. CV was used to study the electrochemical behaviour of PAA, Co and PAA-Co at a SPCE. The diffusion coefficient, formal potential and peak separations were calculated. The cyclic voltammogram of PAA-Co NP composite showed the incorporation of Co NP into PAA. The cyclic voltammogram of PAA-Co NP displayed the current peaks that were present in both the PAA and Co NP cyclic voltammogram. FTIR confirmed the functional groups that are present in PAA and confirmed that PAA was synthesized. SEM showed clusters of PAA with big surface areas. The electrochemical characterization of PAA, Co NP and PAA-Co NP showed that the materials were electroactive.

Norfloxacin was electrochemically detected using cyclic voltammetry and square wave voltammetry at bare SPCE, PAA-SPCE and PAA/Co NP-SPCE. The limit of detections were calculated for the bare electrode and the modified electrode sensor. PAA, Co NP and PAA-Co NP were electrodeposited on to SPCE and Norfloxacin was detected in 0.1 M pH7.04 PBS. The decrease in the current peaks of PAA with increase in concentration of Norfloxacin observed in the PAA-SPCE and PAA-Co NP SPCE cyclic voltammograms was caused by the adsorption of Norfloxacin species onto the surface of the electrodes. The Norfloxacin signal appeared between 0.70 V-0.85 V (vs Ag/AgCl). The calculated limit of detection was  $14.7 \times 10^{-3}$  M for PAA-SPCE which is high compared to the ones previously reported in literature. The bare SPCE had an average limit of detection of  $37.1 \times 10^{-4}$  M. Although the limit of detection in this study for the modified electrode with PAA is greater compared to the ones previously reported in literature the steps required for modification of the electrodes in this work were not complicated.

A screen printable ink was successful developed by bulk modification, mixing different amounts of PAA with commercial carbon ink. Not a lot of work has been reported on polymer based screen printable ink for electrodes fabrication. Most work that has been reported on polymer based electrodes uses two printing techniques where the polymer is inkjet-printed onto the carbon black working electrode. Screen printing technology offers a quicker, inexpensive way to develop electrodes. The electrodes were successfully printed onto photo paper by screen print technology. The electrodes were further characterised by SEM to study

the surface morphology and CV to study the electrochemical behaviour of the electrodes. The SEM images showed as the amount of PAA present in the working electrode increased the surface of the electrode became less rough and more uniform surface was observed compared to the commercial carbon ink electrode with no PAA which showed a rough surface with flake like particles therefore PAA was successfully incorporated into the commercial carbon ink. The electrochemical behaviour was studied in 0.1 M pH7.04 PBS as well as 5 mM  $K_3FeCN_6$  prepared in 0.1 M KCl. The 20%PAA-commercial ink electrode showed the best electrochemical behaviour compared to all other commercial carbon ink blended electrodes as well as the MWCNT blended electrodes. However the main outcome of the polymer blended electrodes, is the fact that commercial inks can be readily modified with semi-conductive polymers such as PAA, to impart their superior properties for redox electrochemistry onto the novel paper based printed electrodes. This successful demonstration of blended polymer screen printed electrodes, opens up a world of possibilities for producing highly efficient electrocatalysts for a wide range of applications, by using simple bulk modification method and cost effective screen printing onto paper. Norfloxacin was perhaps not the best analyte to demonstrate the quantitative analytical reporting of the novel electrode systems effectively. However the success achieved with this challenging example bodes well for future investigations of this class of compounds.



## Future works:

Improving reproducibility of the screen printed paper based electrodes: Reproducibility is one of the major challenges that screen printed electrodes faces. Things like curing process of the ink, ink viscosity, ink composition, screen type used for printing, screen printing equipment etc. can have an effect on the repeatability of the results. One of the ways we can go about to improve the repeatability of the results is by developing our own ink instead of using commercial ink as we don't really know what is in the commercial ink because manufacturers do not share all the information related to the composition of the ink. By developing our ink we will know the contents present the ink and also know whether what is in the ink is compatible with other conductive materials that we would like to add in the ink to improve electron transfer rate, conductivity and sensitivity. We can also try and incorporate different polymers to the working electrode. Further we can compare commercial ink electrodes with synthesised ink electrodes and see which of the electrodes give better results.

Printing Methods: In this work screen printing method was used to fabricate the electrodes. We can also use screen printing method with inkjet printing method to fabricate the electrodes. We can do this first by screen printing the carbon ink and inkjet printing the polymer materials or nanomaterials. Other methods to integrate polymer materials onto printed devices such as drop casting, electrodeposition, pen writing etc can also be tried to see which method works best for printing of polymer materials.

Integration of screen printed electrodes into microfluidic devices: We will also focus on integrating the printed electrodes into microfluidic paper analytical devices to fabricate the microfluidic electrochemical paper devices. First we would have to fabricate the microfluidic paper based device that have sample pre-treatment zones, mixing zones and detection zones. We will also integrate portable potentiostats to develop the point of care devices that can be used not only in the laboratory but can also be used outside the laboratory.

# References

- Agbabiaka, A., Wiltfong, M. and Park, C., 2013. Small angle X-ray scattering technique for the particle size distribution of nonporous nanoparticles. *Journal of Nanoparticles*, 2013.
- Akyazi, T., Basabe-Desmonts, L. and Benito-Lopez, F., 2018. Review on microfluidic paper-based analytical devices towards commercialisation. *Analytica Chimica Acta*, 1001, pp.1-17.
- Aleeva, Y. and Pignataro, B., 2014. Recent advances in upscalable wet methods and ink formulations for printed electronics. *Journal of Materials Chemistry C*, 2(32), pp.6436-6453.
- Ansari, S.M., Bhor, R.D., Pai, K.R., Sen, D., Mazumder, S., Ghosh, K., Kolekar, Y.D. and Ramana, C.V., 2017. Cobalt nanoparticles for biomedical applications: Facile synthesis, physiochemical characterization, cytotoxicity behavior and biocompatibility. *Applied Surface Science*, 414, pp.171-187.
- Antuna Jimenez, D., Diaz Diaz, G., Blanco Lopez, M.D.Z., Lobo Castanon, M.J., Miranda Ordieres, A.J. and Tunun Blanco, P., 2012. Molecularly Imprinted electrochemical sensors: past, present, and future. *Molecularly Imprinted Sensors*. 2012.
- Badihi-Mossberg, M., Buchner, V. and Rishpon, J., 2007. Electrochemical biosensors for pollutants in the environment. *Electroanalysis: An International Journal Devoted to Fundamental and Practical Aspects of Electroanalysis*, 19(19-20), pp.2015-2028.
- Chen, M. and Chu, W., 2012. Degradation of antibiotic norfloxacin in aqueous solution by visible-light-mediated C-TiO<sub>2</sub> photocatalysis. *Journal of Hazardous Materials*, 219, pp.183-189.
- Cinti, S., Mazzaracchio, V., Cacciotti, I., Moscone, D. and Arduini, F., 2017. Carbon black-modified electrodes screen-printed onto paper towel, waxed paper and parafilm m<sup>®</sup>. *Sensors*, 17(10), p.2267.

Couto, R.A.S., Lima, J.L.F.C. and Quinaz, M.B., 2016. Recent developments, characteristics and potential applications of screen-printed electrodes in pharmaceutical and biological analysis. *Talanta*, 146, pp.801-814.

da Silva, H., Pacheco, J., Silva, J., Viswanathan, S. and Delerue-Matos, C., 2015. Molecularly imprinted sensor for voltammetric detection of norfloxacin. *Sensors and Actuators B: Chemical*, 219, pp.301-307.

De Groot, M.T. and Koper, M.T., 2008. Redox transitions of chromium, manganese, iron, cobalt and nickel protoporphyrins in aqueous solution. *Physical Chemistry Chemical Physics*, 10(7), pp.1023-1031.

Dungchai, W., Chailapakul, O. and Henry, C.S., 2009. Electrochemical detection for paper-based microfluidics. *Analytical Chemistry*, 81(14), pp.5821-5826.

Elveflowcom.2019.Elveflow. [Online]. [18 March 2019]. Available from: <http://www.elveflow.com/microfluidic-tutorials/microfluidic-reviews-and-tutorials/microfluidics/>

El-Zanfaly, H.T., 2015. Antibiotic resistant bacteria: a factor to be considered in safe drinking water. *Journal of Environment Protection and Sustainable Development*, 1(3), pp.134-143.

Ghoneim, M.M., Radi, A. and Beltagi, A.M, 2001. Determination of norfloxacin by square-wave adsorptive voltammetry on a glassy carbon electrode. *Journal of Pharmaceutical and Biomedical Analysis*, 25(2), pp. 205-210.

Goyal, R.N., Rana, A.R.S. and Chasta, H., 2012. Electrochemical sensor for the sensitive determination of norfloxacin in human urine and pharmaceuticals. *Bioelectrochemistry*, 83, pp.46-51.

Hamnca, S., Phelane, L., Iwuoha, E. and Baker, P., 2017. Electrochemical Determination of Neomycin and Norfloxacin at a Novel Polymer Nanocomposite Electrode in Aqueous Solution. *Analytical Letters*, 50(12), pp.1887-1896.

Hayat, A. and Marty, J., 2014. Disposable screen printed electrochemical sensors: Tools for environmental monitoring. *Sensors*, 14(6), pp.10432-10453.

He, K. and Blaney, L., 2015. Systematic optimization of an SPE with HPLC-FLD method for fluoroquinolone detection in wastewater. *Journal of Hazardous Materials*, 282, pp.96-105.

Heidari, M., Kazemipour, M., Bina, B., Ebrahimi, A., Ansari, M., Ghasemian, M. and Amin, M.M., 2013. A qualitative survey of five antibiotics in a water treatment plant in central plateau of Iran. *Journal of Environmental and Public Health*, 2013.

Hernández, F., Sancho, J.V., Ibáñez, M. and Guerrero, C., 2007. Antibiotic residue determination in environmental waters by LC-MS. *TrAC Trends in Analytical Chemistry*, 26(6), pp.466-485.

Hess, E.H., Waryo, T., Sadik, O.A., Iwuoha, E.I and Baker, P.G., 2014. Constitution of novel polyamic acid/polypyrrole composited films by in-situ electropolymerization. *Electrochimica Acta*, 128, pp.439-447.

Hua, M.Y., Chen, H.C., Chuang, C.K., Tsai, R.Y., Jeng, J.L., Yang, H.W. and Chern, Y.T., 2011. The intrinsic redox reactions of polyamic acid derivatives and their application in hydrogen peroxide sensor. *Biomaterials*, 32(21), pp.4885-4895.

Huang, K.J., Xu, C.X. and Xie, W.Z., 2008. Electrochemical behavior of norfloxacin and its determination at poly (methyl red) film coated glassy carbon electrode. *Bulletin of the Korean Chemical Society*, 29(5), pp.988-992.

Jacobs, M., Nagaraj, V.J., Mertz, T., Selvam, A.P., Ngo, T. and Prasad, S., 2013. An electrochemical sensor for the detection of antibiotic contaminants in water. *Analytical Methods*, 5(17), pp.4325-4329.

Kamal, S.K., Sahoo, P.K., Premkumar, M., Rao, N.R., Kumar, T.J., Sreedhar, B., Singh, A.K., Ram, S. and Sekhar, K.C., 2009. Synthesis of cobalt nanoparticles by a modified polyol process using cobalt hydrazine complex. *Journal of Alloys and Compounds*, 474(1-2), pp.214-218.

Karami, H., Kafi, B. and Mortazavi, S.N., 2009. Effect of particle size on the cyclic voltammetry parameters of nanostructured lead dioxide. *Int. J. Electrochem. Sci*, 4, pp.414-424.

Kit-Anan, W., Olarnwanich, A., Sriprachuabwong, C., Karuwan, C., Tuantranont, A., Wisitsoraat, A., Srituravanich, W. and Pimpin, A., 2012. Disposable paper-based electrochemical sensor utilizing inkjet-printed Polyaniline modified screen-printed carbon electrode for Ascorbic acid detection. *Journal of Electroanalytical Chemistry*, 685, pp.72-78.

Lamas-Ardisana, P.J., Casuso, P., Fernandez-Gauna, I., Martínez-Paredes, G., Jubete, E., Añorga, L., Cabañero, G. and Grande, H.J., 2017. Disposable electrochemical paper-based devices fully fabricated by screen-printing technique. *Electrochemistry Communications*, 75, pp.25-28.

Lee, V.B.C., MOHD-NAIM, N.F., Tamiya, E. and Ahmed, M.U., 2018. Trends in Paper-based Electrochemical Biosensors: From Design to Application. *Analytical Sciences*, 34(1), pp.7-18.

Li, M., Li, Y.T., Li, D.W. and Long, Y.T., 2012. Recent developments and applications of screen-printed electrodes in environmental assays—A review. *Analytica chimica acta*, 734, pp.31-44.

Li, Q., Yang, X., Chen, W., Yi, C. and Xu, Z., 2008, January. Preparation of poly (amic acid) and polyimide via microwave-assisted polycondensation of aromatic dianhydrides and diamines. In *Macromolecular symposia* (Vol. 261, No. 1, pp.148-156). Weinheim: Wiley-VCH Verlag.

Li, X., Ballerini, D.R and Shen, W., 2012. A perspective on paper-based microfluidics: current status and future trends. *Biomicrofluidics*, 6(1), p.011301.

Liana, D.D., Raguse, B., Gooding, J.J. and Chow, E., 2012. Recent advances in paper-based sensors. *Sensors*, 12(9), pp.11505-11526.

Lin, Y., Gritsenko, D., Feng, S., Teh, Y.C., Lu, X. and Xu, J., 2016. Detection of heavy metal by paper-based microfluidics. *Biosensors and Bioelectronics*, 83, pp.256-266.

Liu, F., Wu, J., Chen, K. and Xue, D., 2010. Morphology study by using scanning electron microscopy. *Microscopy: Science, Technology, Applications and Education*, 3, pp. 1781-1792.

Luo, X., Morrin, A., Killard, A.J. and Smyth, M.R., 2006. Application of nanoparticles in electrochemical sensors and biosensors. *Electroanalysis*, 18(4), pp.319-326.

Maduraiveeran, G. and Jin, W., 2017. Nanomaterials based electrochemical sensor and biosensor platforms for environmental applications. *Trends in Environmental Analytical Chemistry*, 13, pp.10-23.

Materials evaluation and engineering. 2001. Fourier transform infrared spectroscopy (FTIR). [ONLINE] Available at <https://www.mee-inc.com/hamm/fourier-transform-infrared-spectroscopy-ftir/> [Accessed 14 July 2019]

Materials evaluation and engineering. 2001. Fourier transform infrared spectroscopy (FTIR). [ONLINE] Available at <https://www.mee-inc.com/hamm/scanning-electron-microscopy-sem/> [Accessed 14 July 2019]

Matongo, S., Birungi, G., Moodley, B. and Ndungu, P., 2015. Pharmaceutical residues in water and sediment of Msunduzi River, kwazulu-natal, South Africa. *Chemosphere*, 134, pp.133-140.

Mettakoonpitak, J., Boehle, K., Nantaphol, S., Teengam, P., Adkins, J.A., Srisa-Art, M. and Henry, C.S., 2016. Electrochemistry on Paper-based Analytical Devices: A Review. *Electroanalysis*, 28(7), pp.1420-1436.

Muntteanu, F.D., Titoiu, A., Marty, J.L. and Vasilescu, A., 2018. Detection of antibiotics and evaluation of antibacterial activity with screen printed electrodes. *Sensors*, 18(3), p.901.

Nery, E.W. and Kubota, L.T., 2013. Sensing approaches on paper-based devices: a review. *Analytical and Bioanalytical Chemistry*, 405(24), pp. 7573-7595.

Nie, Z., Nijhuis, C.A., Gong, J., Chen, X., Kumachev, A., Martinez, A.W., Narovlyansky, M. and Whitesides, G.M., 2010. Electrochemical sensing in paper-based microfluidic devices. *Lab on a Chip*, 10(4), pp.477-48.

Noah, N.M., Omole, M., Stern, S., Zhang, S., Sadik, O.A., Hess, E.H., Martinovic, J., Baker, P.G. and Iwuoha, E.I., 2012. Conducting polyamic acid membranes for sensing and site-directed immobilization of proteins. *Analytical biochemistry*, 428(1), pp.54-63.



Nyman, M. and Fullmer, L., 2015. SMALL ANGLE X-RAY SCATTERING OF GROUP VPOLYOXOMETALATES. *Trends in Polyoxometalates Research*, pp.151-170.

Padavan, D.T. and Wan, W.K., 2010. Synthesis and characterization of a novel versatile poly (amic acid) derived from ethylenediaminetetraacetic dianhydride. *Materials Chemistry and Physics*, 124(1), pp.427-433.

Pant, M., Dadare, K. and Khatri, N.C., 2012. Application and UV spectrophotometric methods for simultaneous estimation of norfloxacin and tinidazole in bulk and tablet dosage forms. *Der Pharma Chemica*, 4(3) pp.1041-1046.

Peng, H., Zhang, L., Soeller, C. and Travas-Sejdic, J., 2009. Conducting polymers for electrochemical DNA sensing. *Biomaterials*, 30(11), pp.2132-2148.

Pilehvar, S., Dardenne, F., Blust, R. and De Wael, K., 2012. Electrochemical sensing of phenicol antibiotics at Gold. *International Journal of Electrochemical Science*, 7(6), pp.5000-5011.

Rahman, M.D., Kumar, P., Park, D.S. and Shim, Y.B., 2008. Electrochemical sensors based on organic conjugated polymers. *Sensors*, 8(1), pp.118-141.

Rassaei, L., Marken, F., Sillanpaa, M., Amiri, M., Cirtiu, C.M. and Sillanpaa, M., 2011. Nanoparticles in electrochemical sensors for environmental monitoring. *TrAC Trends in Analytical Chemistry*, 30(11), pp. 1704-1715.

Ruecha, N., Rodthongkum, N., Cate, D.M., Volckens, J., Chailapakul, O. and Henry, C.S., 2015. Sensitive electrochemical sensor using a graphene–polyaniline nanocomposite for simultaneous detection of Zn (II), Cd (II), and Pb (II). *Analytica Chimica Acta*, 874, pp.40-48.

Schnablegger, H. and Singh Y., 2011. The SAXS guide: getting acquainted with the principles. Austria: Anton Paar GmbH.

Seifrtová, M., Nováková, L., Lino, C., Pena, A. and Solich, P., 2009. An overview of analytical methodologies for the determination of antibiotics in environmental waters. *Analytica Chimica Acta*, 649(2), pp.158-179.

Smith, S., Bezuidenhout, P., Mbanjwa, M., Zheng, H., Conning, M., Palaniyandy, N., Ozoemena, K. and Land, K., 2017, February. Development of paper-based electrochemical sensors for water quality monitoring. In *Fourth Conference on Sensors, MEMS, and Electro-Optic Systems* (Vol. 10036, p. 100360C). International Society for Optics and Photonics.

Tang, C.Y. and Yang, Z., 2017. Transmission electron microscopy (TEM). In *Membrane Characterization*, pp. 145-159. Elsevier.

Wang J., (2000). Analytical Electrochemistry, second edition. New Mexico: Wiley inc Publication.

Wang, J., Tian, B., Nascimento, V.B. and Angnes, L., 1998. Performance of screen-printed carbon electrodes fabricated from different carbon inks. *Electrochimica Acta*, 43(23), pp.3459-3465.

Wang, P., Wang, M., Zhou, F., Yang, G., Qu, L. and Miao, X., 2017. Development of a paper-based, inexpensive, and disposable electrochemical sensing platform for nitrite detection. *Electrochemistry Communications*, 81, pp.74-78.

Xu, Y., Liu, M., Kong, N. and Liu, J., 2016. Lab-on-paper micro-and nano-analytical devices: fabrication, modification, detection and emerging applications. *Microchimica Acta*, 183(5), pp.1521-1542.

Xu, Y., Liu, M., Kong, N. and Liu, J., 2016. Lab-on-paper micro-and nano-analytical devices: fabrication, modification, detection and emerging applications. *Microchimica Acta*, 183(5), pp. 1521-1542.

Xue, Q., Qi, Y. and Liu, F 2015. Ultra-high performance liquid chromatography electrospray tandem mass spectrometry for the analysis of antibiotic residues in environmental waters. *Environmental Science and Pollution Research*, 22(21), pp. 16857-16867.

Yamanaka, K., Vestergaard, M.D. and Tamiya, E., 2016. Printable electrochemical biosensors: A focus on screen-printed electrodes and their application. *Sensors*, 16(10), p.1761.

Ye,Z., Wang, L. and Wen, J., 2015. A simple and sensitive method for determination of norfloxacin in pharmaceutical preparations. *Brazilian Journal of Pharmaceutical Sciences*, 51(2), pp.429-437.

Zacco, E., Adrián, J., Galve, R., Marco, M.P., Alegret, S. and Pividori, M.I., 2007. Electrochemical magneto immunosensing of antibiotic residues in milk. *Biosensors and Bioelectronics*, 22(9-10), pp.2184-2191.

Zhang, X., Cui, Y., Lv, Z., Li, M., Ma, S., Cui, Z. and Kong, Q., 2011. Carbon nanotubes, conductive carbon black and graphite powder based paste electrodes. *Int J Electrochem Sci*, 6(12), pp.6063-6073.

Zhang, Z. and Nagrath, S., 2013. Microfluidics and cancer: are we there yet?. *Biomedical Microdevices*, 15(4), pp.595-609.

